

Development of Qualitative and Quantitative Analytical Methods for the Analysis of Per- and Polyfluoroalkyl Substances (PFAS) in Environmental Samples by UHPLC-MS/MS

by

Danyang Wang

A dissertation submitted to the Graduate Faculty of
Auburn University
in partial fulfillment of the
requirements for the Degree of
Doctor of Philosophy

Auburn, Alabama
December 9, 2023

Keywords: PFAS, method development, liquid chromatography,
mass spectrometry, solid phase extraction, environmental distribution

Copyright 2023 by Danyang Wang

Approved by

Joel S. Hayworth, Chair, Associate Professor of Civil and Environmental Engineering
Vanisree Mulabagal, Research Fellow III of Civil and Environmental Engineering
Mark O. Barnett, Professor of Civil and Environmental Engineering
David M. Blersch, Associate Professor of Biosystems Engineering

Abstract

Per- and polyfluoroalkyl substances (PFAS) are synthetic compounds widely used in industrial and consumer products. Over the years, these substances have been distributed in environmental media, human populations, and wildlife species. Detecting trace amounts of PFAS in environmental systems can be challenging due to their complex transport and transformation pathways, and limitations in detection techniques. The primary goal of this research is to develop analytical methods for detecting and measuring PFAS in environmental samples. To achieve this, ultra-high performance liquid chromatography paired with triple quadrupole mass spectrometry (UHPLC-QqQ-MS/MS) was used to design three analytical methods that can identify 35 types of PFAS. The first method focused on identifying 17 PFAS, including perfluoroalkyl carboxylic acids (PFCAs), perfluoroalkyl sulfonic acids (PFSAs), and perfluoroalkyl ether acids (PFECAs). The second method was developed to identify five perfluoroalkyl sulfonamides (FASAs) in environmental samples. The third method targeted 6 isomers of perfluorooctanoic acid (PFOA) and 7 isomers of perfluorooctyl sulfonate (PFOS). Each method involved sample preparation and UHPLC-MS/MS conditions optimization, validation, and application to environmental water samples. Also, the developed methods were applied further to analyze PFAS in several collaborative research projects at Auburn University. Sample preparation methods were optimized to detect trace-level PFAS in various samples such as water, sediment, fish, oysters, mussels, and algae. Each chapter comprehensively summarizes the study's methodology, application, and results.

Acknowledgments

I am deeply grateful to Dr. Joel S. Hayworth, my advisor, for his exceptional support, motivation, and guidance throughout my academic program. Dr. Hayworth's mentorship has been instrumental in providing me with countless opportunities to explore my interests and collaborate on various research projects. I would like to extend my sincere appreciation to Dr. Vanisree Mulabagal for her exceptional mentorship and guidance throughout my research program. Her patience and specialized knowledge were instrumental in elevating my research skills and aiding me in realizing my academic goals. I also wish to express my heartfelt appreciation to Dr. Mark Barnett, Dr. David Blersch, and Dr. Jennifer Panizzi for their invaluable feedback and guidance. Their extensive knowledge and expertise have been beneficial to my research career.

I have been incredibly fortunate to have my family's unwavering support and encouragement. I owe a debt of gratitude to my parents, YongBin Wang and Baoxian Yang, and my husband, Pingzhou Yu, for their constant belief in my abilities. Their support has been a driving force behind my academic achievements.

I would like to express my gratitude to my colleagues and friends, Mengwei Xuan, Meredith Feltman, Roger Viticoski, Bushra Tasnim, Sai Deepthi Yeddula, Ayesha Alam, and Lan Liu, for their support during my academic journey. Their contribution was crucial to my academic achievements, for which I am truly grateful. Finally, I am thankful to the Civil and Environmental Engineering Department of Auburn University for providing me with vital facilities and resources that significantly contributed to the success of my academic career.

Table of Contents

Abstract.....	2
Acknowledgments.....	3
Table of Contents.....	4
List of Tables	8
List of Figures.....	10
List of Abbreviations	12
Chapter 1. Introduction.....	14
1.1 Background	14
1.2 Classification.....	15
1.3 Timeline of PFAS Productions and Applications	19
1.4 PFAS Manufacturing Process	21
1.4.1 Electrochemical Fluorination.....	21
1.4.2 Telomerization	22
1.5 Source and Transformation of PFAS	23
1.5.1 Industrial production.....	24
1.5.2 Contamination of Fluorine-containing Firefighting Foams.....	25
1.5.3 Landfill Leachate	27
1.5.4 Transformation of PFAS.....	30
1.6 Distribution and Impact of PFAS.....	31
1.6.1 PFAS in Environmental Water Systems.....	32
1.6.2 PFAS in Soil and Sediment.....	33

1.6.3	PFAS in Wildlife and Humans	35
1.7	PFAS Regulations	37
1.8	Analytical Approaches	40
1.8.1	Total Fluorine (TF)/ Total Organofluorine (OF) Methods	40
1.8.2	Advanced Analytical Techniques	42
1.9	Challenges of PFAS analysis	47
1.10	Goals and Objectives.....	49
1.11	Instrument Selection for This Study.....	50
Chapter 2. Detection of Perfluoroalkyl Carboxylic Acids (PFCAs), Sulfonic Acids (PFSAs), and Ether Carboxylic Acids (PFECAs) in Surface Water by UHPLC-MS/MS		52
2.1	Background Information	52
2.2	Materials and Methods.....	58
2.2.1	Chemicals, Reagents, and Materials	58
2.2.2	Sample Collection.....	59
2.2.3	Sample Preparation- Solid Phase Extraction (SPE).....	61
2.2.4	Preparation of Working PFAS Standard Solutions.....	62
2.2.5	UHPLC-MS/MS Method Development	62
2.2.6	Method Validation	65
2.3	Results and Discussion.....	65
2.3.1	Part 1. Rapid UHPLC-MS/MS Method for Perfluoroalkyl Ethers (PFECAs)	65
2.3.2	Part 2. UHPLC-MS/MS Quantitative Method for 17 PFAS.....	70
2.3.3	Method Validation	76
2.4	Target PFAS in Surface Water Samples	79
2.4.1	Mobile Bay Surface Water Samples.....	79
2.4.2	Method Application to Large Batch of Surface Water Samples.....	84

2.5	Conclusion.....	87
Chapter 3. A Quantitative UHPLC-MS/MS Method for the Analysis of Perfluoroalkyl Sulfonamides (FASAs) in the Environment		
		89
3.1	Introduction	89
3.2	Method	97
3.2.1	Chemical, Reagents and Materials.....	97
3.2.2	Stock Solution and Calibration Solution Preparation	98
3.2.3	Instrumental Conditions.....	99
3.2.4	Extraction Method Selection.....	106
3.2.5	Method Validation and Quality Control	107
3.3	Results and Discussion.....	108
3.3.1	Optimum UHPLC-MS/MS Conditions	108
3.3.2	Sample Extraction Method Selection.....	111
3.3.3	Result of Method Validation and Quality Control.....	113
3.4	Application to Surface Water Samples	117
3.4.1	Sample Collection.....	117
3.4.2	Sample Preparation	120
3.4.3	Quality Control	121
3.4.4	Target PFAS in Water Samples	122
3.5	Conclusion.....	126
Chapter 4. Qualitative Profiling of PFOA and PFOS isomers -Method Development.....		
		126
4.1	Introduction	126
4.2	Method Development.....	132
4.2.1	Chemicals, Reagents and Materials	132
4.2.2	Standard Preparation.....	135

4.2.3	UHPLC-MS/MS Method Development	135
4.3	Results and Discussion.....	137
4.3.1	Optimizing Chromatographic Separation of PFOA and PFOS Isomers.....	138
4.3.2	Optimization of MS and MS/MS Conditions	142
4.3.3	Identification of PFOA and PFOS Isomers	144
4.4.	Conclusions	145
Chapter 5.	A Summary of Scientific Contributions	146
5.1	Summary	146
5.2	Research Novelty and Contribution	147
5.3	Research Limitation and Future Work.....	149
Appendix	152
References	174

List of Tables

Table 2.1 CAS, molecular weight and structure of the target analytes and internal standard in this study.....	57
Table 2.2 Sampling location coordinate details (SW1-SW7).....	60
Table 2.3 UHPLC-MRM conditions optimized for the analysis of PFECAs.....	68
Table 2.4 Optimized UHPLC-MRM Conditions for target PFAS analysis.....	75
Table 2.5 Optimized MRM parameters for target PFAS.....	76
Table 2.6 PFAS recovery (%) data obtained from experiments conducted with spiking concentration 2ng (1A, 2A and 3A) and 10 ng (1B, 2B and 3B) concentration.....	77
Table 2.7 Short-chain PFAS detected in surface water samples collected from Alabama (Unit: ng/L).....	82
Table 2.8 Range (min-max) and average (in parenthesis) of analytes for each of the analyzed rivers. Overall detection frequencies (DF) are also displayed. Concentrations are expressed in ng/L.	85
Table 3.1 CAS, molecular weight, and structure of the target FASAs, internal standard and surrogate standard in this study.....	97
Table 3.2 Mobile phases and modifier combination tested for chromatographic separation.	100
Table 3.3 The Peak Area of each Target FASAs under Various Fragmentor Voltages.	104
Table 3.4 Recovery Rate (% recovery) of Matrix Effect Experiment.	108
Table 3.5 Optimal conditions for UHPLC.....	109

Table 3.6 Optimal conditions for Ionization Source and Mass Spectrometer (MS).....	110
Table 3.7 MRM Conditions for Each Target FASAs.	110
Table 3.8 Percent recovery rate (Unit: %) of the two extraction protocols for each target PFAS. (Mean ± Standard deviation)	112
Table 3.9 The Accuracy of the Calibrations.	115
Table 3.10 Results of Precision Experiment (ng/mL).	116
Table 3.11 Details of Sampling Locations.....	118
Table 3.12 The Recovery Rate of Surrogate Standard MPFOS in Surface Water Samples and Quality Control.	122
Table 3.13 Results of Surrogate Standard Recovery, Quality Control Recovery and FASAs in Chattooga Surface Water (Unit: ng/L).....	125
Table 4.1 Molecular weight, and structures of the target PFAS and isomers, and internal standard in this study.	133
Table 4.2 Optimal conditions for UHPLC-MS/MS.....	136
Table 4.3 MRM Conditions for each target isomers.....	137

List of Figures

Figure 1.1 Classification of PFAS (ITRC, 2021)	18
Figure 1.2 ECF process for PFAS production (Buck et al., 2011).	22
Figure 1.3 Telomerization Process for PFAS production (Buck et al., 2011).	23
Figure 1.4 Industrial Facilities with Suspected Discharges of PFAS (Hayes et al., 2019).	25
Figure 1.5 Military Sites with Known and Suspected Discharges of PFAS (Hayes & Faber, 2020).	27
Figure 1.6 Municipal Solid Waste Management from 1960 to 2018 (USEPA, 2022b).	28
Figure 1.7 Categories of Municipal Solid Waste in 2018 (USEPA, 2022b)	29
Figure 1.8 Internal structure of Agilent Jet Stream Ion Source (Agilent Technologies, 2023).	45
Figure 1.9 Comparison of ionization technologies (Gross, 2017).	46
Figure 1.10 UHPLC-JetStream ESI-QqQ-MS/MS System.	51
Figure 2.1 Location map for surface water (SW1-SW7) collected from Alabama.	60
Figure 2.2 Optimal FV (60 V) for perfluoro(4-oxapentanoic) acid 1, perfluoro (5-oxa-6-methoxyhexanoic) acid 2, and perfluoro(3,6-dioxaheptanoic) acid 3.	66
Figure 2.3 PI spectra with optimized collision cell energies (eV) for ethers 1-3.	67
Figure 2.4 Extracted UHPLC-MRM chromatograms of compounds 1-6.	69
Figure 2.5 Calibration curves developed for PFECAs.	70
Figure 2.6 Extracted UHPLC-MRM Chromatograms for target PFAS.	73
Figure 2.7 Calibration Curves Developed for PFCAs and PFSAs.	79

Figure 2.8 Spatial Distribution of PFAS in Alabama. Σ_6 PFAS concentrations (in ng/L) are displayed for sampling locations. The 10 largest metropolitan areas are highlighted for spatial reference (Viticotski et al. 2022). 86

Figure 3.1 Structure of Perfluoroalkane sulfonamides (FASAs)..... 89

Figure 3.2 ECF process for manufacturing PFOS and derivatives..... 92

Figure 3.3 Metabolic Pathways for the biotransformation of NEtFOSA. 93

Figure 4.1 The Optimal Chromograms for Each Target Isomer..... 140

List of Abbreviations

AFFF	aqueous film forming foam
ADONA	dodecafluoro-3H-4,8-dioxanonanoate
ATSDR	Agency for Toxic Substances and Disease Registry
API	atmospheric pressure ionization
APPI	atmospheric pressure photoionization
APCI	atmospheric pressure chemical ionization
amu	atomic mass unit
CE	collision energy
CIC	combustion ion chromatography
CLC	capillary liquid chromatography
CERCLA	Comprehensive Environmental Response, Compensation and Liability Act
DI	deionized water
ECF	electrochemical fluorination
ESI	electrospray ionization
EWG	Environmental Working Group
FDA	Food and Drugs Administration
FTICR	Fourier-transform ion cyclotron resonance
FV	fragmentor voltage
FASAs	perfluoroalkane sulfonamides
FTOH	fluorotelomer alcohols
HFPO-DA	hexafluoropropylene oxide-dimer acid
HRMS	high-resolution mass spectrometer
HDPE	high-density polyethylene
LOD	limit of detection
LOQ	limit of quantitation

LHA	lifetime health advisory
MCL	Maximum Contaminant Level
MRM	multiple reaction monitoring
MRL	Minimal Risk Level
nd	non-detectable
PI	product ion
POSF	perfluorooctane sulfonyl fluoride
PTFE	polytetrafluoroethylene
PFAS	per- and polyfluoroalkyl substances
PFAAs	perfluoroalkyl acids
PFCAs	perfluoroalkyl carboxylic acids
PFSAs	perfluoroalkane sulfonic acids
PFECA	perfluoroalkyl ether carboxylic acids
PIGE	particle-induced gamma ray emission
SNUR	Significant New Use Rules
SIM	single ion monitoring
SPE	solid phase extraction
SDWA	Safe Drinking Water Act
TSCA	Toxic Substances Control Act
TF	total fluorine
TOP	total oxidizable precursor
TOF	time of flight
UCMR	Unregulated Contaminant Monitoring Rule
UHPLC-MS/MS	ultrahigh-performance liquid chromatography-tandem mass spectrometry
US EPA	United States Environmental Protection Agency
WWTP	wastewater treatment plant
¹⁹ F NMR	fluorine-19 nuclear magnetic resonance spectroscopy

Chapter 1. Introduction

1.1 Background

The study of modern organic chemistry can be traced back to the 1820s when Frederick Wohler synthesized the organic compound urea in the laboratory using inorganic material ammonium cyanate (Keen, 2005). Since then, an increasing number of organic chemicals have been created and extensively utilized in various civil and military applications. While the rapid development of synthetic organic chemistry has significantly contributed to economic growth and societal progress, it has also introduced potential environmental and health risks to ecosystems.

In recent decades, concerns have grown regarding the adverse effects of certain toxic and recalcitrant organic chemicals. To address this issue, the Stockholm Convention proposed the term “Persistent Organic Pollutants (POPs)” in 2001, along with corresponding provisions to regulate the use of these persistent chemicals. POPs have the characteristic of persistent in environment, long-range transport, bioaccumulation, and high-level toxicity (Stockholm Convention, 2001). Among the POPs list, per- and polyfluoroalkyl substances (PFAS) have gained significant attention due to their widespread presence in the environment and consumer products. PFAS constitute a broad class of manufactured chemicals characterized by similar stable structures and persistent properties. These chemicals consist of a carbon- fluorine skeleton of varying carbon lengths and a functional group. The carbon- fluorine bond is one of the strongest covalent bond in organic chemistry that cause these compounds to exhibit high thermal stability, chemical resistance, and low surface tension (Siegemund et al., 2000). PFAS, therefore, have extensive applications in multiple industrial and consumer products in the United States. Since the 1940s, a wide variety of PFAS have been mass-produced and utilized in water, fire, and grease resistance materials, such as surfactants, fire retardants, stain-resistant products, nonstick cookware and food

packaging (AWWA, 2019). The superior performance of PFAS-coated products led to their worldwide popularity in the last century, resulting in their prevalent use in most American households. However, the same properties that make PFAS desirable also cause them to be extremely persistent and difficult to break down in the environment. Decades of heavy use have resulted in a wide distribution of PFAS across the globe, not only in the environment but also in the blood of humans and animals. PFAS contamination poses a global threat to the entire environmental system and human populations on the earth.

Comprehensive toxicological and epidemiological studies of PFAS have only started in this century. Human exposure to PFOA and PFOS has been associated with an increased risk of immune dysfunction, thyroid disorders, endocrine disruption and getting malignant tumors (Cooke, 2017). However, most research to date has focused on PFOA and PFOS, which represent only a small portion of the entire PFAS family. Thousands of undetected and unknown PFAS have been released into the environment, posing risks to all living organisms. Due to the lack of analytical methods for detecting and monitoring these emerging chemicals, our understanding of their toxicity, environmental behavior, and transport pathways remains limited. Addressing this pressing challenge is a priority for the community and society.

1.2 Classification

PFAS comprise a large and continuously expanding group of substances. Among them, over 6000 have been assigned specific CAS (Chemical Abstracts Service) numbers, and more than 5000 of these have a defined chemical structure (Evich et al., 2022). PFAS have the highly fluorinated carbon backbones that contain the perfluoroalkyl moiety C_nF_{2n+1} and a functional group on the end (Buck et al., 2011). Based on their chemical structures, PFAS can be classified

into two primary categories: nonpolymers and polymers, with various subclasses within each category (Figure 1.1).

Non-polymeric PFAS are considered more threatening to the environment and organisms, and thus are the focus of most current studies. Polymeric PFAS are less reactive and bioaccessible due to their large molecular size. However, non-polymeric PFAS can be transformed from polymers and released into the environment during the manufacturing process. According to the fluorinated degree of their carbon chains, non-polymeric PFAS can be further classified into polyfluoroalkyl substances (where fluorine atoms replace only part of the attached hydrogen atoms, excluding hydrogens in functional groups) and perfluoroalkyl substances (where fluorine atoms replace all of the attached hydrogen atoms, excluding hydrogens in functional groups) (Buck et al., 2011). Within the subclass of PFAS, perfluoroalkyl acids (PFAAs) are the most frequently detected perfluoroalkyl substances in the environment. PFAAs are recognized to be the terminal PFAS since they are not degradable in the environment. Other PFAS subclasses that can degrade or transform to PFAAs under chemical or biological processes in the environment are referred to as PFAA precursors.

Perfluoroalkyl carboxylic acids (PFCA) and perfluoroalkane sulfonic acids (PFSA) are PFAAs that are the most widely distributed in the environment, wildlife, and human, such as perfluorooctanoic acid (PFOA), perfluorohexanoic acid (PFHxA), and perfluorobutanoic acid (PFBA), perfluorooctanoic sulfonic acid (PFOS), perfluorohexane sulfonic acid (PFHxS), perfluorobutane sulfonic acid (PFBS). To differentiate between PFCAs and PFSAs, a simplified classification method is based on the length of carbon chains, dividing them into short-chain and long-chain PFAS. Long chain PFAS refers to PFCAs with 7 and more perfluoroalkyl carbons and PFSAs with 6 and more perfluoroalkyl carbons (EU, 2020). Short-chain PFAS indicates PFCAs

with 6 or fewer perfluoroalkyl carbons, and PFSA with 5 and fewer perfluoroalkyl carbons. For instance, PFOA ($C_7F_{15}COOH$) and PFOS ($C_8F_{17}SO_3H$) are classified to be long-chain PFAS, PFBA (C_3F_7COOH) and PFBS ($C_4F_9SO_3H$) are classified into short-chain PFAS.

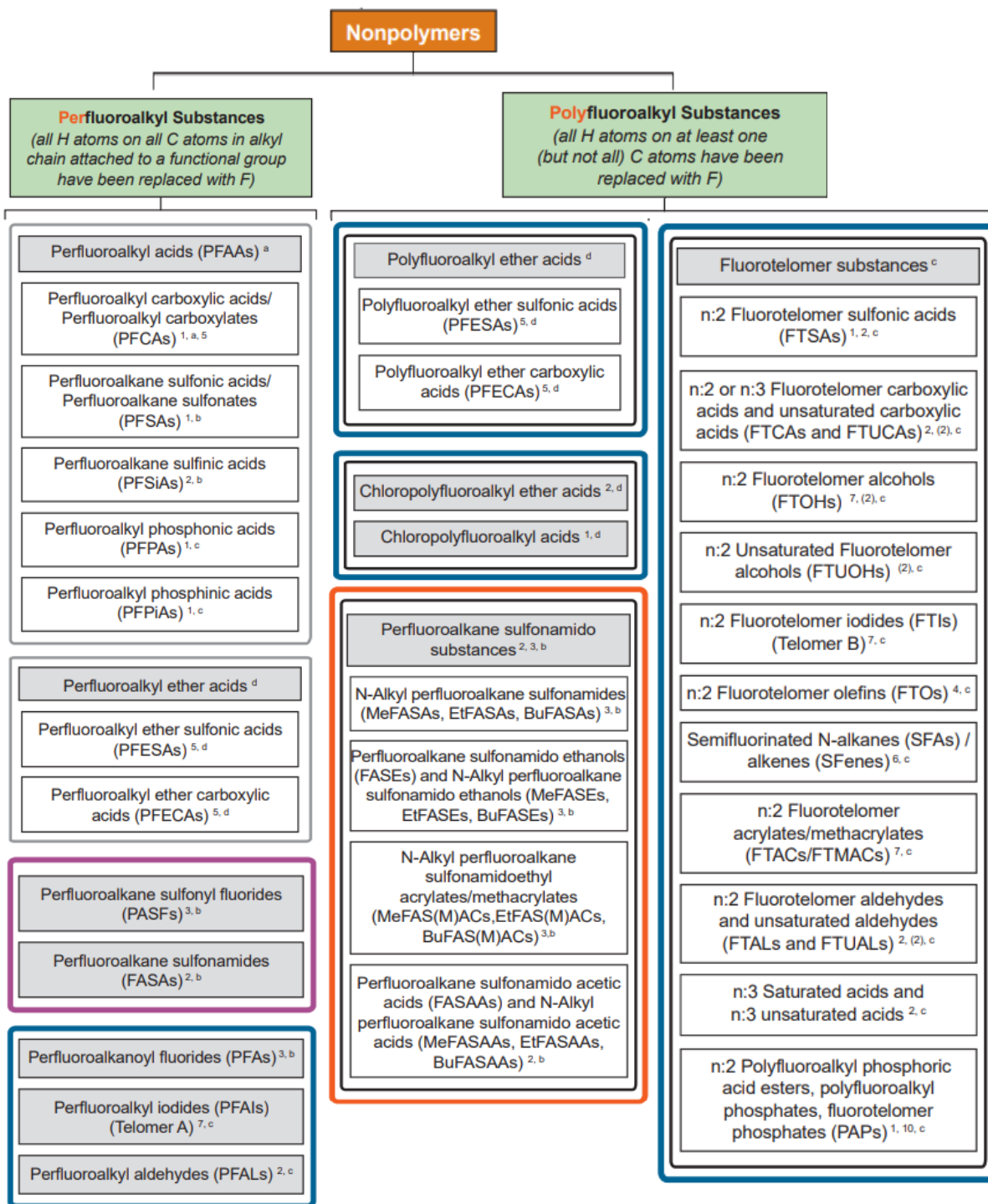


Figure 1.1 Classification of PFAS (ITRC, 2021)

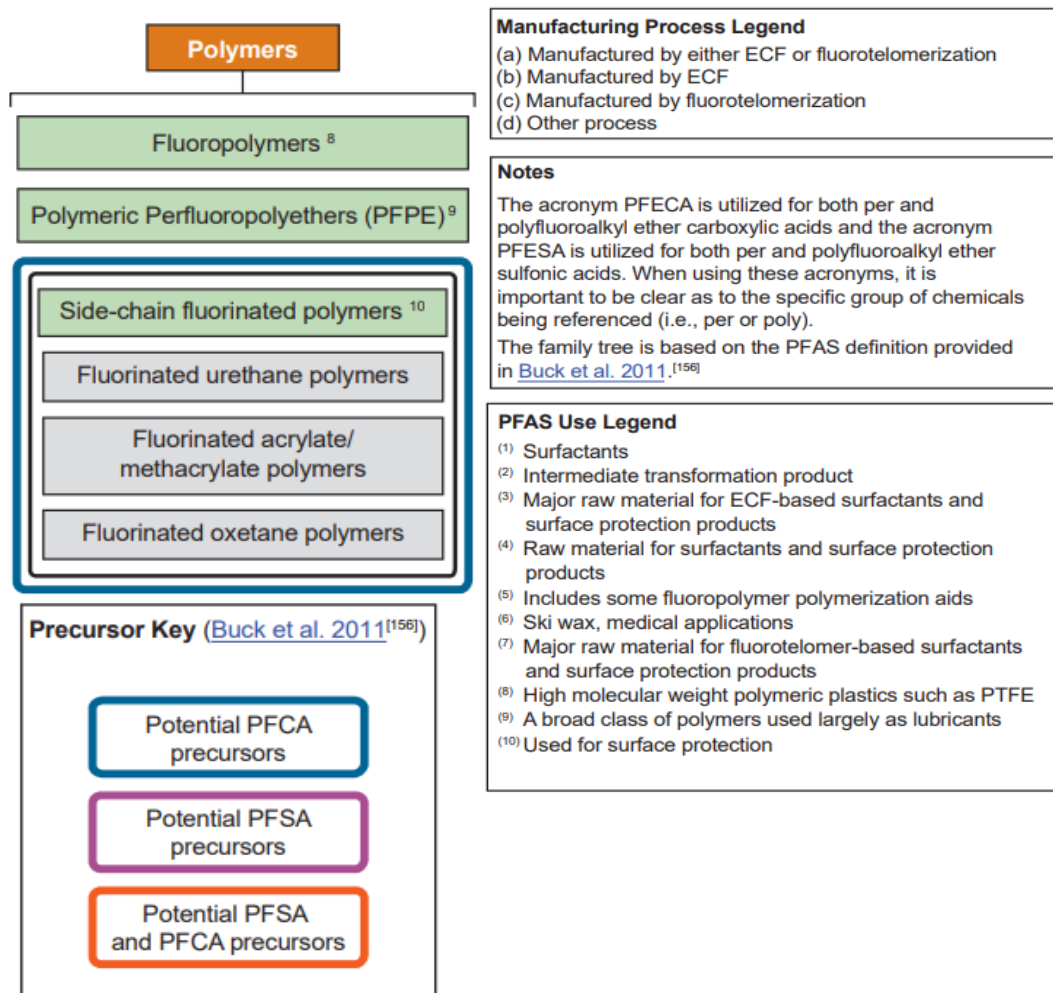


Figure 1.1 Classification of PFAS (ITRC, 2021) (Continued).

1.3 Timeline of PFAS Productions and Applications

PFAS have been used in a broad range of industrial and consumer products worldwide for over seven decades. Polytetrafluoroethylene (PTFE), the first perfluorinated compound, was accidentally created by Roy J. Plunkett at DuPont’s laboratory in 1938 while developing a new chlorofluorocarbon refrigerant (Plunkett, 1986). This substance exhibited exceptional chemical and thermal properties, leading to the commercialization of PTFE as Teflon in 1945 as a coating-material in industrial production. In 1947, 3M (Minnesota Mining and Manufacturing Company) developed PFOA and initiated mass-production for military use. By 1951, DuPont had purchased

PFOA from 3M and began using it as a surfactant in the production process of PTFE-based products. In 1962, the U.S. FDA (Food and Drug Administration) approved the use of Teflon coating in non-stick cookware, which led to the widespread popularity of Teflon products in households worldwide. During the same period, PFOS was developed for stain repellents. First created by 3M in 1949, PFOS was used in their Scotchgard products as a fabric protector. In 1960s, the U.S. Navy collaborated with 3M to develop the aqueous film-forming foam (AFFF), a firefighting foam containing PFOA and PFOS. AFFF can effectively extinguish flammable liquid fires, and rapidly became widely used in military sites, firefight training centers and airports worldwide. However, as the use of PFOA and PFOS increased sharply, their adverse effects started to emerge and were studied. From the 1960s to the 1990s, 3M and Dupont conducted multiple PFOA and PFOS-related research projects, revealing that these substances were toxic to laboratory animals and could accumulate in human blood. The increasing evidence proved the risks PFOA and PFOS posed to humans and the environment, leading to the phasing out of these PFAS. In 2000, 3M announced to voluntarily phase out PFOS, PFHxS, PFOA and related precursors, with the phase-out completed by 2008 (3M, 2000; USEPA, 2017). From 2006 to 2015, all major PFAS manufacturers in the U.S. phased out PFOA, PFOS and related long-chain PFAS under the U.S. EPA's voluntary Stewardship Program (USEPA, 2017). However, after ceasing the use of long-chain PFAS, chemical manufacturers began developing short-chain PFAS as substitutes. Since 2003, one of the C4 PFAS, PFBS, has been used as a replacement for PFOS in 3M's Scotchgard products. Since 2009, DuPont developed HFPO-DA (also known as GenX chemicals), a perfluoroether substance, as a replacement for PFOA. Like long-chain PFAS from the 1960s to the 1990s, emerging short-chain PFAS are now produced on a large scale and used in a wide

variety of products. (ITRC, 2021; Lindstrom et al., 2011; *Toxic timeline: A brief history of PFAS*, 2019)

Apart from non-stick cookware, PFAS are also used in food packaging and containers, such as microwave popcorn bags and fast-food wrappers. Consumer products containing PFAS can be found in many households, including stain-resistant furniture and carpets, waterproof clothing, and shoes, as well as personal care products and cosmetics. In addition to their use in household products with resistance to grease, oil, water, and heat, perfluorinated chemicals have applications in various sectors, such as aerospace, medical, automotive and industrial fields (Buck et al., 2011; ITRC, 2021).

1.4 PFAS Manufacturing Process

PFAS are produced through two principal manufacturing processes: electrochemical fluorination (ECF) and telomerization process. ECF was the major process for PFAS production in the United States from the 1950s to 2002, while telomerization process, developed in 1970s, became the dominant process in recent years since ECF was phased out.

1.4.1 Electrochemical Fluorination

The ECF process was developed by Simons in 1944 and was used for synthesizing long-chain PFAS by the 3M Company since 1956 (Cheremisinoff, 2016). ECF is an organofluorine chemistry technology in which an organic compound reacts with anhydrous hydrogen fluoride in an electrolytic cell, leading to the replacement of all hydrogen atoms by fluorine atoms (Hydrocarbon + HF + e⁻ → Fluorocarbon) (Banks et al., 2013; Buck et al., 2011). ECF is a cost-effective process for PFAS production; however, it yields low quantities of the required PFAS (e.g., linear PFOA and PFOS). It is an impure process that causes the breakage and rearrangement of carbon chains and produces a mixture of straight (70-80%) and branched (20-30%) homologues

(Reagen et al., 2007). ECF technology was the primary process used for producing PFOA and PFOS in the last century; the processes are present in Figure 1.2.

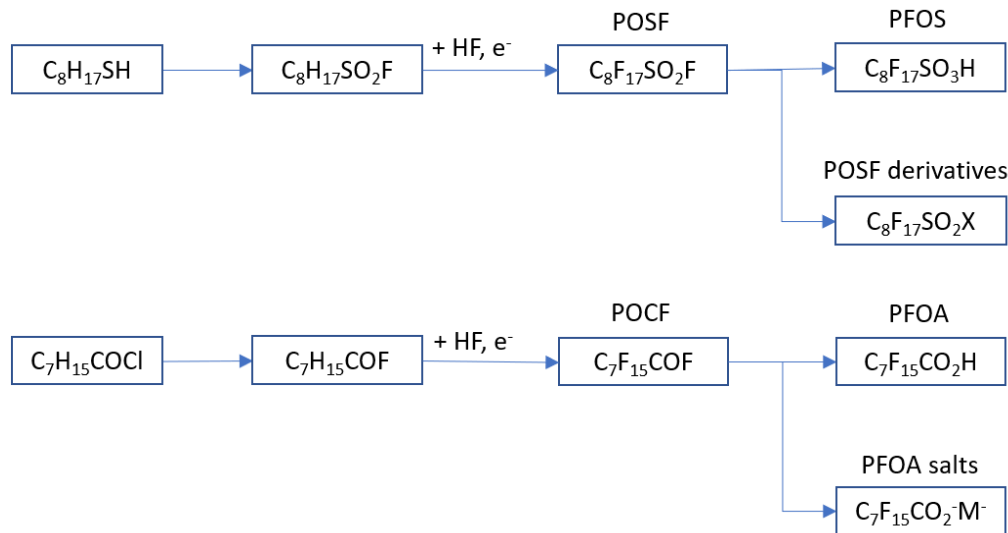


Figure 1.2 ECF process for PFAS production (Buck et al., 2011).

1.4.2 Telomerization

The telomerization technique was originally developed and used by DuPont in the 1970s to produce PFOA. Telomerization is a synthetic process for producing polymers with shorter chains, which have the structure of two to ten repeating units (Cheremisinoff, 2016). Because it retains the structure of initial telogens, this method is an isomeric pure synthetic process that primarily produces structurally linear PFAS. Telomerization became the primary manufacturing process for multiple PFAS since the 2000s as a substitute for the ECF process. The producing process of PFOA, PFNA, FTOHs by telomerization process is illustrated in Figure 1.3.

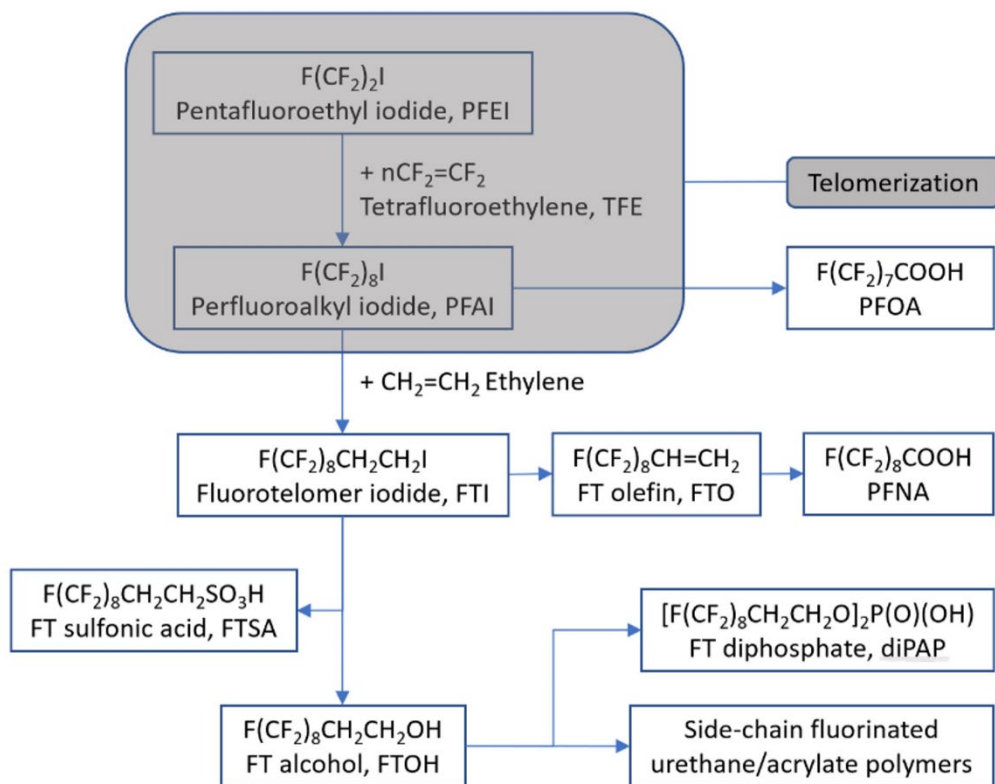


Figure 1.3 Telomerization Process for PFAS production (Buck et al., 2011).

1.5 Source and Transformation of PFAS

PFAS are manmade chemicals, and their presence in the environment and biota can be traced back to their extensive production, usage, or the degradation of these input PFAS. The large-scale production and usage is often referred to as the direct source of PFAS, including emissions from industrial production, fluorine-containing firefighting foam, landfill leachate, wastewater treatment plants, and release during the lifecycle of consumer products (ITRC, 2021). Indirect sources of PFAS involve the transformation of precursor substances through biotic or abiotic degradation processes in the environment. These transformations increase the diversity of the PFAS, complicating the tracking of manufactured PFAS in environment media and biota (ITRC, 2021).

1.5.1 Industrial production

Industrial PFAS-containing wastes are generated in both primary and secondary manufacturing facilities. Primary manufacturing facilities produce PFAS through ECF or telomerization processes, which result in a range of PFAS byproducts, including linear PFAS with varying carbon-chain lengths and branched isomers. Prior to the 2000s, ECF was the major process for PFAS production, leading to the release of both linear and branched byproducts into the environment. After the 2000s, the production process shifted to telomerization, reducing the release of branched byproducts. However, due to lack of PFAS-related regulations on industrial discharges, mixtures of linear byproducts and manufactured PFAS continue to be released into the environment. For instance, perfluorooctane sulfonyl fluoride (POSF) is one of the most produced PFAS. Its historical global production was estimated to be 122.5 kiloton from 1970 to 2012, including usable industrial materials and unusable wastes; approximately 36.9% of the produced POSF has been released to the environment (Paul et al., 2009). Secondary manufacturing facilities process PFAS-containing products and use PFAS as raw material or surfactant to produce industrial and consumer products, such as PTFE coatings, firefighting foams or surface treatments of papers and textiles.

PFAS-containing wastes from these manufacturing plants can be released into the environment through air emissions, wastewater, and solid waste disposal. However, currently, no treatment strategies employed by these facilities can effectively remove PFAS from wastewater or gas before discharging into water and air. According to an analysis by the Environmental Working Group (EWG), at least 475 industrial facilities in the United States use PFAS and could be discharging PFAS contaminants into the surrounding environment (Hayes et al., 2019). Such

industrial facilities include carpet, paper, electroplating, semiconductor, tannery, and wire manufacturing plants, as well as other known users of PFAS (Figure 1.4).

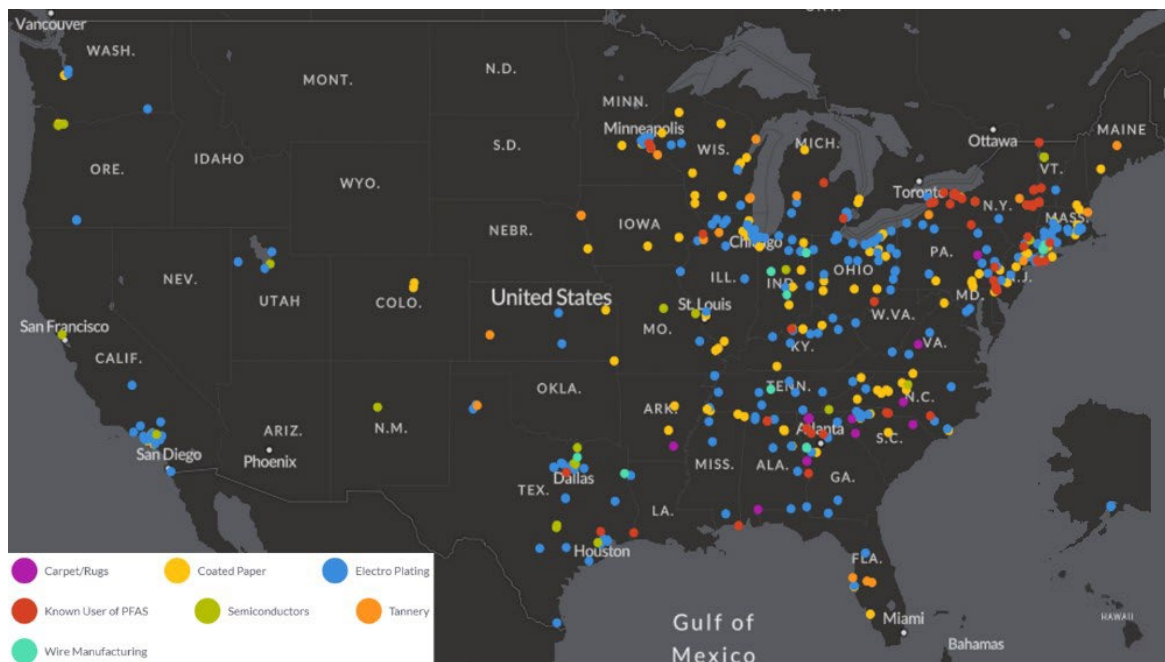


Figure 1.4 Industrial Facilities with Suspected Discharges of PFAS (Hayes et al., 2019).

1.5.2 Contamination of Fluorine-containing Firefighting Foams

Aqueous film forming foam (AFFF) is one of the most used fluorinated foams designed for extinguishing flammable liquid fires. Since the 1970s, AFFF has been extensively used and stored in many facilities for firefighting training or emergency response, including military and domestic airports, petroleum refineries, municipal fire departments, storage sites, and offshore fire protection facilities (Hu et al., 2016). Prior to 2002, the ingredients of AFFF were long-chain PFCAs and PFASs homologues produced by the ECF process, including PFOA, PFOS, PFHxA and their precursors. After the ECF process phased out, the second generation of AFFF was telomer-based foams, dominated by PFOA and its precursors (8:2 FTS). By 2016, the

manufacturing of long-chain PFAS discontinued, and short-chain fluorotelomers (6:2 and 4:2 FTS) became the predominant ingredients of the surfactant solution in AFFF (Dalton, 2018).

The fluorinated chemicals in AFFF were not formulated to be a specific mixture of PFAS and contained both known and unknown PFAS (ITRC, 2021). These PFAS were released into the environment through fire suppression activities, firefighting training or leaks during transport and storage. As a result, it is difficult to estimate the volume of PFAS released from firefighting foams, whether for total PFAS or any individual PFAS. Although the production of long-chain PFAS has been phased out, regulations did not ban the use of old generation AFFF that was already stored in military and civilian facilities. Due to the persistent property of PFAS chemicals, large numbers of historically stored firefighting foam are still being used in most of these facilities. Currently, the use of old and modern-generation AFFF has made both long-chain and short-chain PFAS environmental contaminants in the surrounding area.

Among all these facilities, military sites are known to use most firefighting foams. A high volume of PFAS-containing firefighting foams is discharged to the training site during every periodical training exercise. Hundreds of military facilities and installations are distributed across all 50 states in the United States. According to a report by the EWG, 678 military sites are known or suspected of discharging PFAS chemicals, and 328 of them have been confirmed to have caused different levels of contamination in surrounding drinking water or groundwater (Figure 1.5) (Hayes & Faber, 2020).

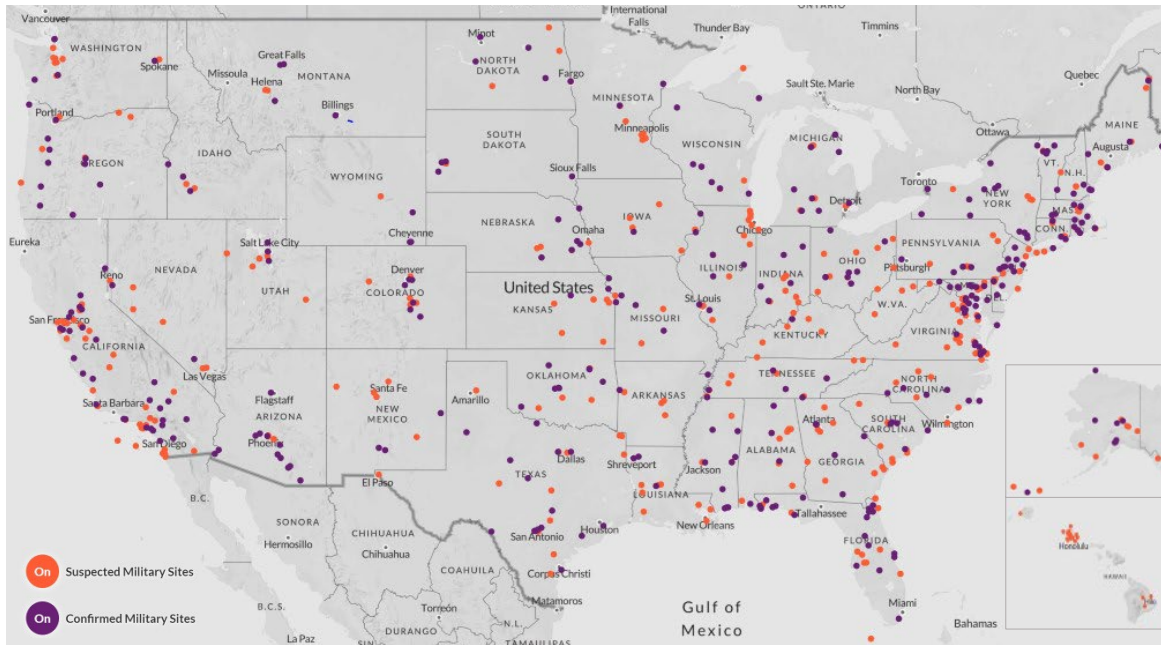


Figure 1.5 Military Sites with Known and Suspected Discharges of PFAS (Hayes & Faber, 2020).

1.5.3 Landfill Leachate

Landfill leachate is the liquid that is formed when precipitation comes into contact with and percolates through waste in a landfill. The leachate reaches groundwater by permeating into the soil or reaches surrounding rivers through stormwater runoff. PFAS-containing leachate is generated from municipal or industrial solid waste landfills.

The extensive use of PFAS has led to their presence in the municipal landfills all over the world. These contaminants originate from discarded consumer products, including fast-food packaging, photographic products, shampoo, paints, and non-stick cookware, where they can leach out into the surrounding environment. EPA records from 1960 to 2018 report that more than 50% of municipal solid waste was directed to landfills every year (Figure 1.6). In 2018 alone, 292.4 million tons of municipal solid waste were generated, with the various categories of waste illustrated in Figure 1.7. Several types of solid waste, such as textiles, rubber, leather, wood

(including furniture paint), paper, paperboard, metal, and plastic, are potential sources of PFAS. These PFAS-containing wastes were landfilled, and the substances were released into the environment through the leachate over time (USEPA, 2022b).

Municipal Solid Waste Management: 1960–2018

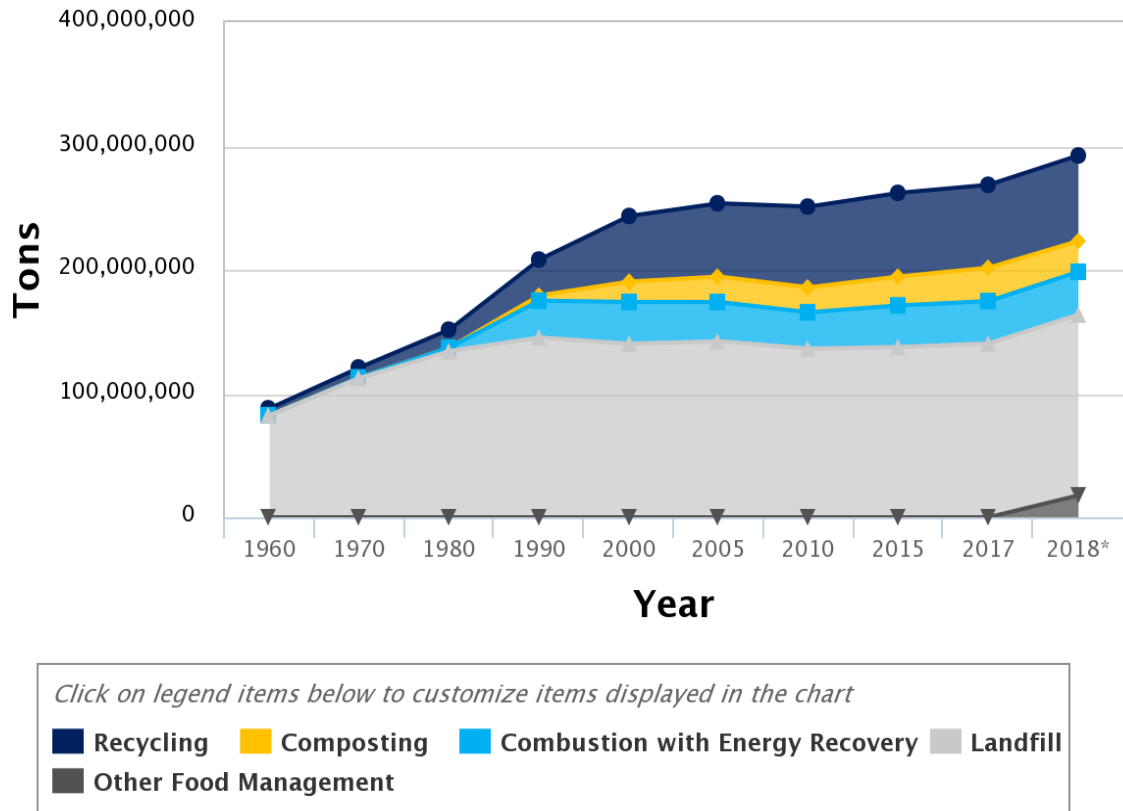


Figure 1.6 Municipal Solid Waste Management from 1960 to 2018 (USEPA, 2022b).

Total MSW Generated by Material, 2018

292.4 million tons

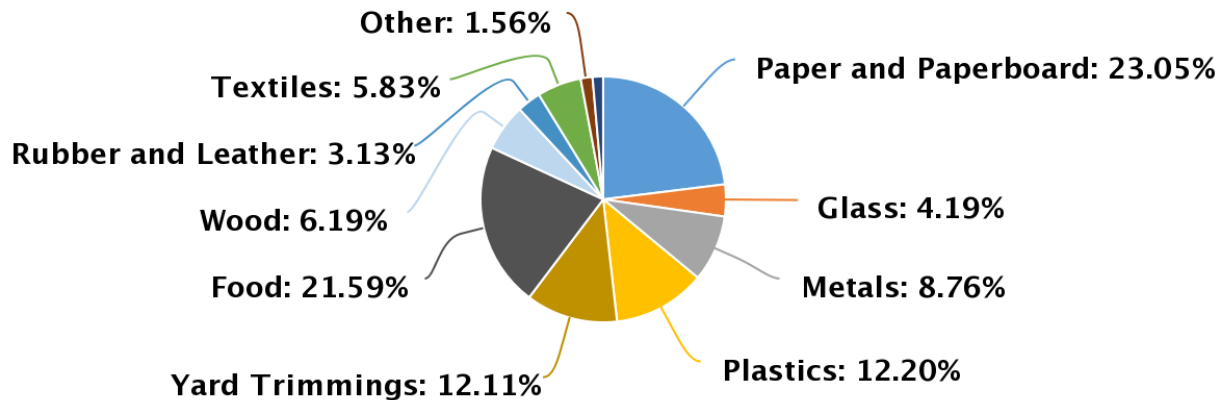


Figure 1.7 Categories of Municipal Solid Waste in 2018 (USEPA, 2022b)

PFAS-containing industrial solid waste originates from facilities that either produce PFAS chemicals or utilize them to make products. Some of the non-hazardous waste is processed along with municipal solid waste. For the handling of hazardous industrial waste, the EPA has established specific standards to minimize the risk of release into the environment. These standards include leak detection systems, controls for leachate collection and removal, and controls for runoff, runoff, and wind dispersal. This regulation is designed to minimize the leachate from hazardous waste landfills, however, the ongoing and long-term monitoring and maintenance for these landfill infrastructures is required to prevent potential leaks (USEPA, 2023a).

1.5.4 Transformation of PFAS

Fully fluorinated PFAS, such as PFCAs and PFSA, are the end products of the PFAS transformation process in the environment. These final PFAS have many precursors, which are partially fluorinated and contain one or more breakable chemical bonds under environmental conditions, such as carbon-oxygen bonds. The transformation processes of PFAS in the environment can be achieved through biotic processes, abiotic processes, or a combination of both. Biotransformation of precursors occurs under aerobic conditions through digestion and metabolism in organisms (Dinglasan et al., 2004; Wang, Szostek, Buck, et al., 2005; Wang, Szostek, Folsom, et al., 2005). Abiotic pathways include the hydrolysis, photolysis, and oxidation processes that occur in environmental soil, water, or atmosphere (ITRC, 2021). Both PFCAs and PFSA, as well as their precursors distributed in the environment, originate from decades of massive production. For example, POSF-based and fluorotelomer-based substances, the major raw materials for fluorinated surfactants and surface protection products, can degrade into PFCAs and PFSA (Buck et al., 2011). POSF-based substances produced by ECF process are major precursors of PFSA, especially PFOS; however, during this process, a small amount of PFCA precursors is generated as impurities as well (Prevedouros et al., 2006). Fluorotelomer-based substances synthesized by telomerization process primarily degrade into PFOA in the environment. Other PFCAs with varying chain lengths, such as PFHpA, PFHxA, PFPeA, PFBA and PFPrA, can be transformed from specific fluorotelomer-based intermediates through a series of chain unzipping processes under complex environmental conditions (Buck et al., 2011). The degradation of precursors can occur anywhere under appropriate conditions, including natural environment, production lines in factories, or wastewater treatment processes. While the degradation of precursors frequently happens under ambient conditions, they account for a small portion of PFCA and PFSA emissions compared to direct industrial releases. In an estimation of global PFCAs

emissions, the total historical emissions of PFCAs from the degradation of POSF-based precursors and fluorotelomer-based precursors are approximately 1-30t in 1960-2002 and 6-130t in 1974-2004 separately, taking a small percentage of the total PFCAs source emissions (3200-7300t) (Prevedouros et al., 2006). Nevertheless, understanding the transformation pathways of PFAS is currently a challenging task since a degradation process can release multiple intermediates and final products, significantly increasing the diversity and complexity of PFAS in environmental media and biota. In addition to non-polymer precursors, the degradation of fluorinated polymers also contributes to the abundance of PFAS in the environment.

1.6 Distribution and Impact of PFAS

PFAS have been ubiquitously found in the environment and organisms, including water, air, sediment/soil, microorganisms, plants, animals, and humans. In general, most PFAS, such as PFAAs and some of their precursors, are ionic; they are less volatile than other organic chemicals and highly soluble in water at ambient temperature. A small number of PFAS are neutral PFAS, such as fluorotelomer alcohols (FTOHs), fluorotelomer acrylates (FTAs), and some perfluorooctane sulfonamido alcohols; they are more volatile than ionic PFAS. In addition to accumulating in the water environment, these volatile and semi-volatile PFAS can disperse into the atmosphere and transport to remote areas (Xie et al., 2015). A portion of the PFAS distributed in the environment ends up entering and accumulating in organisms by taking in PFAS-contaminated air, water, or food, and then passing to the upper trophic levels. PFAS have been circulated in the global environment through various pathways, including water cycles, atmospheric routes, organism uptake, and transmission through food webs. Among all identified PFAS, PFOA and PFOS are the most frequently detected in all environmental media, mainly due to massive production and their non-degradable property.

1.6.1 PFAS in Environmental Water Systems

Environmental water systems are the major media for the transportation of PFAS; they have been extensively detected worldwide in surface water, seawater, wastewater, groundwater, rain/snow water, as well as drinking water.

Among all identified PFAS, PFAA, especially PFCA and PFSA, have been present in all these aquatic environments, originating from either long-term production or degradation of precursors. In recent decades, the PFAAs detected in environmental water samples commonly have a higher shorter-chain (C4-C8) content, including PFBA, PFBS, PFPeA, PFHxA, PFHxS, PFHpA, PFOA, PFOS. The detection of these PFAA in surface water across the world is presented in Appendix A.1. In addition to the discontinuation of long-chain PFAS production, PFAAs with shorter carbon chain lengths exhibit high mobility and long-distance transportation ability in aquatic environments (Brendel et al., 2018), while long-chain PFAS tend to sorb to sediment or soil in the environment (Zhao et al., 2016). Additionally, short-chain PFAAs have already been detected in remote areas, such as Tibetan Plateau (Yamazaki et al., 2016) and Antarctic region (Cai, Yang, et al., 2012). These short-chain PFAAs are degraded from volatile precursors which can transport long distances via the atmosphere (Brendel et al., 2018).

In contrast to the widely distributed PFAAs, partially fluorinated PFAS, like PFAA precursors and perfluoroethers, are more frequently detected in waters close to contamination sources than in general water bodies. Samples collected in water bodies near PFAS-contaminated areas, such as firefighting training sites, manufacturing facilities, and wastewater treatment plants, usually contain high concentrations and a great variety of PFAS. For example, Chen et al. conducted a study of the rivers around Bohai Sea, one of the most polluted sea areas in China, which is close to two famous fluorochemical industrial parks. They found 21 PFAS in the area

with the highest total concentration up to 41700ng/L, including 17 PFAAs, 2 precursors (FASAs) and 2 perfluoroethers (PFESAs) (Chen et al., 2017).

PFAS contamination has become a global environmental issue, threatening the safety and health of humans. Current PFAS removal techniques cannot effectively capture or eliminate these chemicals in water, which means wastewater treatment plants and water supply plants cannot provide adequate treatments for PFAS. The PFAS that are widely distributed in the environment have invaded the drinking water systems of the United States. According to a report by the EWG in 2018, more than 1500 drinking water systems, serving up to 110 million Americans, were contaminated with PFOA, PFOS and similar PFAS (Walker, 2018).

1.6.2 PFAS in Soil and Sediment

The primary sources of PFAS in soil and sediment are PFAS-based firefighting foam, industrial/municipal landfill leachate, and deposition of PFAS from aqueous or atmospheric systems (Ahmed et al., 2020). Among these sources, the use of AFFF is the most significant contributor to PFAS contamination in soils. A review by Brusseau et al. indicated that the majority of PFAS-contaminated soils studied in the literature were collected from fire training areas or other AFFF-utilizing locations. PFOS and PFOA are the predominant PFAS reported in these sites, with concentrations reaching up to 460,000ng/g for PFOS and exceeding 50,000ng/g for PFOA (Brusseau et al., 2020). Similar to the situation in water systems, the concentration of PFAS in the sediment/soil varies depending on the distance from contamination sources. However, trace levels of PFAS have been detected in soils worldwide, even in regions that are away from direct PFAS sources. Brusseau et al. investigated 1400 sampling locations across all continents that were not directly impacted by PFAS sources. The global background level of total PFAS in these soils ranged from <0.001 to 237 ng/g (Brusseau et al., 2020). PFAS levels in sediments have been found

to be high in various water bodies, such as Lake Ontario in Canada (Yeung et al., 2013), Charleston Harbor in the US (White et al., 2015), Bohai coastal watersheds in China (Zhu et al., 2014), and Jucar river in Spain (Campo et al., 2016). PFOA and PFOS are the most prevalent PFAS in these river sediments as well. The concentration and diversity of PFAS in sediments/soils are influenced by numerous biotic or abiotic processes, including sorption to solid phases, uptake by microorganisms and plants, or degradation of some precursor PFAS.

The sorption and accumulation of PFAS in soil and sediment are among the primary factors affecting the fate and transport of PFAS in the environment. Numerous studies have investigated the partitioning of PFAS between liquid and solid phases, revealing that some PFAS can bind to solids. The binding of PFAS to sediment/soil is associated with the functional groups, chain length and hydrophobic properties of the PFAS, as well as the characteristics of the sediment/soil, such as organic matter content, salinity, and pH. Higgins & Luthy suggested the main sorption mechanism was attributed to the hydrophobic interaction between the carbon chain of the PFAS and organic matter in the sediment; another minor mechanism is the electrostatic interactions between the functional groups of the PFAS and the charged composition of the sediment. Studies have confirmed that PFAS sorption increased with increasing chain length, and PFAS with sulfonate functional head groups (PFSAAs) adsorbed more strongly onto soil than PFAS with carboxylic head groups (PFCAs) (Higgins & Luthy, 2006; Pereira et al., 2018). A study by Milinovic et al. supported this conclusion by comparing the sorption of PFOS, PFOA and PFBA in soil. They reported that the affinity sequence of the three PFAS in soils was PFOS > PFOA > PFBS (Milinovic et al., 2015). In addition to the physicochemical properties of PFAS, the conditions of sediments and soils largely affect the partitioning of PFAS to solid phases, with organic matter content being a key factor (Johnson et al., 2007). Moreover, environmental factors

such as charge composition, pH, salinity, and mineral content play crucial roles in the sorption process. For example, Pereira et al. noted that cation effects likely have a more pronounced effect on shorter-chained PFAS, promoting their bonding to humic and fulvic acids, whereas the sorption of longer-chained PFAS is more strongly related to pH values, suggesting a higher affinity for sorbing to humic acid in soils (Pereira et al., 2018).

1.6.3 PFAS in Wildlife and Humans

The presence of PFAS in the blood and organ tissues of a wide range of wildlife, as well as humans, has raised concerns regarding potential health risks associated with the exposure to these synthetic chemicals.

PFAS have been detected in various wildlife species inhabiting different regions worldwide, such as fish, birds, marine mammals, even polar bears living far from human settlements. A review by Giesy and Kannan (2001) reported PFOS concentrations in wildlife from diverse geographical locations, including three continents in the north hemisphere, the Pacific, the Arctic, and the Antarctic Oceans. Varying levels of PFOS were detected in the plasma, livers, eggs, and muscles of a broad range of wildlife, such as in aquatic mammals from <3g/ng (plasma of ringed seals, Canadian Arctic) to 3680ng/g (liver of minks, Midwestern USA), in birds from <1ng/g (plasma of polar skua, Terra Nova Bay, Antarctica) to 2570ng/g (plasma of bald eagle, Midwestern USA), and in fish from <6ng/g (muscle of brown trout, Michigan waters, USA) to 380ng/g (eggs of lake whitefish, Michigan waters, USA) (Giesy & Kannan, 2001). Oral ingestion of PFAS-containing food, air or water is the primary pathway for these chemicals to enter the internal systems of wildlife. Once these persistent chemicals enter the body of an organism, a portion of them will build up in cells rather than excrete by metabolism or digestion. Numerous laboratory or field studies have indicated that long-chain PFAS tend to accumulate in cells more

readily and pose higher bioaccumulation risks to wildlife compared to shorter-chain PFAS. These long-chain PFAS, once accumulated in organisms, can transfer and magnify between trophic levels through the food web (Fang et al., 2014). As a result of their bioaccumulation potential, long-chain PFAS have been the most extensively studied to date, particularly PFOA and PFOS. Research on PFOA and PFOS have shown that they are both toxic to laboratory animals, causing adverse effects on reproduction, development, and systemic health (Cooke, 2017). However, PFAS bioaccumulation varies significantly among different species, even among mammals. Pizzurro et al (2019) reviewed the half-lives of several PFAS in monkeys, rodents, and humans, indicating that PFAS persist much longer in humans than in the other two species. The half-lives of PFHxS, PFOA and PFOS are 2.3-15.5 years in humans, 20-200 days in monkeys, and 1.9 hours-83 days in rodents. The half-lives of C4 PFAS, such as PFBA and PFBS, are much shorter, remaining in human and monkeys for only a few days and in rodents just hours (Pizzurro et al., 2019).

Currently, studies on the health effects of PFAS in humans primarily focus on long-chain PFAS due to their ability to bioaccumulate in human body. A study by Calafat et al. (2007) estimated that long-chain PFAS, including PFOS, PFOA, PFHxS and PFNA, were present in the serum of more than 98% of U.S. population (Calafat et al., 2007). PFAS can accumulate in humans for years and disrupt normal physiological functions. Human epidemiological studies have identified associations between PFOA/PFOS exposure and a series of diseases, such as high cholesterol, thyroid disorders, pregnancy-induced hypertension, testicular and kidney cancers, and endocrine disruption (Cooke, 2017). Since the phase-out of long-chain PFAS, their concentrations in the general population have been decreasing over the past two decades. Calafat et al. (2007) compared PFAS concentrations in the serum of participants between 1999-2000 and 2003-2004, finding significant decreases of approximately 32%, 25%, and 10% for PFOS, PFOA and PFHxS,

respectively (Calafat et al., 2007). Jain (2018) investigated the concentration levels of more long-chain PFAS in the U.S. population from 2003 to 2014, observing declines of 27% for PFOA, 75% for PFOS, 32% for PFDA, 27% for PFHxS, and 30% for PFNA (Jain, 2018). Despite the considerable decline in legacy PFAS concentrations in the U.S. population following discontinued production, they are still detectable in the blood of general populations in recent years (Yu et al., 2020). Moreover, low levels of short-chain PFAS, such as PFBA, PFBS, PFHxA, have been frequently detected in human blood after replacing long-chain PFAS (Nilsson et al., 2013; Poothong et al., 2017; Song et al., 2018). Although short-chain alternatives are considered to have lower bioaccumulation potential, the lack of understanding regarding their toxicity profile in human body remains a challenge for scientists.

1.7 PFAS Regulations

Over the past twenty years, the federal government has taken actions to regulate PFAS production and address PFAS contamination to protect humans and the environment. The United States Environmental Protection Agency (USEPA) began working with PFAS manufacturers and processors in 2000 to eliminate long-chain PFAS. Between 2000 and 2008, the 3M company completed the phase-out of PFOS, PFOA and POSF-related chemicals (3M, 2000; USEPA, 2017). In 2006, USEPA initiated the PFOA Stewardship Program, aimed at regulating the long-chain PFAS production by eight major manufacturing companies (Arkema, Asahi, BASF Corporation, Daikin, 3M/Dyneon, Dupont and Solvay Solexis) (USEPA, 2006). From 2010 to 2015, all eight companies successfully achieved the goals, meeting a 95% reduction of PFOA and its precursors by 2010, and completed elimination by 2015 (USEPA, 2017).

To complement the PFOA Stewardship Program, the USEPA issued several versions of Significant New Use Rules (SNUR) under the Toxic Substances Control Act (TSCA) to regulate

any future use or production of certain PFAS. SNUR requires PFAS manufacturers and processors to notify the EPA before commercializing these PFAS and related products. In March 2002, the first SNUR was published, including 13 PFAS that were voluntarily phased out by 3M between 2000 and 2002. In December, a SNUR for an additional 75 PFAS was issued. In October 2007, the EPA finalized the third SNUR for another 183 PFAS. In 2013, a SNUR for new uses of certain PFOA-related chemicals in carpets production was issued. The latest SNUR, proposed in January 2015 and finalized in July 2020, required manufacturers (including importers) to notify the EPA at least 90 days before starting to resume new uses of long-chain PFAS that had been phased out in the United States. From 2002 to the present, there has been 330 non-Confidential Business Information (CBI) PFAS chemicals reported to the EPA, and the SNURs have been supplementing and amending to improve the regulation on PFAS uses (USEPA, 2002).

In addition to restricting PFAS production and use, the EPA also has taken actions on monitoring PFAS in drinking water systems. In 1996, the EPA issued the Unregulated Contaminant Monitoring Rule (UCMR) under the Safe Drinking Water Act (SDWA) to monitor unregulated contaminants in public water systems (USEPA, 1996). In the third Unregulated Contaminant Monitoring Rule (UCMR3), published in 2012, the EPA monitored six PFAS between 2013 and 2015, including PFOS, PFOA, PFNA, PFHxS, PFHpA, and PFBS (USEPA, 2012). UCMR3 collected data of the six PFAS in approximately 6000 public water systems. As of now, no Maximum Contaminant Levels (MCLs) have been set for any PFAS. Nevertheless, the EPA has developed health advisories for PFOS and PFOA. In 2009, the EPA published the provisional health advisories of 200ng/L for PFOS and 400ng/L for PFOA (USEPA, 2009). After years of evaluating the exposure and toxicity, the EPA published the lifetime health advisory (LHA) for PFOA and PFOS in 2016, with a combined limit of 70ng/L in drinking water (USEPA,

2016). In June 2022, interim updated LHAs were issued, setting the levels at 0.004 ng/L for PFOA and 0.02ng/L for PFOS. Additionally, final health advisories for two other PFAS, PFBS and GenX chemicals, were published, with limits of 10ng/L and 2000ng/L, respectively (USEPA, 2022a). However, these LHA levels for PFAS did not serve as enforcement regulations. It was in April 2023 that the EPA took a key step to protect public health by announcing the proposed National Primary Drinking Water Regulation (NPDWR), which proposed legally enforceable levels for six PFAS: PFOA, PFOS, PFNA, HFPO-DA, PFHxS and PFBS. The regulation will be finalized and implemented by the end of 2023. Once in effect, it is anticipated to prevent thousands of deaths and reduce tens of thousands of serious PFAS-attributable illnesses (USEPA, 2023b).

The EPA, in conjunction with the Agency for Toxic Substances and Disease Registry (ATSDR), began the regulatory development process to classify PFOA and PFOS as “hazardous substances” under Comprehensive Environmental Response, Compensation and Liability Act (CERCLA), also known as Superfund. This allows the EPA to initiate the clean-up programs for contaminated sites and hold responsible parties accountable for contamination. In response to the PFAS superfund program, ATSDR developed Minimal Risk Levels (MRLs) in 2018 for PFOA, and PFOS, PFHxS and PFNA. MRLs are screening levels used to identify environmental exposures that might cause adverse health effects in humans. To evaluate drinking water exposures, ATSDR converted these MRLs to equivalent drinking water concentrations. For adults, the reference concentrations for PFOA, PFOS, PFHxS and PFNA in drinking water are 78ppt, 52ppt, 517ppt, and 78ppt, respectively. Children, who are more vulnerable from PFAS, have reference concentrations of 21ppt (PFOA), 14ppt (PFOS), 140ppt (PFHxS) and 21 ppt (PFNA). If any of the four PFAS concentrations in drinking water exceed these levels, people in the area may face health risk from PFAS contaminants (ATSDR, 2018; USEPA, 2019).

Outside the United States, PFAS regulations vary by countries. In Canada, the maximum acceptable concentration (MAC) for PFOS and PFOA in drinking water is 600ppt and 200ppt, respectively. In Australia, drinking water guidelines are 70ppt for PFOS and PFHxS, and 560ppt for PFOA. In Europe, PFOS drinking water guidelines are 90ppt in Sweden, 100ppt in Denmark, 530ppt in the Netherlands (for surface water used for drinking), 100-500ppt for different populations in Germany, and 100ppt in the United Kingdom (Seow et al., 2020).

1.8 Analytical Approaches

Analytical approaches for PFAS detection and monitoring have evolved over time. As PFAS are widely distributed in the environment at trace amounts, accurate and sensitive methods are necessary to capture, identify and quantify the broad range of PFAS. The development of advanced analytical instrumentation techniques since the 1990s has enabled the detection of PFAS in the environment at low concentrations (Pitt, 2009). Presently, analytical methods for PFAS can be divided into two primary categories: total fluorine methods and liquid/gas chromatograph coupled with mass spectrometry methods.

1.8.1 Total Fluorine (TF)/ Total Organofluorine (OF) Methods

TF/TOF Analysis is a non-specific analytical approach used for quantifying the total mass of fluorine or organofluorine in environmental and biological samples. TF is the sum of inorganic fluorine (IF) and organofluorine (OF). Although these methods cannot separate and analyze individual PFAS, they offer several advantages, such as cost-effectiveness, rapid analysis, and the ability to capture all fluorine in the samples, including known and unidentified PFAS. These methods can be performed together with solid phase extraction (SPE) as a pretreatment step for samples, providing a rapid screening test for total PFAS in various sample types. This approach helps identify samples with high levels of PFAS and offer valuable information for subsequent

analysis using more specific techniques, such as Liquid/Gas chromatography-Mass Spectrometry (LC/GC-MS) methods. Some common TF/OF methods include Particle-induced gamma ray emission (PIGE) spectroscopy, Fluorine-19 nuclear magnetic resonance spectroscopy (^{19}F NMR), Instrumental neutron activation analysis (INAA), Combustion ion chromatography (CIC), High-resolution molecular absorption spectrometry (HR-MAS), X-ray fluorescence spectrometry (TXRF), Total oxidizable precursor assays (TOP), and others.

CIC is commonly used for measuring halogens (F, Cl, Br and I) and Sulphur in all types of combustible samples. The extractable organic fluorine (EOF) assay using CIC has been applied to a wide range of samples, including surface water (Koch et al., 2019; Koch et al., 2021), sediment (Codling et al., 2014; Yeung et al., 2013), and biological samples (Koch et al., 2019; Miaz et al., 2020). In CIC, samples are combusted at high temperatures, generating combustion products. The gaseous portion of these products is collected using absorption solvents and subsequently analyzed through ion chromatography. To improve sensitivity, extraction or fractionation procedures are typically performed before the EOF assay to remove impurities. For example, the chloride content in the samples may replace the fluoride ions and interfere the chromatography peak of fluorine (Koch et al., 2020). Additionally, the CIC method can also directly measure TF without destructing the samples.

The TOP assay is the most selective non-specific method, capable of quantifying the total amount of PFAA precursors by comparing the PFAS content before and after oxidization of the samples. This assay provides information on the total PFAA precursors content (including unidentified precursors) and the carbon chain length of these precursors. The TOP assay is commonly used for aqueous samples, such as water samples (Houtz et al., 2018; Martin et al., 2019).

The ^{19}F NMR method is used for analyzing organofluorine compounds by identifying variations in chromatography associated with the chemical shift of CH_3 groups. This technique can provide structural information of organic fluorine chemicals and determine the degree of branched isomers (Guy et al., 1976; Moody et al., 2001).

PIGE is a non-destructive analytical method for total fluorine with low matrix effects and good sensitivity (ppm levels). This approach is often combined with LC-MS or GC-MS for analyzing target-PFAS in solid materials, such as food packaging, textiles and papers (Ritter et al., 2017; Robel et al., 2017; Schaidler et al., 2017). With little to no sample pretreatment required, PIGE is a promising method for field-screen PFAS in solid-phase samples. However, due to its maximum penetration depth of $250\mu\text{m}$, this method is not suitable to environmental water samples (Koch et al., 2020).

In published research to date, CIC and TOP are the most applied for non-specific PFAS analysis. The ^{19}F NMR and PIGE methods show promise for rapid screening before target PFAS analysis. INAA, HR-MAS, TXRF and other TF methods are widely applied in chemistry, but there are few publications using them for PFAS analysis. These non-specific methods offer the most economical and efficient way to measure the total fluorine weight of samples (including unknown and uncaptured PFAS) and can be performed before specific methods to improve the accuracy of results.

1.8.2 Advanced Analytical Techniques

Chromatography Techniques

Chromatography is a critical technique for sample separation in PFAS analysis, which includes liquid chromatography (LC) and gas chromatography (GC). Chromatography techniques

effectively separate mixtures of chemicals based on their differing migration speeds through a stationary phase (solid) while being carried by a mobile phase (liquid or gas).

LC encompasses high performance liquid chromatography (HPLC), ultra-high-performance liquid chromatography or ultra-performance liquid chromatography (UHPLC/UPLC), and capillary liquid chromatography (CLC). The mixture of chemicals is carried by an organic solvent to the LC column and separated through interactions between the solid stationary phase (LC column) and liquid mobile phase (chemical mixture). Fragments are separated based on their migration speed, which is determined by molecular weight, ion interactions, hydrophilicity or hydrophobicity, adsorption or desorption, or a combination of these factors (Snyder, 2009). LC is commonly used for analyzing ionic PFAS, such as PFSA and PFCA. As ionic PFAS are highly soluble in water, LC is preferred for detecting PFAS in aqueous samples (Nakayama et al., 2019a).

The separation mechanism of GC involves interactions between the solid stationary phase (GC column) and gas mobile phase. Volatile chemicals are vaporized and carried by an inert or unreactive gas, such as helium and nitrogen, into the GC column, where they are separated under specific oven temperatures (Turner, 2021). GC is predominantly used for analyzing neutral PFAS in air samples or volatile and semi-volatile PFAS in solids, such as FTOH or FASE (Nakayama et al., 2019a).

Mass Spectrometry (MS)

The principle of mass spectrometry is to generate ions from analytes and quantify the abundance of each ion based on their mass-to-charge ratio (m/z). A mass spectrometer consists of an ionization source and a mass detector. The selection of proper ionization sources is based on the inherent polarity, stability, and size of analyte molecules, which is critical for future analysis

of chemicals in mass analyzers. In ion sources, neutral analytes are desolvated and converted into molecular ions (charged) before being transferred to the mass detector. Chemical ionization (CI) and electron impact (EI) sources are commonly used in GC-MS. EI sources provide high-energy electrons that collide with the gas-phase sample and fragment the molecules, while CI is a soft ionization process that does not cause the fragmentation of molecules. Atmospheric pressure ionization (API) is another soft ionization method and is typically coupled with LC-MS for PFAS analysis. This category includes electrospray ionization (ESI), atmospheric pressure photoionization (APPI), and atmospheric pressure chemical ionization (APCI). Compared to GC-MS, an API source coupled with LC-MS can provide reliable and selective analysis for a broader range of compounds.

Electrospray ionization (ESI) is an advanced technique in mass spectrometry, facilitating the ionization and desolvation of samples. Agilent Jet Stream (AJS) technology significantly enhances sensitivity relative to standard electrospray ionization compared to the conventional ESI. This technology utilizes superheated nitrogen as a sheath gas, effectively confining the nebulizer spray and improving the desolvation process of ions. It improved ion generation and sampling efficiencies, leading to amplified signals, and minimized noise. Notably, it delivers a five-to-tenfold increase in sensitivity over traditional ESI at conventional flowrates ranging from 50 $\mu\text{L}/\text{min}$ to 2.5 mL/min . Additionally, it maintains consistent operating parameters across a broad spectrum of flow rates, reducing the need for re-optimization. The internal structure of Agilent Jet Stream Ion Source is shown in Figure 1.8. (Agilent Technologies, 2023)

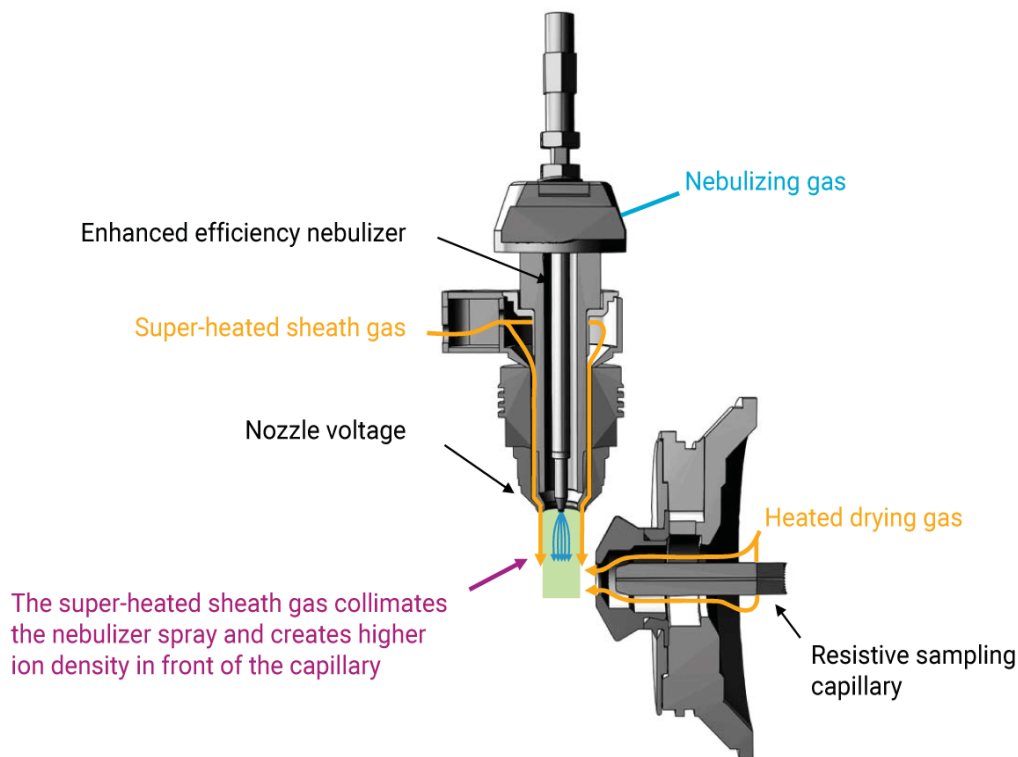


Figure 1.8 Internal structure of Agilent Jet Stream Ion Source (Agilent Technologies, 2023).

A single ionization method does not fit all chemicals; therefore, selecting a suitable ionization source based on the properties of analytes will maximize the accuracy and efficiency of the instrument. (Harrata, 1995; ThermoFisher, 2006) The comparison of different types of ionization technologies is presented in Figure 1.9.

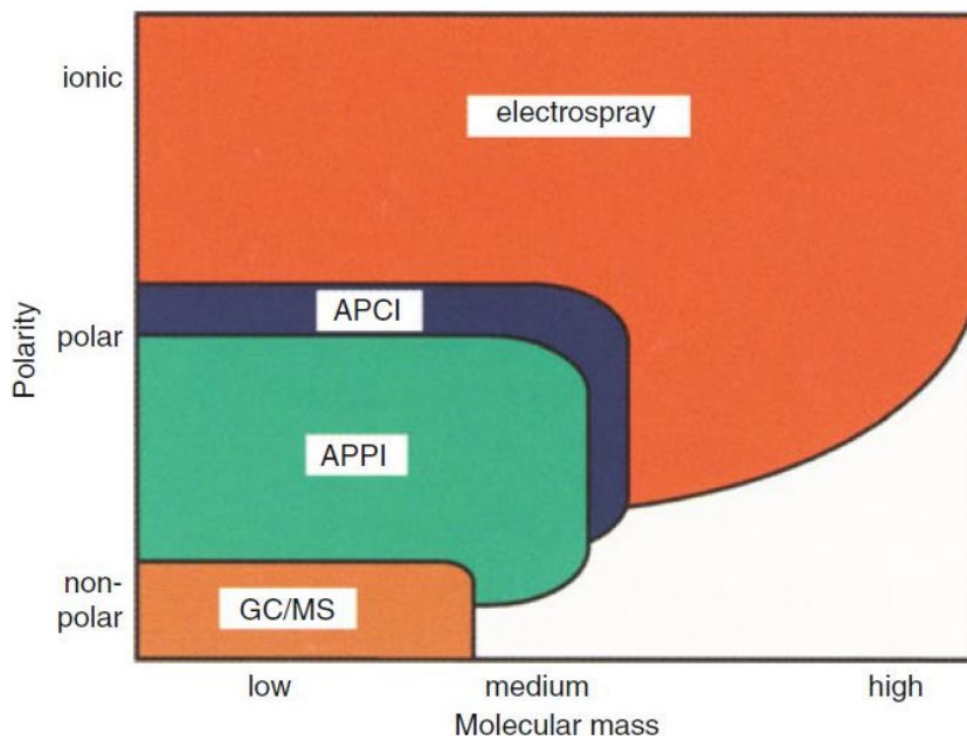


Figure 1.9 Comparison of ionization technologies (Gross, 2017).

The molecular ions are transferred into the mass detector and collided into smaller fragments (product ions); the abundance of both molecular ions and product ions are quantified here. PFAS analysis methods can be classified into target and non-target methods, depending on whether analytical standards are applied. These methods are used in different situations. The most commonly employed mass detectors for target PFAS are single and tandem mass spectrometers which are typically coupled with either an LC or GC system. These mass spectrometry systems can effectively gather mass information of specific PFAS and accurately quantify their concentrations in the sample. LC-MS/MS and GC-MS have been extensively employed in monitoring target PFAS with specific standards and reference calibrations due to their high sensitivity and selectivity of methods (Al Amin et al., 2020). The primary method of non-target PFAS identification involves applying high-resolution mass spectrometer (HRMS) technology.

HRMS instruments include Time of flight (TOF), Orbitrap and Fourier-transform ion cyclotron resonance (FTICR), which provide the possibility for unknown PFAS discovery. HRMS systems coupled with LC (LC-HRMS) can detect the formula of polar PFAS in the sample, including both known and unknown PFAS. To discover new or unidentified PFAS, LC-MS/MS systems are usually combined with LC-HRMS to analyze the portions of known PFAS and unknown PFAS separately (Yanna Liu et al., 2019).

1.9 Challenges of PFAS analysis

Analyzing PFAS compounds presents numerous challenges due to their diverse chemical properties and complex behaviors in the environment, as well as limitations associated with existing analytical approaches and sample preparation strategies.

One primary challenge in PFAS analysis is the vast number of PFAS compounds and their varied chemical properties. With over 6000 PFAS compounds estimated in total and 2060 of them found on the global market (Evich et al., 2022; KEMI, 2015), it becomes exceedingly difficult to develop a universal analytical method suitable for all PFAS. Additionally, the lack of reference standards poses a significant limitation for identifying and characterizing unknown and novel PFAS. This makes it difficult to differentiate these novel compounds from the vast array of known PFAS and other co-occurring chemicals. Consequently, researchers encounter considerable challenges when developing accurate and efficient methods for detecting and quantifying the diverse group of PFAS compounds in environment samples.

Apart from challenges arising from PFAS properties, the complexity of the environmental sample media represents another significant challenge. Environmental samples often contain complex matrices that can interfere with the analysis, impacting the reliability of the results. Minimizing matrix effects from varying samples should be considered during sample preparation.

Moreover, PFAS sometime occur at extremely low concentrations in the general environment, which requires efficient concentration strategies and highly sensitive analytical methods.

Due to the uncertainties of PFAS, the analysis processes of these chemicals are time-consuming and costly. A precise procedure, including sample collection, purification, detection, quantification, and quality control, is essential for producing reliable data. Throughout PFAS sampling and testing, multiple challenges can arise that may lead to inaccurate results or detection errors. Contamination can be introduced at any stage of the experimental process, from sampling to instrumental analysis, potentially originating from laboratory supplies containing or coated with PFAS, residual PFAS in instruments, and background contamination in calibration blanks. Maintaining the stability of targets analytes and determining their transformation pathways present another challenge, as PFAS degradation mechanisms vary under different environmental conditions. Most detectable PFAS are usually the most recalcitrant ones, such as PFAS with 4 to 8 carbons. Some of these stable PFAS transform from their precursors, with the degradation process potentially occurring during samples transport to the lab. Another analytical challenge arises from instrumental quantitative analysis, which involves effectively tracing multiple compounds, controlling the variability of environmental samples, and maximizing instrument efficiency based on limitations in resolution, sensitivity, and selectivity. Additionally, the extraction and concentration protocol of PFAS from various sample matrices can impact the results, with inefficient extraction potentially leading to low recovery rates and underestimation of PFAS concentrations.

Addressing these challenges requires the improvement of the overall understanding of PFAS properties, occurrence, and behaviors in the environment, along with advancement in analytical techniques.

1.10 Goals and Objectives

The primary focus of this study was to develop highly effective and reliable techniques for analyzing various types of per- and polyfluoroalkyl substances (PFAS) in environmental samples using the ultra-high performance liquid chromatography-tandem mass spectrometry (UHPLC-MS/MS) method. Specifically, we focused on the following PFAS classes: perfluoroalkyl carboxylic acids (PFCAs), perfluoroalkyl sulfonic acids (PFSAs), perfluoroalkyl ether carboxylic acids (PFECAs), perfluoroalkyl sulfonamides (FASAs), and perfluorooctanoic acid (PFOA) and perfluorooctane sulfonate (PFOS) isomers. These substances have been found to persist in the environment and are associated with a range of adverse health effects in humans and wildlife. Due to their ubiquitous presence in almost all environmental compartments, we have selected these groups of PFAS for method development. Our ultimate objective is to enhance the efficiency and precision of analyzing per- and polyfluoroalkyl substances (PFAS) in complex environmental samples. To achieve this, we aim to meticulously select reverse-phase analytical columns packed with sub-2- μm particles for our ultra-high-performance liquid chromatography (UHPLC) separation methods. This approach will allow us to achieve optimal separation of PFAS compounds from other interfering substances, thereby improving the sensitivity and selectivity of our analysis. In addition, we will carry out extensive testing and evaluation of various tandem mass spectrometry (MS/MS) conditions to optimize the trace-level detection of PFAS with chemical structure certainty. This will help us accurately identify the presence of even the most challenging PFAS compounds in environmental samples. Finally, we will validate and apply our developed methods for multi-class PFAS analysis in complex environmental samples and ensure their robustness for future applications. Implementing our advanced techniques for detecting per- and polyfluoroalkyl substances (PFAS) has the potential to yield significant benefits in accurately identifying their presence in the environment. This, in turn, can lead to a more comprehensive

understanding of these chemical distribution patterns and concentrations, which can guide future efforts to mitigate their harmful effects on both human health and the natural ecosystem.

1.11 Instrument Selection for This Study

The instrument used in this research is an ultrahigh-performance liquid chromatography-triple quadrupole mass spectrometry system with electrospray ionization (UHPLC-ESI-QqQ-MS/MS) (Figure 1.10). This system is preferred for detecting and quantifying target ionic PFAS. Compared to traditional LC and GC, UHPLC offers better performance, higher column efficiency, higher analytical resolution, faster detection speed, and reduced mobile phase consumption (Feng et al., 2019). The QqQ-MS/MS is an advanced tandem mass spectrometry system that enhances the selectivity and sensitivity of methods compared to single mass spectrometry (Gross, 2006). It can detect a wide range of PFAS at pg/L levels with molecular weight labeled standards. Furthermore, since most target PFAS are anionic, the JetStream electrospray ionization (ESI) on negative mode is selected to effectively ionize target PFAS for subsequent analysis in MS/MS.

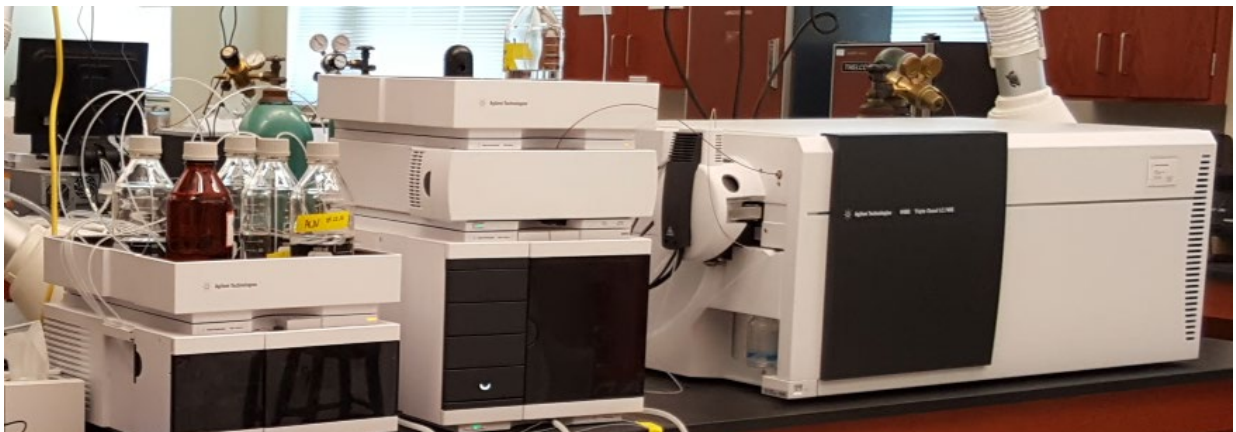


Figure 1.10 UHPLC-JetStream ESI-QqQ-MS/MS System.

Chapter 2. Detection of Perfluoroalkyl Carboxylic Acids (PFCAs), Sulfonic Acids (PFSAs), and Ether Carboxylic Acids (PFECAs) in Surface Water by UHPLC-MS/MS

2.1 Background Information

Perfluoroalkyl Carboxylic Acids (PFCAs) and Sulfonic Acids (PFSAs) are two subclasses of perfluoroalkyl acids (PFAA), which have a fully fluorinated carbon backbone connected with a carboxylic function group end ($C_nF_{2n+1}-COOH$) or a sulfonic function group end ($C_nF_{2n+1}-SO_3H$). Due to the stability of the C-F bond, these chemicals are extremely recalcitrant and unable to degrade through any biotic or abiotic process under environmental conditions. The major source of PFSA and PFCA is the long-term massive production and emission of the PFAS manufacturing and processing facilities. Before 2000, due to the lack of regulation on PFAS, these chemicals were manufactured on a large scale and unrestrictedly released into the environment. During that time, PFAS with a carbon chain greater than 8 were the dominant fluorinated chemicals that were mass-manufactured, which were primarily long-chain (C_8-C_{18}) PFAA and some of their precursors. Among them, PFOA and PFOS were the most produced PFCA and PFSA in traditional PFAS manufacturing plants. The production of long-chain PFAS lasted over five decades, until 2000, EPA started to take action on regulating long-chain PFAS. From 2000 to 2015, under the regulating actions of USEPA, major PFAS manufacturing companies discontinued the production of long-chain PFAS (USEPA, 2006) and transferred to short-chain alternatives (C_4-C_7). Massive production of PFCAs and PFSAs have been continuously discharging PFAS contaminants into the environment. In addition to directly discharging, another source of these chemicals is the transformation from their precursors, such as POSF-based and fluorotelomer-based substances, which were essential industrial materials that were produced in large scale as well. The PFCA and

PFSA detected in the environment are from either manufacturer direct discharge, or breakdown of precursors, or both.

Perfluoroalkyl ether carboxylic acids (PFECAs) represent an emerging class of PFAS characterized by a non-fully-perfluorinated backbone containing carbon-oxygen bonds. This group of chemicals presents less bioaccumulation possibility and distinct degradation behaviors compared with the full-carbon-chain PFAAs (Bentel et al., 2020), and hence were created as an alternative for traditional PFAS. Over the past decades, the use of novel perfluoroether substances has increased rapidly. Among them, HFPO-DA (commercially known as GenX) and ADONA (dodecafluoro-3H-4,8-dioxanonanoate) are two prominent perfluoroethers developed to replace PFOA since 2009. The increased use of these novel PFAS has resulted in the frequent detection of various PFECAs or other perfluoroether substances in surface water globally, including in countries such as China, the United States, the United Kingdom, Sweden, Germany, the Netherlands, and Korea (Pan et al., 2018). A study investigating PFECAs in Xiaoqing River, China, found 10 out of 11 target PFECAs present, with concentrations reaching up to 20200ng/L. Among those detected, PFECAs, PF4OPeA, PF5OHxA and HFPO-DA were found at concentrations ranging from non-detectable to 114ng/L, non-detectable to 37.2ng/L, and 1.04 to 4340ng/L, respectively (Yao et al., 2021). Additionally, the novel PFECAs have been found in residents living near fluorochemical plants, with detection in over 95% of human serum samples collected from industrial areas in China (Yao et al., 2020). This high detection frequency suggests potential health risks associated with exposure to these novel chemicals. Further studies have also found evidence of bioaccumulation and biomagnification of PFECAs in the estuarine food web (Li et al., 2023; Li et al., 2021), thereby raising concerns regarding potential health impacts from consuming contaminated aquatic products.

Scientific studies related to PFAS have escalated dramatically since the 2000s. Over the past decade, analytical approaches for PFAS were mostly focused on several long-chain PFAS, such as PFOA, PFOS and their precursor compounds, in various environmental or biological samples. Most toxicological and epidemiological studies related to PFAS were targeted to these long-chain PFAS as well. In recent years, the public's attention to emerging PFAS continues to grow. However, there is lack of systemic understanding regarding their environmental impacts, bioaccumulation risks and toxic patterns in wildlife and humans. This deficiency is primarily due to the absence of analytical approaches that can identify and quantify these PFAS in complex environmental and biological media at low concentrations. Given the recent changes within the fluorochemical industry, efficient and accurate quantitative methods that include emerging alternatives are needed to determine the distribution of these novel PFAS, and to understand their behaviors and fate in the environment. However, due to the complexity of various samples, limitations on quantification techniques and continuous development of alternatives with similar structures, there are many and ever-increasing challenges in profiling and quantifying PFAS (Nakayama et al., 2019b; Wang et al., 2017).

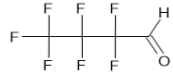

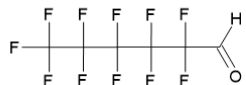

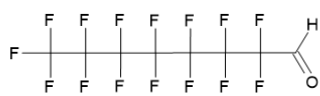
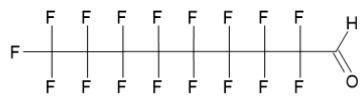

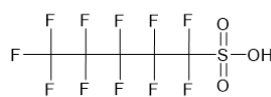




Liquid chromatography coupled to tandem mass spectrometry (LC-MS/MS) is a powerful tool that provides advanced analysis on chemical identification and quantification at low concentration levels in complex mixtures. Over recent decades, LC-MS/MS has been commonly used to analyze PFAS in environmental and biological samples due to its advanced separation capacity, high sensitivity, selectivity, and high throughput. The number of publications for analytical methods using LC-MS/MS has significantly increased in the past decade, with the methods targeting a broad range of PFAS from different subclasses across various environmental and biological matrices (Androulakakis et al., 2022; Coggan et al., 2019). This includes water

samples such as drinking water, seawater, surface water, and wastewater. For example, Coggan et al. developed a method to detect 53 PFAS from 14 compound classes in aqueous matrices (wastewater, surface water and drinking water) (Coggan et al., 2019), while Huerta et al developed a method for determining 15 PFAS with carbon chain lengths from C₅ to C₁₂ in environmental water samples (Huerta et al., 2022). However, the majority of current analytical methods primarily focus on PFAS detection at contaminated sites like wastewater treatment plants (Semerád et al., 2020), Aqueous Film-Forming Foam (AFFF) impacted areas (Barzen-Hanson et al., 2017), or fluorochemical manufacturing facility surrounding area (Meng et al., 2021). Since PFAS concentrations at these contamination sites are typically at a high level, these methods may not be directly applicable to general environmental water samples for routine monitoring and background concentration determination. The uncertainties in environmental matrices and the ever-expanding numbers of alternative PFAS cause the ongoing requirement of novel analytical methods for profiling and analyzing PFAS at trace concentrations within various environmental systems. In addition to aqueous samples, analytical methods have also been developed to identify and quantify PFAS in human and wildlife samples, different food matrices and plant tissues. Validated methods were established by researchers such as Frigerio et al. for 30 PFAS in human plasma (Frigerio et al., 2022), by Androulakakis et al. for 56 PFAS in various animal species from central and northern Europe (Androulakakis et al., 2022), by Theurillat et al. for 57 PFAS in seven different food matrices (Theurillat et al., 2023), and by Nassazzi et al for 24 PFAS in plant tissues (Nassazzi et al., 2022).

These analytical methods usually cover multiple classes of PFAS that include legacy and emerging PFAS as well as some of their precursors. Although these methods can be used in the detection of a broad range of PFAS, they are usually time-consuming and costly for

routine monitoring of PFAS in general environmental waters. Some of these long-chain PFAS and precursors are only temporarily present in waterbodies near contaminated sites, while in places away from sources, they are rarely detected. During their transport in the environmental system, these PFAS may degrade into persistent PFAS or attach to sediments and soils. To monitor the distribution of prevalent PFAS in the global general water system, a fast, economical, sensitive, and reproducible analytical method is required. The aim of this chapter is to establish a reliable analytical technique for regularly monitoring 17 commonly occurring and new PFAS in coastal surface waters in Alabama. These targeted PFAS are divided into three subclasses based on type of functional groups and carbon chain length (C₄ - C₉), namely PFCAs, PFSAs, and PFECAs. The separation and quantification of PFAS were carried out using ultra-high performance liquid chromatography coupled with a JetStream electrospray ion source (ESI) and a triple quadrupole mass spectrometry (UHPLC-QqQ-MS). Furthermore, this chapter outlines an effective method for solid phase extraction cleanup of environmental water samples and introduces a highly sensitive method development and validation procedure for the targeted PFAS. The chapter is divided into two parts; Part 1 focuses on creating a fast and efficient analytical method for emerging perfluoroalkyl ethers (PFECAs), while Part 2 combines analytical methods for perfluoroalkyl carboxylic acids (PFCAs), perfluoroalkyl sulfonic acids (PFSAs), and perfluoroalkyl ethers (PFCECAs).

Table 2.1 CAS, molecular weight and structure of the target analytes and internal standard in this study.

Chemicals	Acronym	CAS	Molecular Weight (g/mol)	Molecular Formula	
Perfluoroalkyl carboxylic acids (PFCAs)					
1	Perfluorobutyric acid	PFBA	375-22-4	214.04	
2	Perfluoropentanoic acid	PFPeA	2706-90-3	264.05	
3	Perfluorohexanoic acid	PFHxA	307-24-4	314.05	
4	Perfluoroheptanoic acid	PFHpA	375-85-9	364.06	
5	Perfluorooctanoic acid	PFOA	335-67-1	414.07	
6	Perfluorononanoic acid	PFNA	375-95-1	464.08	
Perfluoroalkane sulfonic acids (PFSAs)					
7	Perfluorobutane sulfonate acid	PFBS	375-73-5	300.10	
8	Perfluoropentyl sulfonate acid	PFPeS	2706-91-4	349.9	
9	Perfluorohexane sulfonate acid	PFHxS	355-46-4	399.9	
10	Perfluoroheptane sulfonate acid	PFHpS	375-92-8	449.9	
11	Perfluorooctyl sulfonate acid	PFOS	1763-23-1	500.13	
12	Perfluorononyl sulfonate acid	PFNS	68259-12-1	550.1	

Perfluoroalkyl ether carboxylic acids (PFECAs)					
13	Ammonium 4,8-dioxo-3H-perfluorononanoate	ADONA	958445-44-8	395.10	
14	Hexafluoropropylene oxide dimer acid	HFPO-DA (GenX)	13252-13-6	330.05	
15	Perfluoro (4-oxapentanoic) acid	PF4OPeA	377-73-1	280.04	
16	Perfluoro (5-oxa-6-methoxyhexanoic) acid	PF5OHxA	863090-89-5	380.04	
17	Perfluoro (3,6-dioxaheptanoic) acid	3,6-OPFHpA	151772-58-6	296.04	
Internal Standard					
IS	Sodium perfluoro-1-[1,2,3,4- ¹³ C ₄]octane sulfonate	MPFOS	960315-53-1	526.08	

2.2 Materials and Methods

2.2.1 Chemicals, Reagents, and Materials

The study utilized high purity perfluoroalkyl carboxylic acids (PFCAs), perfluoroalkyl sulfonic acids (PFSAs), and perfluoroalkyl ether carboxylic acids (PFECAs) procured from Wellington Laboratories in Canada. Table 2.1 presents a comprehensive list of the PFAS analytes that were targeted. VWR International in Suwanee, GA supplied the LC/MS grade solvents, including acetonitrile, methanol, and water, as well as analytical grade ammonium hydroxide and

ammonium acetate reagents. An RRHD Eclipse Plus C18 analytical column (2.1 × 100 mm, 1.8 μm, p/n 959758-902), a guard column (Agilent ZORBAX Eclipse Plus C18, 2.1 × 5 mm, 1.8 μm, p/n 821725-901), a 5M ammonium formate solution with a purity of 98.1%, and Captiva premium syringe layered filters (0.2 μm, p/n 5190-5132) were purchased from Agilent Technologies (Wilmington, DE). The Oasis WAX (6cc, 200mg, p/n 186002493) extraction cartridges and a 20-position vacuum manifold were obtained from Waters Corporation in Milford, MA, USA, while Sigma Aldrich (St. Louis, MO) supplied the Whatman glass microfiber filters (90mm, p/n 1827-090).

2.2.2 Sample Collection

For this study, surface water samples were collected from seven distinct locations within Alabama between June and September 2019. The objective of the investigation was to identify any seasonal variations in surface water quality. Duplicate water samples were collected from each location using pre-cleaned high-density polyethylene (HDPE) containers and transported in a cooler with ice at a temperature of 4°C to the laboratory to prevent any changes in water quality. The samples were brought to the laboratory and stored at -20°C until they were processed. Figure 2.1 and Table 2.2 provide detailed information about the sampling locations, including a map and coordinates.

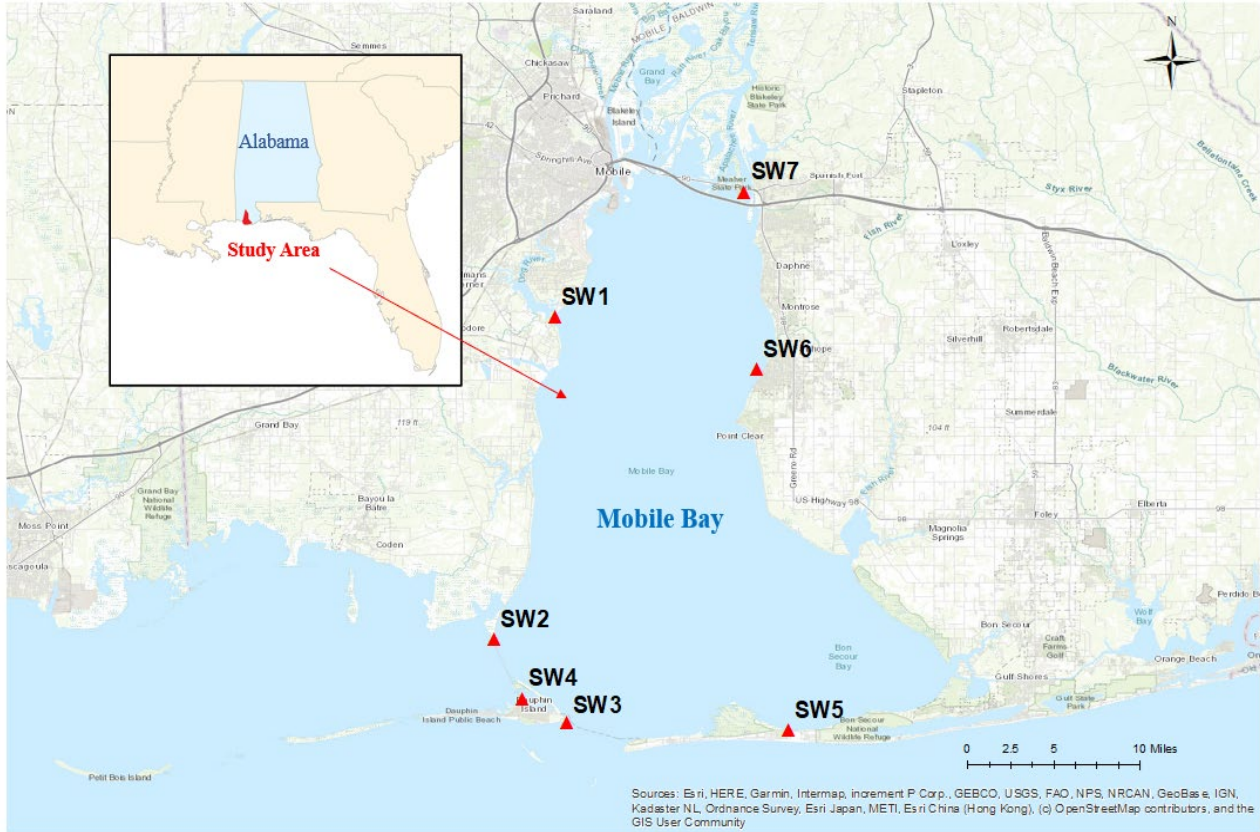


Figure 2.1 Location map for surface water (SW1-SW7) collected from Alabama.

Table 2.2 Sampling location coordinate details (SW1-SW7)

Samples	Coordinates		Location	Time			
	Lat	Long		June	July	August	September
SW1A	30.5673	-88.0869	Dog River, Mobile, AL	6/27/2019 11:15am	7/31/2019 11:45am	8/31/2019 3:00pm	9/21/2019 12:50pm
SW2A	30.3114	-88.138	Mobile Bay, Coden, Mobile, AL	6/27/2019 11:50am	7/31/2019 12:20pm	8/31/2019 3:40pm	9/21/2019 2:15pm
SW3A	30.2457	88.0773	Gulf of Mexico, Dauphin Island, Mobile, AL	6/27/2019 12:30pm	7/31/2019 1:00pm	8/31/2019 4:00pm	9/21/2019 3:00pm

			Dauphin Island Bay, Dauphin Island, Mobile, AL	6/27/2019 12:15pm	7/31/2019 12:35pm	8/31/2019 3:50pm	9/21/2019 2:30pm
SW4A	30.2642	- 88.1143					
			Bon Secour Bay Hwy 180, Fort Morgan, Baldwin, AL	6/27/2019 2:50pm	7/31/2019 2:00pm	8/31/2019 5:10pm	9/21/2019 5:45pm
SW5A	30.2393	- 87.8902					
			Mobile Bay, Fairhope, Baldwin, AL	6/27/2019 9:24am	7/31/2019 10:00am	8/31/2019 1:45pm	9/21/2019 11:50am
SW6A	30.5258	-87.917					
			Blakeley River, Spanish Fort, Baldwin, AL	6/27/2019 10:15am	7/31/2019 11:00am	8/31/2019 2:20pm	9/21/2019 11:00pm
SW7A	30.6663	- 87.9273					

2.2.3 Sample Preparation- Solid Phase Extraction (SPE)

Water samples were thawed at room temperature and filtered through a GE Whatman glass microfiber filter using a micro-filtration assembly under vacuum to remove all the suspended solid particles. The sample filtration process was repeated twice for each sample. The filtered water samples were cleaned up using the solid phase extraction (SPE) method. Prior to the SPE, the pH of the samples was tested using the pH testing paper and adjusted to an appropriate pH value (around 6.5). Adjusting the pH is crucial for the effectiveness of the SPE process to achieve optimal recovery of the target analytes. Solid phase extraction (SPE) purification was then conducted using Waters Oasis WAX cartridges (150mg, 6cc) on a Waters 20-position vacuum manifold. Before sample loading, cartridges were pre-conditioned with 4mL of 0.1% ammonium hydroxide in methanol, 4mL methanol, and 4mL LC-grade water. Each 500 mL filtered water sample, pre-spiked with 5ng MPFOS as an internal standard, was loaded onto the cartridges at a controlled rate of one drop per second, ensuring target analytes were retained on the cartridge until the water fraction was eluted. Post-sample loading, cartridges were rinsed with 4mL of a pH4 LC water

buffer containing 25 mM ammonium acetate to remove potential impurities. Target analytes were subsequently eluted using a two-step process with 4mL of 0.1% ammonium hydroxide in methanol, followed by 4mL methanol. Both fractions were combined and filtered through 0.2 μ m glass fiber nylon membrane filters. The extracts were concentrated under vacuum and were analyzed using UHPLC-MS/MS.

2.2.4 Preparation of Working PFAS Standard Solutions

To prepare PFAS stock solutions, high-purity analytical standards of each target analyte were diluted in a solvent mixture of methanol and water (9:1, v/v) until the desired concentration of μ g/mL was achieved. Independent stock solutions of 0.1 μ g/mL and 0.01 μ g/mL were prepared for each target PFAS. An internal standard solution was also prepared in methanol at a concentration of 0.1 μ g/mL. To create seven levels of calibration solution mixtures, the stock solutions were diluted in a mixture of methanol and water (9:1, v/v) to achieve a concentration ranging from 0.05- 50 ng/mL. A seven-point calibration curve was developed for quantitation purposes.

2.2.5 UHPLC-MS/MS Method Development

A methodology for the detection of specific PFAS was developed using an Agilent Technologies UHPLC-ESI-MS/MS system. The system comprises a 1290 Infinity II UHPLC system, a 6460 Triple Quadrupole MS, and a Jet Stream ESI source. Different C₁₈ analytical columns and mobile phase combinations with modifiers such as acetonitrile, methanol, and water were tested to separate the target analytes. Parameters such as flow rate, injection volume, and column temperature were optimized through chromatography experiments. Chromatographic separation for PFECAs was achieved using an Agilent RRHD Eclipse Plus column and a gradient elution method. Ammonium formate was used as a solvent modifier to achieve maximum peak

resolution. The mass spectrometry conditions, and ionization source parameters were also optimized through various experiments such as full (MS²) scan, single ion monitoring (SIM) scan, product ion (PI) scan, and multiple reaction monitoring (MRM). Both negative and positive ionization modes were employed to determine the best conditions such as collision cell energy, fragmentor voltage, MRM transition for each target PFAS, cell accelerator voltage, delta EMV, gas temperature and flow, sheath gas temperature and flow, nebulizer pressure, capillary voltage, and nozzle voltage. These experiments were essential to ensure the accuracy and reliability of the results obtained.

Full Scan/MS² Scan Analysis

To identify the precursor/molecular ion of the target analytes, a full scan analysis was conducted. Each group of analytes was scanned individually across a wide mass range (50-2000) using a 0.1 µg/mL stock solution. The initial fragmentor voltage was set at 100V. The appropriate scan mode was determined by comparing peak responses in dual scan mode, ultimately selecting the negative scan mode.

Single Ion Monitoring (SIM) Scan Analysis

In order to find the best voltage for detecting a specific substance, known as the target analyte precursor ion, Single Ion Monitoring (SIM) scan experiments were conducted at different fragmentor voltages. This technique is more sensitive than a full scan analysis because it only looks at a narrow range of mass. For PFAS, the SIM experiments at various fragmentor voltages (FV) for each precursor ion, ranging from 60-200V were tested. SIM scan analysis was performed at 0.1 µg/mL stock solution to confirm the molecular ions and identify the best fragmentor voltage for each target.

Product Ion (PI) Scan Analysis

Conducting product ion scan experiments can provide valuable information about the structure of a particular target analyte. By subjecting precursor ions obtained from SIM scan experiments to PI scan using a broad range of collision cell energies (0 to 60eV) and selective fragments, we can obtain specific information about chemical structure. In this study, PI scan analysis was conducted on each PFAS at 0.1 μ g/mL to determine the most abundant product ions and their corresponding collision cell energies. Performing these experiments can help identify the chemical structure of a substance with a high degree of certainty.

Multiple Reaction Monitoring (MRM) Analysis

The Multiple reaction monitoring (MRM) method is a highly sensitive and selective mass spectrometric technique. MRM experiments combined and integrated all optimized parameters derived from previous analyses, including molecular ions with optimized fragmentor voltage, the major product ions, and their corresponding collision cell energies. The MRM technique enables the specific detection and quantification of target analytes at trace levels, leading to improved accuracy and sensitivity in the analysis of target compounds in complex environmental samples. Method optimization was achieved with 0.01 μ g/mL PFAS stock solutions. To enhance the sensitivity of PFAS analysis, a series of optimizations were performed on several key parameters. Specifically, gas temperature, gas flow, nebulizer pressure, nozzle voltage, and capillary voltage were carefully adjusted using MRM parameters to achieve the desired outcome. This meticulous approach ensured that the analysis was as accurate and effective as possible, allowing for the detection of even the most minute traces of PFAS.

2.2.6 Method Validation

The developed quantitative method was evaluated for its specificity, linearity, sensitivity, precision, accuracy, and recoveries. Method specificity was tested by monitoring target analyte in spiked matrix sample with those of solvent banks. A calibration curve was developed for target PFAS, and its accuracy and linearity were assessed at concentrations ranging from 0.05 to 50 ng/mL. Method sensitivity was assessed by measuring the limit of detection and limit of quantitation recommended by validation guidelines. Accuracy and precision were determined by analyzing spiked samples at different concentrations at different days. Method recovery and matrix effects were assessed by analyzing blank matrix samples before and after spiking with target PFAS.

2.3 Results and Discussion

2.3.1 Part 1. Rapid UHPLC-MS/MS Method for Perfluoroalkyl Ethers (PFECAs)

Analytical grade PFECA stock solutions were accurately weighed and dissolved in methanol and water (9:1, v/v) to achieve mg/mL concentration. Working solutions were prepared by diluting stock solutions in methanol and water (8:2, v/v) to obtain 0.1 and 0.01 µg/mL concentrations for method development. All analytes were analyzed using a full scan (MS2 Scan) at a 0.1 µg/mL concentration to obtain selective precursor ions in negative and positive ionization modes. Optimal Fragmentor voltage (FV) conditions were obtained through single ion monitoring (SIM) ion scan experiments with 60 to 200 V. PI scan experiments with collision cell energies (CEs) ranging from 0 to 60 eV were conducted to identify product ions specific to each analyte structure. Optimal fragmentor voltage and CE conditions for perfluoro(4-oxapentanoic) acid **1**,

perfluoro (5-oxa-6-methoxyhexanoic) acid **2**, and perfluoro(3,6-dioxahexanoic) acid **3** are presented in Figures 2.2 and Figure 2.3.

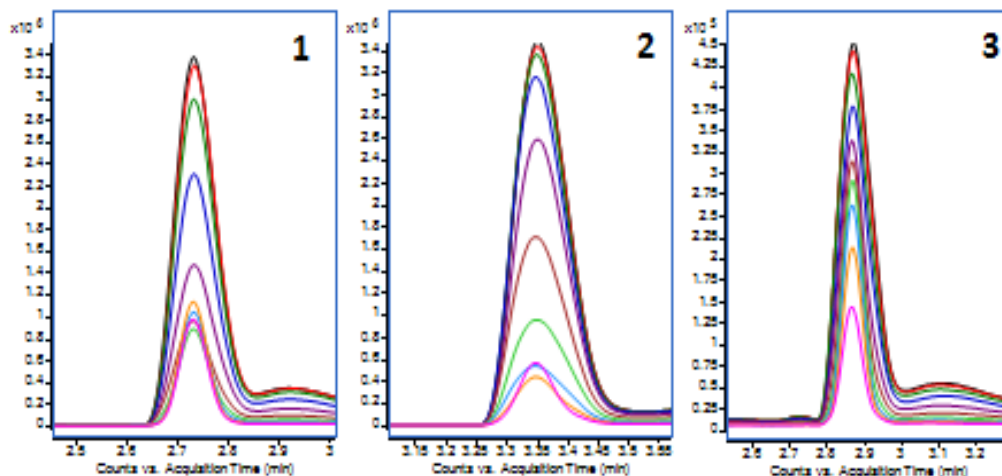
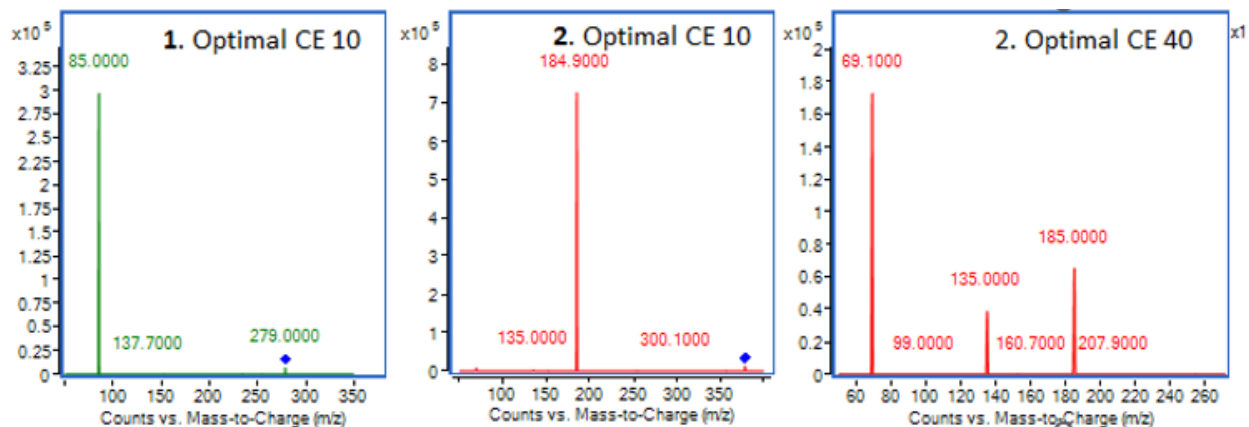


Figure 2.2 Optimal FV (60 V) for perfluoro(4-oxapentanoic) acid 1, perfluoro (5-oxa-6-methoxyhexanoic) acid 2, and perfluoro(3,6-dioxahexanoic) acid 3.



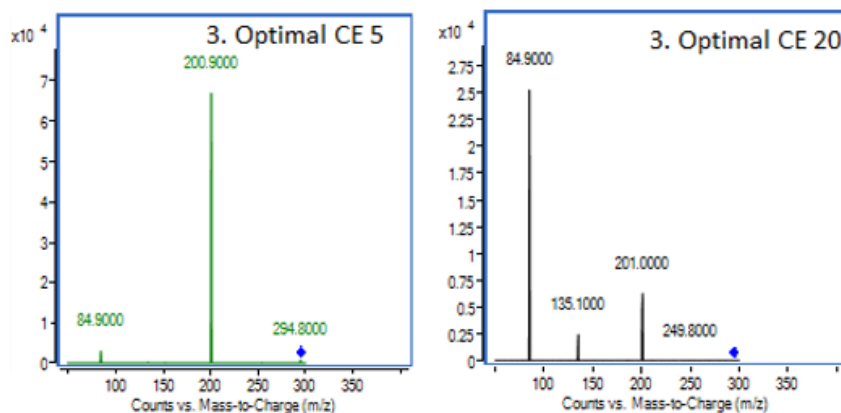


Figure 2.3 PI spectra with optimized collision cell energies (eV) for ethers 1-3.

Selective precursor and product ions for each analyte with optimal method conditions were obtained before setting up MRM experiments. The total run time analysis was 7 minutes, with samples sent to the detector from 2 to 4.5 minutes for analysis (Figure 2.3) dwell time, cell accelerator voltage, and capillary voltage conditions were optimized for MRM method development. Different concentrations of test solutions for the internal standard (M3HFPO-DA) were evaluated to achieve relevant spike concentrations in quantitative analysis. Quantitation was performed using M3HFPO-DA as an internal standard at 1 ng/mL concentration. Agilent Qualitative and Quantitative software version B.3.0 was used for data analysis. Optimal UHPLC-MRM conditions are summarized in Table 2.3a & 2.3b.

Selective precursor and product ions for each analyte with optimal method conditions were obtained before setting up MRM experiments. The total run time analysis was 7 minutes, with samples sent to the detector from 2 to 4.5 minutes for analysis (Figure 2.4).

Table 2.3a UHPLC-MRM conditions optimized for the analysis of PFECAs.

	Analyte	Precursor ion m/z	Product ions m/z	Fragmentor voltage (v)	Dwell time (ms)	Collision energies (eV)	Polarity
1	Perfluoro (4-oxapentanoic) acid	278.9	235.0/84.9	60	20	10/10	Negative
2	Perfluoro (5-oxa-6-methoxyhexanoic) acid	378.9	184.9/134.9/69.0	60	20	10/30/40	Negative
3	Perfluoro (3,6-dioxahexanoic) acid	295	200.9/84.9	60	20	5/20	Negative
4	NaDONA	376.9	250.9/184.9	80	20	10/30	Negative
5	HFPO-DA (GenX)	328.9	284.9/169.0	70	20	5/15	Negative
6 (IS)	M3HFPO-DA (IS)	332	287	70	20	5	Negative

Table 2.3b UHPLC-MRM conditions optimized for the analysis of PFECAs.

Optimized UHPLC-MRM Conditions for target analyte analysis	
UHPLC Condition	
Analytical Column	Agilent RRHD Eclipse Plus C18 (2.1×100mm, 1.8µm, p/n 959758-902)
Mobile phase	A. 5mM ammonium formate in water B. 95% methanol, 5% water
Gradient method conditions	Time (min), B% 0 (30); 0.2 (30); 0.5 (70); 6 (80); 6.2 (99); 6.5 (99); 7 (30)
Post run	3 min
Total run time analysis	7 min
Column temperature	40°C
Injection volume	5µL
Gas temperature	225°C
Gas low	10L/min
Nebulizer	45 Psi
Sheath gas temperature	350°C
Sheath gas flow	11 L/min
Capillary voltage	3600
Nozzle voltage	1500
Delta EMV	400 v
Cell acceleration voltage	4 v
MS1 and MS2 resolution	Unit
Ionization mode	Negative

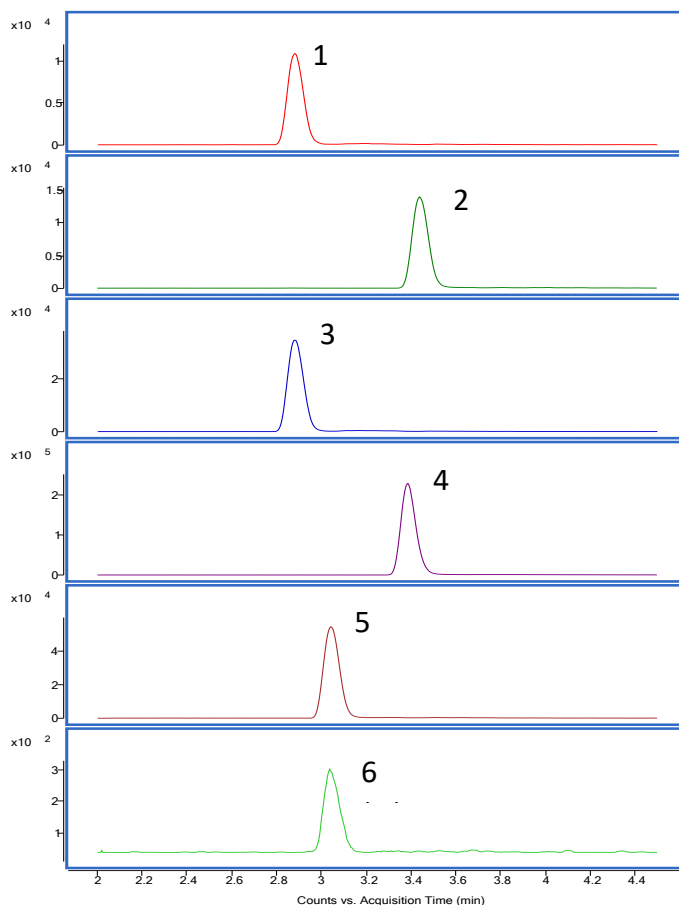


Figure 2.4 Extracted UHPLC-MRM chromatograms of compounds 1-6.

Calibration curves were established for each analyte with concentrations ranging from 0.1 to 25 ng/mL (Figure 2.5). Calibration curves show good linearity with regression (r^2) values >0.99 . To determine the limit of detection (LOD) and limit of quantification (LOQ), signal-to-noise ratios of 3 and 10 were used, respectively. The LOD values achieved for analytes 1-5 in the current method are 0.18, 0.15, 0.14, 0.15, and 0.19 pg/injection, respectively. The LOQ values for 1-5 are 0.60, 0.49, 0.46, 0.49, and 0.62 pg/injection, respectively. In conclusion, a surrogate ethers-based quantitative method was developed to monitor and quantify PFECAs in various environmental media. This is the first UHPLC-MRM method developed for some ethers using triple quadrupole

mass spectrometry. The developed method is employed in laboratory and field studies to help understand PFECA sorption behavior and bioaccumulation potential.

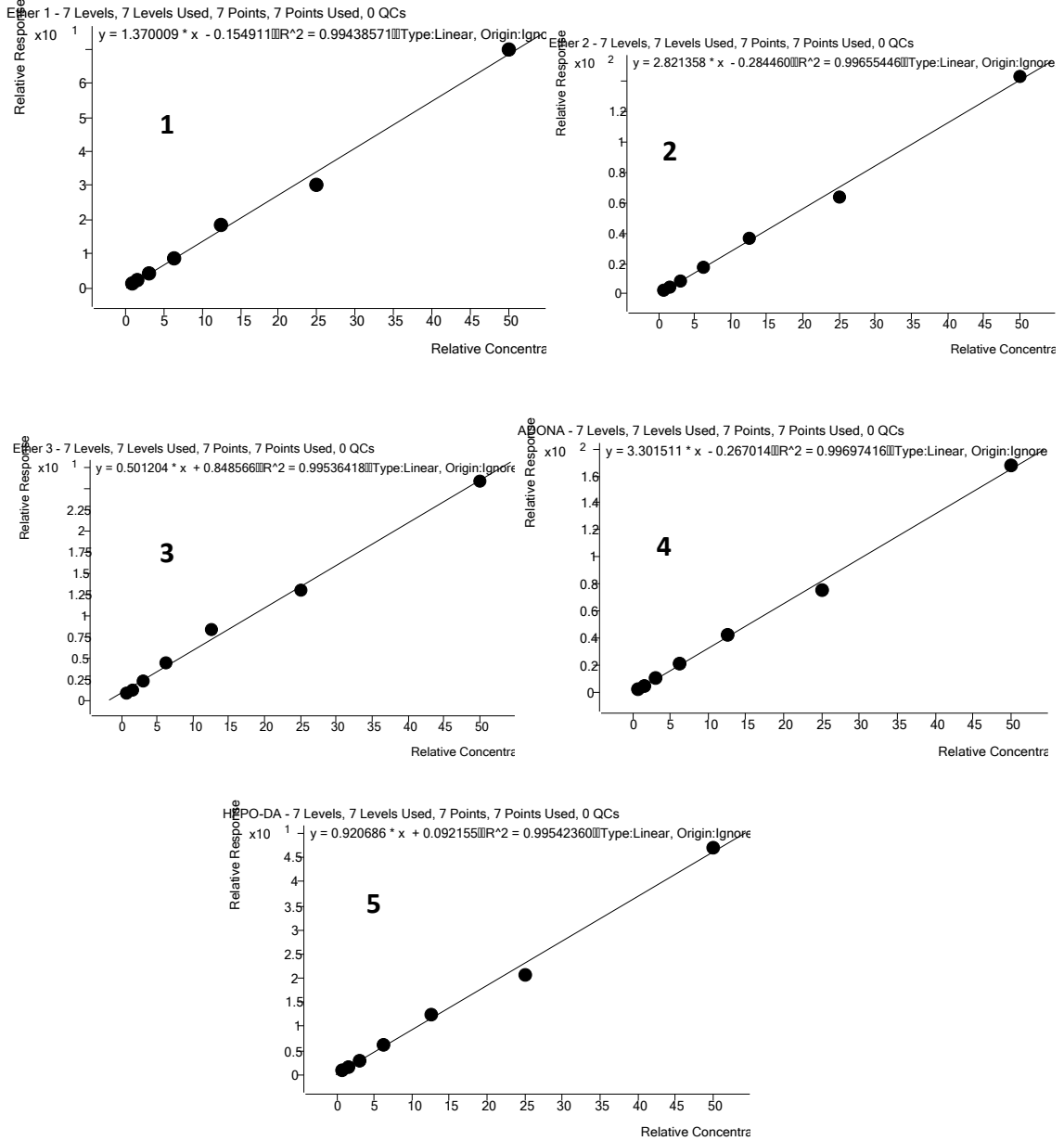


Figure 2.5 Calibration curves developed for PFECAs.

2.3.2 Part 2. UHPLC-MS/MS Quantitative Method for 17 PFAS

Optimization of UHPLC-MS/MS Conditions for PFCAs, PFSA and PFECAs

This part of work was planned to improve the sensitivity and reliability of the UHPLC-MS/MS method for analyzing PFAS in complex environmental water samples. We modified the analytical method published by Mulabagal et al. (2019) to ensure its efficiency before applying it to surface water samples. While running large batch samples using the old method over a period, we noticed a problem with using methanol as a mobile phase in UHPLC/MS, resulting in frequent back pressure on the column. Methanol consistently produced higher back pressures than other solvents (Smith et al. 2015). We used nano bore column components and solvents that could withstand high pressures during continuous analysis to overcome this issue. After conducting extensive tests using acetonitrile and methanol/acetonitrile as mobile phase solvents, we ultimately chose acetonitrile as the organic mobile phase. This enabled us to optimize the separation efficiency without compromising the symmetry or sensitivity of PFAS peaks during large batch analysis, and without any column backpressure issues. Total run time of analysis was 9 min and target PFAS were separated within five minutes of run time analysis with gradient mobile phase. The extracted UHPLC-MRM Chromatograms for target PFAS are presented in Figure 2.6. The UHPLC mobile phase composition and conditions optimized were summarized in Table 2.4. The injection needle of the multi-sampler was rinsed with a mixture solution of methanol, acetonitrile, and water (40/40/20, v/v) to prevent any target compound carryover during analysis and reduce contamination. Also, MS/MS source conditions and MRM parameters for PFAS (Table 2.4) are revised to achieve better peak sensitivity with low detection limits in this method. Also, we have revised MS/MS conditions and MRM parameters for PFAS to achieve better sensitivity with low detection limits in this study. Optimal ionization conditions were achieved by utilizing the following settings: a gas temperature of 225°C, a gas flow rate of 10mL/min, a nebulizer pressure of 45psi, a sheath gas temperature of 350°C, a sheath gas flow rate of 11mL/min, a capillary

voltage of 3600V, and a nozzle voltage of 1500V. Details of MS/MS parameters, including delta EMV and cell acceleration voltage were shown in Table 2.5. In the conducted research, a highly effective MRM method was utilized to optimize MRM parameters for emerging perfluoroalkyl ethers (PFECAs) such as PF4OPeA, PF5OHxA, and 3,6-OPFHpA. This was achieved through various scan experiments using the UHPLC-QqQ-MS/MS system coupled with Agilent JetStream ESI. The outcome of the study was noteworthy, as it provided valuable insights into the behavior and characteristics of PFECAs. In the conducted research, a highly effective MRM method was utilized to optimize MRM parameters for emerging perfluoroalkyl ethers (PFECAs) such as PF4OPeA, PF5OHxA, and 3,6-OPFHpA. This was achieved through various scan experiments using the UHPLC-QqQ-MS/MS system coupled with Agilent JetStream ESI. The outcome of the study was noteworthy, as it provided valuable insights into the behavior and characteristics of PFECAs.

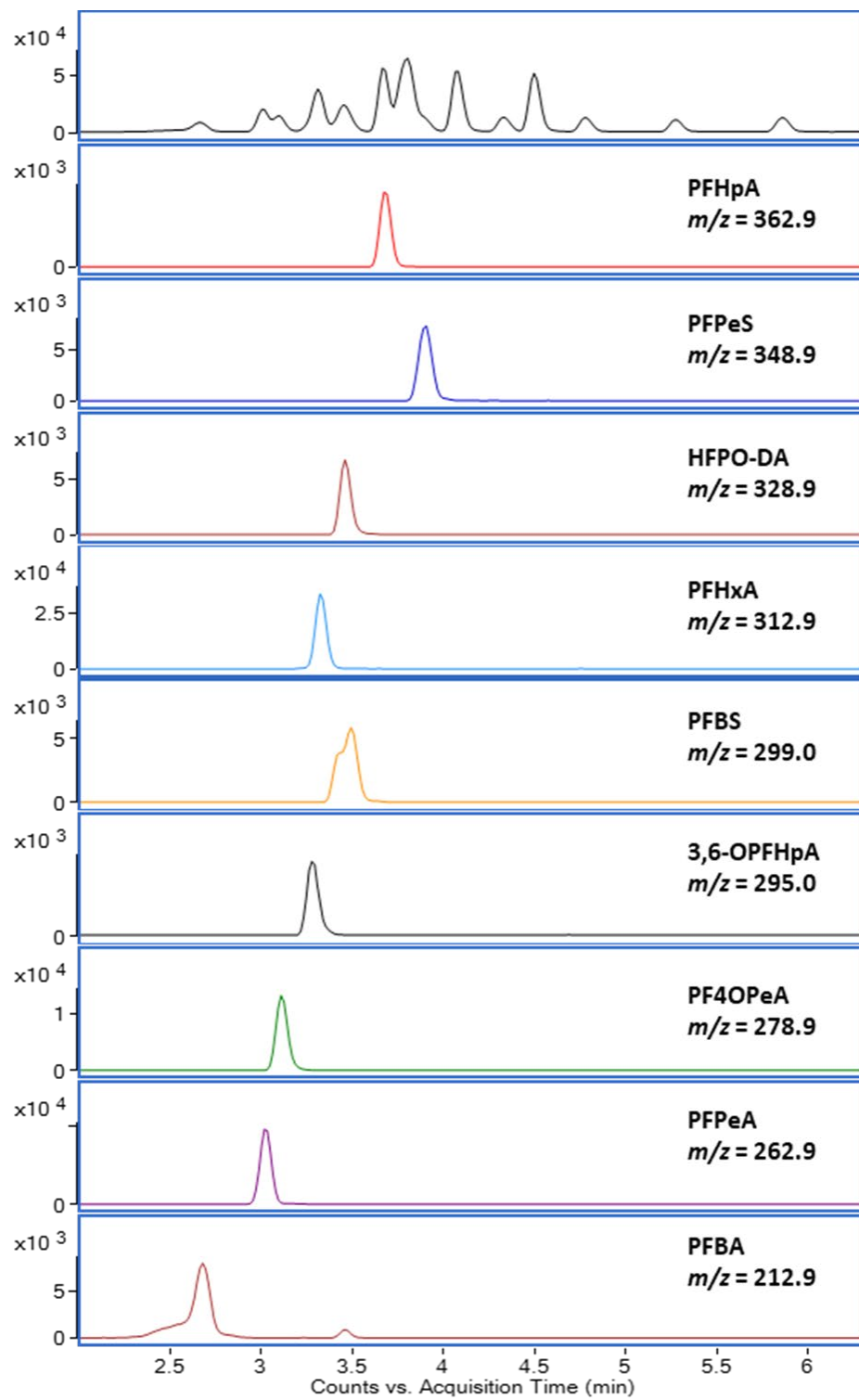


Figure 2.6 Extracted UHPLC-MRM Chromatograms for target PFAS.

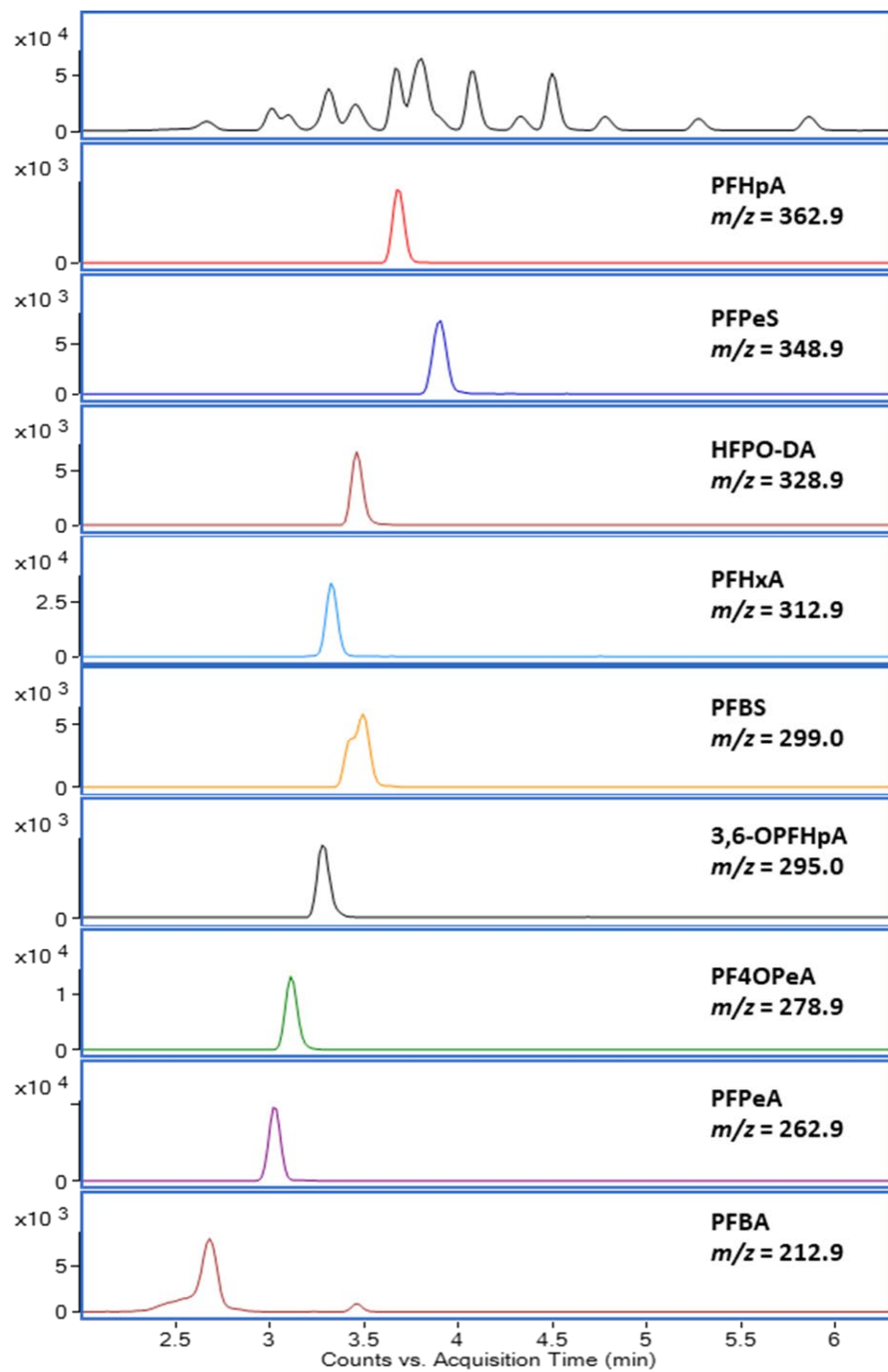


Figure 2.6 Extracted UHPLC-MRM Chromatograms for target PFAS. (continued)

Table 2.4 Optimized UHPLC-MRM Conditions for target PFAS analysis.

UHPLC Conditions	
Pump	Agilent Infinity 1290 II
Analytical column	Agilent RRHD Eclipse Plus C18 (2.1 × 100 mm, 1.8 μm, p/n 959758-902)
Guard column	Agilent ZORBAX Eclipse Plus C18 (2.1 × 5 mm, 1.8 μm, p/n 821725-901)
Mobile phase	A. 5mM ammonium formate in water/acetonitrile (95/5, v/v) B. acetonitrile/water (95/5, v/v)
Gradient method conditions	Time (min), B% 0 (20); 0.5 (20); 1 (40); 2 (50); 3 (60); 5 (70); 7 (80); 8 (99); 8.5 (99); 8.8 (20); 9 (20)
Post run	2 min
Flow rate	0.2mL/min
Total runtime	9 min
Column temperature	40 °C
Injection volume	10 μL
Injection part wash solvent	Methanol/acetonitrile/water (40/40/20, v/v)
MS/MS Conditions	
Gas temperature	225 °C
Gas flow	10 L/min
Nebulizer	45 Psi
Sheath gas temperature	350 °C
Sheath gas flow	11 L/min
Capillary voltage	3600V
Nozzle voltage	1500V
Delta EMV	400V
Cell acceleration voltage	4
MS1 and MS2 resolution	Unit/wide
Ionization mode	Negative

Table 2.5 Optimized MRM parameters for target PFAS.

Target Analytes	Retention Time (min)	Precursor Ion (m/z)	Product Ions (m/z)	Fragmentor Voltage (V)	Collision Energy (eV)
1 PFBA	2.307	212.9	169	70	5
2 PFPeA	2.905	262.9	218.8	70	5
3 PFHxA	3.167	312.9	268.8	70	5
4 PFHpA	3.489	362.9	168.9/319	70	15/5
5 PFOA	3.864	413.1	169.1/369.1	70	15/5
6 PFNA	4.274	463.1	169.1/419	80	20/5
7 PFBS	3.299	299	80/99	70	35/35
8 PFPeS	3.667	348.9	80/99	70	35/35
9 PFHxS	4.086	398.8	80/99	70	40/40
10 PFHpS	4.509	448.9	80/99	70	45/45
11 PFOS	4.942	498.9	80/99	70	50/50
12 PFNS	5.441	549.1	80/99	70	55/55
13 HFPO-DA	3.288	328.9	169/284.9	70	15/5
14 ADONA	3.618	376.9	84.9/250.9	80	30/10
15 PF4OPeA	2.990	278.9	84.9/235	60	10/5
16 PF5OHxA	3.571	378.9	69/134.9/184.9	60	40/40/10
17 3,6-OPFHpA	3.127	295	84.9/200.9	60	20/5
IS MPFOS	4.944	503.1	80.1/99	170	50/50

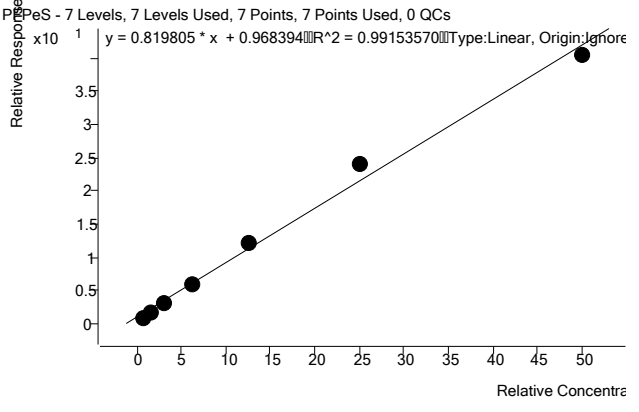
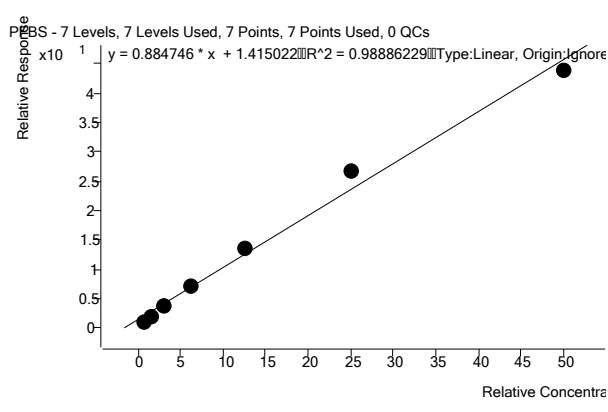
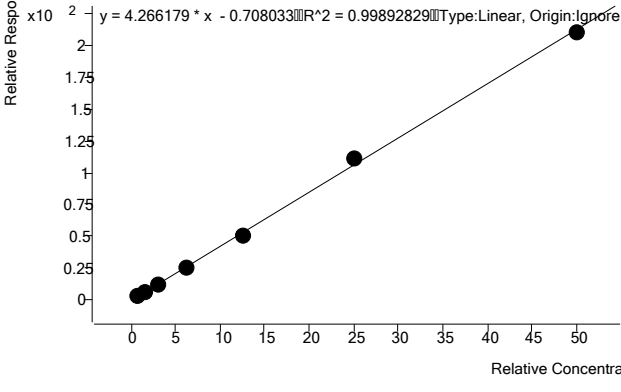
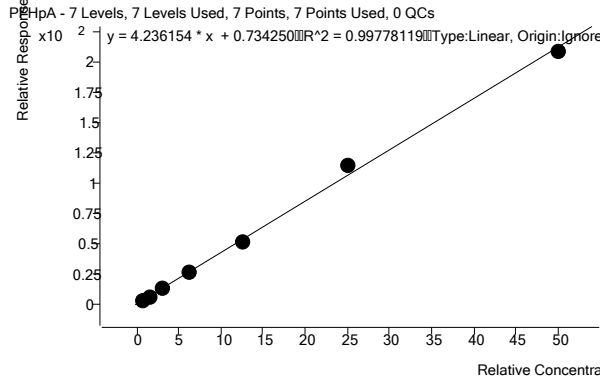
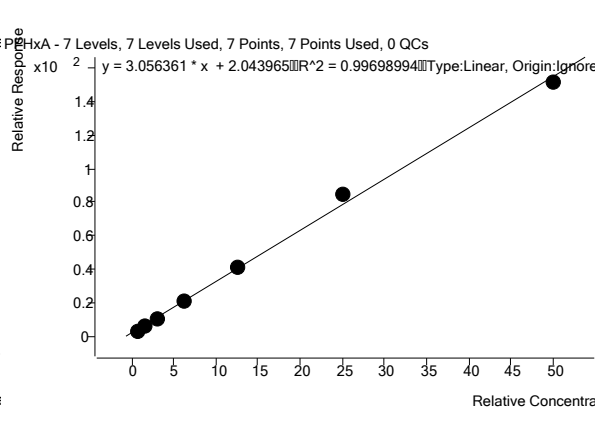
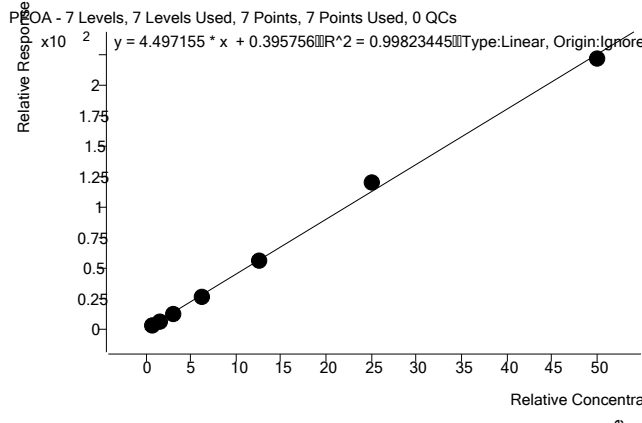
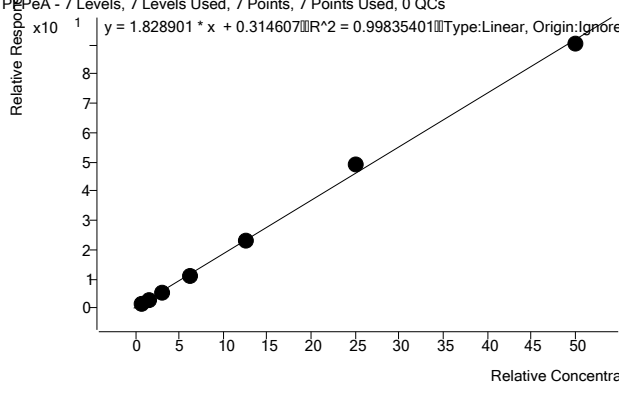
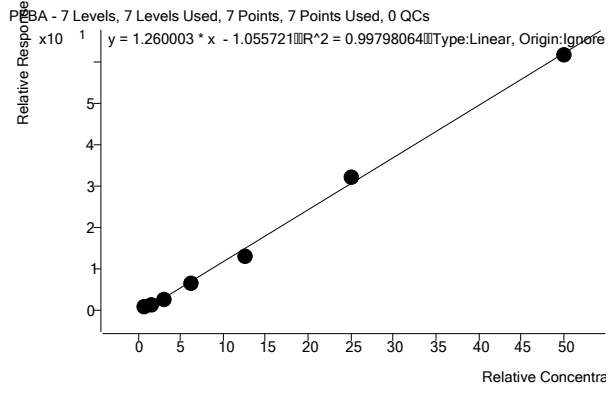
2.3.3 Method Validation

The method underwent a thorough validation process to ensure that it fulfilled the necessary criteria for sensitivity, linearity, accuracy, and repeatability. Calibration curves developed were tested for its linearity and accuracy and the results have been presented in Figure 2.7. Method recovery experiments were conducted by spiking multiple sets of samples with 2 ng and 10 ng concentrations. Samples were processed and analyzed using this method and recovery data have been provided in Table 2.6. The Limit of Detection (LOD) and Limit of Quantitation (LOQ) values of PFAS were found to vary between 0.13 and 0.32 ng/L and 0.42 and 1.08 ng/L,

respectively. These values represent the lowest concentrations of a substance that can be reliably detected and accurately quantified using the analytical method employed in the study. It is worth noting that LOD and LOQ are critical parameters to consider when assessing the sensitivity and accuracy of an analytical method, particularly when working with trace amounts of target compounds. To prevent any interference or contamination during the analysis, we conducted numerous solvent blanks and meticulously cleaned the injection port for every batch. The data was analyzed using the MassHunter Qualitative analysis software, version B07.00.

Table 2.6 PFAS recovery (%) data obtained from experiments conducted with spiking concentration 2ng (1A, 2A and 3A) and 10 ng (1B, 2B and 3B) concentration.

PFAS	1A	2A	3A	1B	2B	3B
PBA	90.4	83.9	90.5	100.1	108.8	112.6
PFBS	90.7	80.8	90.9	97.5	104.7	109.9
PFPeA	99.9	91.9	99.7	96.5	105.0	111.2
PFPeS	91.0	83.2	89.6	99.2	107.5	110.8
PFHxA	98.8	90.1	99.5	96.4	104.3	107.7
HFPO-DA	90.6	84.6	91.4	102.3	110.7	113.6
PFHxS	90.2	83.3	89.8	99.2	107.3	110.9
PFHpA	101.6	94.0	102.2	96.6	106.2	110.3
ADONA	95.0	86.9	95.7	97.1	105.7	110.8
PFHpS	86.3	82.0	85.2	98.2	104.3	109.5
PFOA	96.5	87.4	95.6	97.7	105.3	110.0
PFOS	89.0	81.5	89.3	98.8	108.7	111.4
PFNA	95.0	87.0	95.7	97.7	105.2	109.8
PFNS	86.9	82.7	89.1	100.6	107.9	111.2
PFDA	92.1	85.0	92.7	97.7	105.1	110.3



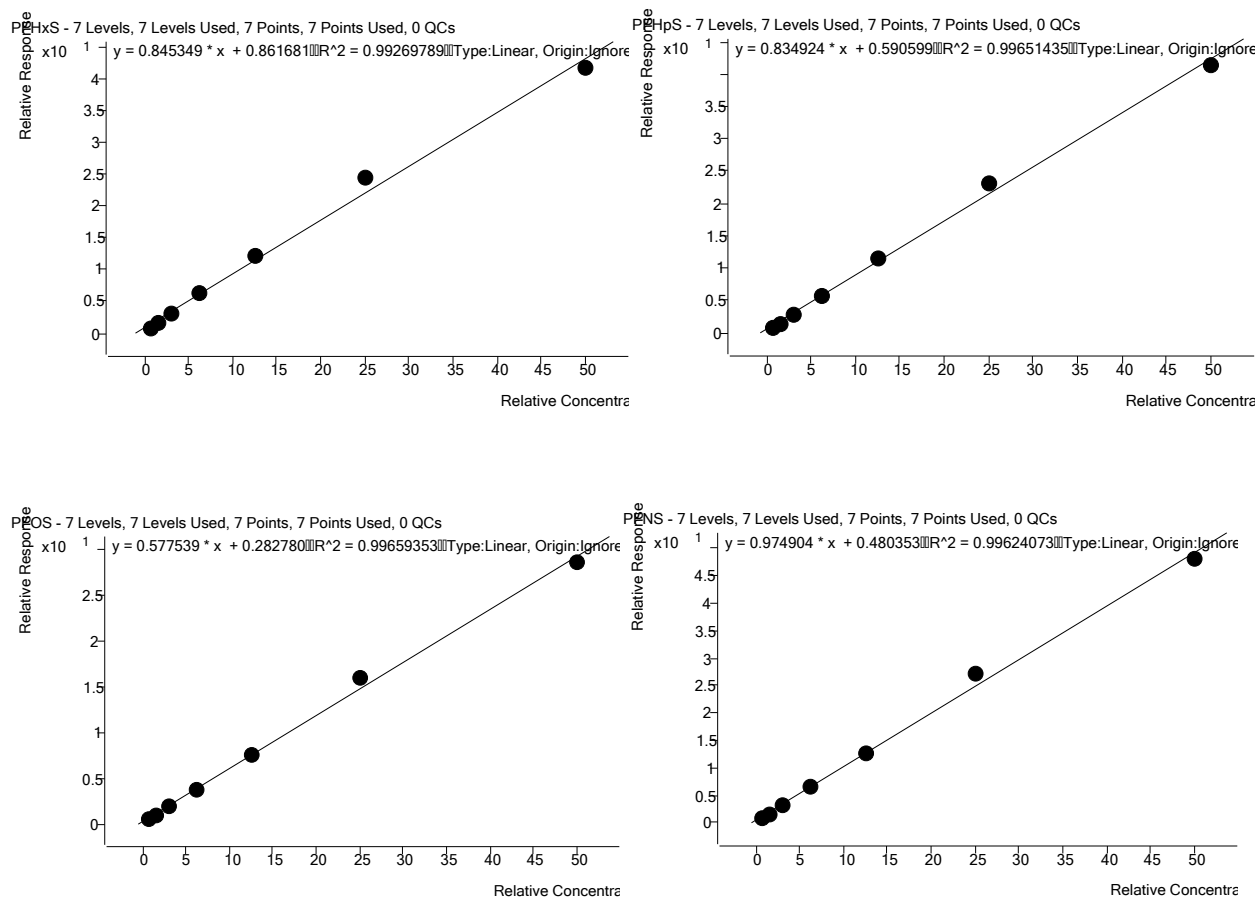


Figure 2.7 Calibration Curves Developed for PFCAs and PFSAs.

2.4 Target PFAS in Surface Water Samples

2.4.1 Mobile Bay Surface Water Samples

A comprehensive analysis was conducted on short-chain PFAS levels in surface water samples collected across Alabama from June to September 2019. The study aims to present its findings through a detailed discussion and interpretation of the data collected to conclude the distribution and trends of PFAS contamination across the samples. The objective of this study was to analyze 17 different short-chain PFAS from surface samples. The results obtained from the analysis of seven different sampling locations consistently detected several target PFAS, which included PFPeA, PFHxA, PFHpA, PFOA, and PFOS, all of which were found in each of the

samples collected. Additionally, PFBS was detected in most of the samples. However, the presence of PFNA and PFBA was less frequent. It is worth noting that none of the perfluoroethers, including HFPO-DA, NaDONA, PF4OPeA, PF5OHxA, and 3,6-OPFHpA, or sulfonic acids, such as PFPeS, PFHxS, PFHpS, and PFNS, were detected in any of the samples collected from the seven different locations. The individual and total PFAS levels present in surface water samples collected from seven different locations were recorded and presented in Table 2.7.

Among the seven distinct sampling locations, the Blakeley River in Spanish Fort, designated as Location 7, emerged as the site with the most pronounced Σ PFAS (Σ , summation) concentrations. In June, the recorded average for this location stood at 77.1 ng/L; in September, it was marginally higher at 78.4 ng/L. This result contrasts the findings from the Gulf of Mexico site at Dauphin Island, identified as Location 3. Here, the recorded Σ PFAS concentration averages were notably lower. Specifically, in June, the average concentration was 18.7 ng/L, and it experienced a slight increase to 20.0 ng/L by July. A general trend observed across most locations was the spike in Σ PFAS concentrations in July, except in the Blakeley River location, which exhibited an almost 27% reduction from June (77.1 ng/L) to July (55.9 ng/L). However, an interesting trend was seen in the samples from Bon Secour Bay Hwy 180 (Location 5), which showed a consistent increase in total PFAS concentration in June, July, and September (Σ PFAS: 29.9 to 35.2 ng/L) months.

Individual PFPeA concentration was recorded in Blakeley River in September at 11.7 ng/L, while several locations reported no detectable amounts in July. Dog River and Blakeley River exhibited high concentrations of PFHxA in the initial months (June and July); however, Mobile Bay (Codon) and the Gulf of Mexico sites showed relatively consistent values. Interestingly, PFBS was detected in most of the samples, and the highest concentration was found in Blakeley River

samples in June, at 31.03 ng/L, almost double the values observed at any other location or month. A comparison with global studies supports these this finding, with similar concentrations reported in the Bohai Bay, China (0.61-30.9 ng/L) (Y. Liu et al., 2019) and in the Rhine River, Germany (1.4-40 ng/L) (Heydebreck et al., 2015). Compounds PFHpA and PFOA generally exhibited increased concentration over the months, with notable spikes in September at various locations, as summarized in Table 2.7. PFHpA was often found at similar concentrations in many previous studies, including in a world-wide survey of emerging PFAS conducted by Pan et al. (2018), in which PFHpA concentrations ranged from 0.02 to 5.70 ng/L across the analyzed waterbodies. Several recent studies have also detected PFOA at similar concentrations in coastal areas, including in the coastal waters of South Korea (0.21-16.5 ng/L) (J. W. Lee et al., 2020) and in Biscayne Bay, Florida (0.11-8.14 ng/L) (Li et al., 2022). The discovery of PFOA at these levels, despite the regulations, suggests multiple potential input sources, including continuous production in other countries, indirect environmental degradation, and historical usage and contamination. PFBA and PFNA had non-detectable values in August and September for multiple sites. Understanding the cause of this pattern may require further investigation. While PFOS presence was consistent across months, Blakeley River in September recorded an unusually high concentration of 16.6 ng/L, almost double that of any other value. Several sites, such as Dog River and Mobile Bay sites, peaked in total PFAS concentration in July, followed by a decline in August and September. This pattern suggests a possible seasonal influence or event-based contamination in July. The data also underscores the importance of understanding the sources of contamination for individual PFAS compounds. For instance, the consistent presence of PFOS across all locations, with some sites showing sudden spikes, suggests multiple sources or event-based discharges. The presented data provides crucial insights into the distribution and temporal variation of PFAS in

surface waters across selected Alabama locations. While specific trends like the July spike in several sites are evident, others, like the consistently high PFAS values in Blakeley River, require further investigation. The consistent presence of certain compounds across all sites emphasizes the need for comprehensive monitoring and mitigation strategies.

Table 2.7 Short-chain PFAS detected in surface water samples collected from Alabama (Unit: ng/L).

ID	location	Compounds	June	July	August	September
1	Dog River, Mobile, AL	PFPeA	7.9±0.7	nd	8.7±1.4	9.1±1.2
		PFHxA	7.4±0.4	11.2±0.5	7.8±0.3	7.0±0.4
		PFBS	15.7±0.9	19.9±0.8	17.5±0.9	8.0±0.6
		PFHpA	3.5±0.2	4.8±0.4	6.2±0.1	6.2±0.1
		PFOA	8.5±0.5	11.5±0.3	9.0±0.3	8.1±0.
		PFBA	4.8±0.8	4.5±0.7	nd	nd
		PFNA	1.9±0.1	2.0±0.2	nd	nd
		PFOS	3.9±0.1	8.4±0.6	10.4±0.6	5.1±0.3
		Total	53.6	62.2	59.6	43.5
2	Mobile Bay, Coden, Mobile, AL	PFPeA	5.7±1.0	nd	8.7±1.3	5.8±0.6
		PFHxA	5.5±0.3	9.8±0.4	6.5±0.3	5.8±0.2
		PFBS	9.0±0.5	17.6±1.1	11.4±0.8	8.2±0.6
		PFHpA	2.8±0.1	4.2±0.2	5.9±0.2	5.3±0.1
		PFOA	6.4±0.1	11.0±0.5	8.0±0.4	6.2±0.2
		PFBA	3.5±0.5	3.3±0.4	nd	nd
		PFNA	2.2±0.1	1.9±0.1	nd	nd
		PFOS	5.4±0.3	6.2±0.5	5.2±0.4	2.8±0.2
		Total	40.6	54.0	45.6	34.1
3	Gulf of Mexico, Dauphin Island, Mobile, AL	PFPeA	3.3±0.6	nd	4.2±0.6	4.7±0.7
		PFHxA	2.6±0.3	3.0±0.3	4.4±0.2	4.6±0.1
		PFBS	2.0±0.6	3.2±0.4	2.4±0.3	3.1±0.3
		PFHpA	1.6±0.1	1.6±0.2	4.9±0.0	5.0±0.2
		PFOA	3.5±0.5	4.2±0.2	5.4±0.1	5.9±0.1
		PFBA	3.0±0.4	3.2±0.4	nd	nd
		PFNA	1.4±0.1	1.3±0.1	nd	nd
		PFOS	1.2±0.2	3.5±0.4	2.3±0.1	2.6±0.2
		Total	18.7	20.0	23.7	25.9
4		PFPeA	2.8±0.7	nd	5.6±1.0	4.8±0.7

		PFHxA	1.9±0.1	7.1±0.3	4.8±0.1	4.6±0.1
	Dauphin Island	PFBS	nd	11.1±0.8	5.7±0.3	5.1±0.5
	Bay, Dauphin	PFHpA	1.5±0.1	2.9±0.2	5.1±0.1	5.0±0.1
	Island, Mobile,	PFOA	3.5±0.2	5.4±0.2	6.1±0.1	5.6±0.1
	AL	PFBA	3.4±0.4	4.2±0.6	nd	nd
		PFNA	1.4±0.0	1.5±0.2	nd	nd
		PFOS	1.1±0.1	4.6±0.3	2.8±0.1	2.5±0.1
		Total	15.7	36.8	30.2	27.5
		PFPeA	3.7±0.4	nd	5.0±0.5	6.4±1.2
		PFHxA	3.7±0.2	6.5±0.4	5.1±0.1	5.6±0.1
		PFBS	4.4±0.3	9.1±0.3	6.6±0.5	7.0±0.4
		PFHpA	2.3±0.1	3.0±0.2	5.3±0.1	5.5±0.1
		PFOA	6.1±0.3	7.9±0.29	6.9±0.1	7.4±0.2
	Bon Secour Bay	PFBA	3.5±0.3	2.6±0.3	nd	nd
	Hwy 180, Fort	PFNA	2.2±0.1	1.5±0.1	nd	nd
	Morgan,	PFOS	4.1±0.3	4.5±0.3	3.5±0.2	3.3±0.3
5	Baldwin, AL	Total	29.9	35.0	32.5	35.2
		PFPeA	5.9±0.9	nd	7.4±1.1	7.2±1.1
		PFHxA	6.0±0.3	10.3±0.4	6.3±0.3	6.2±0.2
		PFBS	8.5±0.5	16.4±1.2	11.0±0.7	11.3±0.7
		PFHpA	3.0±0.1	4.7±0.3	5.7±0.1	5.6±0.1
6	Mobile Bay,	PFOA	7.0±0.3	11.8±0.5	7.3±1.1	7.1±0.1
	Fairhope,	PFBA	4.6±0.4	4.4±0.4	nd	nd
	Baldwin, AL	PFNA	1.8±0.1	2.0±0.1	nd	nd
		PFOS	2.8±0.2	6.3±0.2	3.8±0.2	3.3±0.2
		Total	39.6	55.8	41.6	40.7
		PFPeA	11.2±0.3	nd	9.7±1.0	11.7±0.7
		PFHxA	11.3±0.4	9.5±0.8	6.8±0.4	9.6±0.2
		PFBS	31.0±1.4	19.6±1.6	12.6±1.0	22.8±1.4
		PFHpA	4.7±0.2	4.0±0.3	5.8±0.2	6.9±0.1
7	Blakeley River,	PFOA	10.1±0.3	10.6±0.4	7.9±0.3	10.9±0.2
	Spanish Fort,	PFBA	4.3±0.4	4.0±0.4	nd	nd
	Baldwin, AL	PFNA	1.5±0.1	1.8±0.2	nd	nd
		PFOS	3.0±0.2	6.3±0.5	8.0±0.4	16.6±0.7
		Total	77.1	55.9	50.7	78.4

2.4.2 Method Application to Large Batch of Surface Water Samples

The optimized method was applied to a large batch of sample for analysis. The spatial distribution of 17 PFAS and the overall extent of PFAS contamination across Alabama was profiled and evaluated. A total of 74 surface water samples were collected from fourteen river systems within ten major river basins in Alabama, including Alabama Rivers, Black Warrior Rivers, Cahaba Rivers, Chattahoochee Rivers, Choctawhatchee Rivers, Conecuh Rivers, Coosa Rivers, Escatawpa Rivers, Perdido Rivers, Tallapoosa Rivers, Tennessee Rivers, Tombigbee Rivers, Yellow Rivers, and Mobile River and tributaries. In 65 out of the 74 samples taken from various rivers, six PFAS were detected, with an average total concentration of 35.2 ng/L. PFAS were prevalent in the majority river system of Alabama, appearing in 88% of the collected samples, with total PFAS concentration levels reaching as high as 237ng/L. Table 2.8 provides a summary of the range and average concentration of the identified PFAS found in each river system. The spatial distribution of the target PFAS is presented in Figure 2.8. Among the six detected PFAS, the short-chain PFPeA was the most frequently detected PFAS, which was found in 88% of the samples. However, the substance with the highest individual concentration was the short-chain PFBS, which was reaching up to 79.4ng/L.

The results of this study reveal the widespread distribution of PFAS in the majority of rivers and tributaries in Alabama, even in areas with less industrial activity. This finding suggests potential health risks to humans and wildlife. Additionally, the study evaluates the method of tracking PFAS contamination in interconnected river systems flowing through large geographical areas, indicating the existence of a significant number of local contamination sources within the river basins. The PFAS contamination in Alabama could also threaten the estuarine systems and coastal areas that receive water from the state. Due to the bioaccumulation and biomagnification

potential of PFAS, this contamination may pose risks to aquatic animals residing in the estuarine ecosystem. A detailed study report has been published by Vitocotski et al., 2022.

Table 2.8 Range (min-max) and average (in parenthesis) of analytes for each of the analyzed rivers. Overall detection frequencies (DF) are also displayed. Concentrations are expressed in ng/L.

River	PFBS	PFPeA	PFHxA	PFHpA	PFOA	PFOS	∑PFAS
Alabama	28.2-33.3 (30.1)	21.1-23.5 (21.9)	13.2-15.3 (14.1)	7.6-8.2 (7.8)	14.0-15.3 (14.6)	10.7- 13.0 (11.7)	96.4- 107.8 (100.2)
Black Warrior	n/a	2.1-23.1 (8.7)	0.0-11.6 (1.9)	n/a	0.2-6.1 (2.0)	n/a	2.3-40.8 (12.6)
Cahaba	n/a	8.5-15.0 (10.9)	0.0-7.3 (2.8)	n/a	0.0-7.1 (3.8)	n/a	8.5-29.4 (17.6)
Chattahoochee	n/a	8.4-17.5 (12.3)	3.8-10.8 (6.5)	0.0-6.2 (2.1)	4.3-10.2 (7.9)	n/a	21.4-43.5 (28.8)
Choctawhatchee	n/a	0.0-15.7 (7.4)	0.0-15.0 (3.0)	n/a	0.0-14.0 (2.8)	0.0-19.1 (3.8)	0.0-63.8 (17.0)
Conecuh	n/a	n/a	n/a	n/a	n/a	n/a	n/a
Coosa	52.8-79.4 (63.9)	33.8-54.9 (42.1)	22.5-39.3 (30.4)	8.8-13.1 (11.1)	18.3- 30.2 (23.7)	11.0- 29.6 (19.9)	155.0- 237.3 (191.2)
Escatawpa	n/a	n/a	n/a	n/a	n/a	n/a	n/a
Mobile Bay	n/a	4.4-14.7 (11.4)	0.0-6.5 (4.2)	n/a	2.7-7.5 (5.7)	0.0-30.7 (3.4)	8.5-56.7 (24.7)
Perdido	n/a	4.2-13.9 (10.4)	0.0-6.1 (3.7)	n/a	2.6-9.0 (6.5)	n/a	6.9-29.0 (20.5)
Tallapoosa	n/a	5.6-8.5 (7.0)	n/a	n/a	0.0-5.8 (2.8)	n/a	5.6-14.0 (9.8)
Tennessee	n/a	5.3-8.8 (7.4)	0.9-7.0 (4.5)	n/a	3.0-10.7 (5.6)	0.0-9.5 (2.9)	9.2-35.6 (20.4)
Tombigbee	n/a	5.8-9.0 (7.8)	n/a	n/a	0.0-0.6 (0.2)	n/a	6.3-9.0 (7.9)
Yellow	n/a	n/a	n/a	n/a	n/a	n/a	n/a
D.F. (%)	14.9	87.8	58.1	18.9	74.3	21.6	87.8

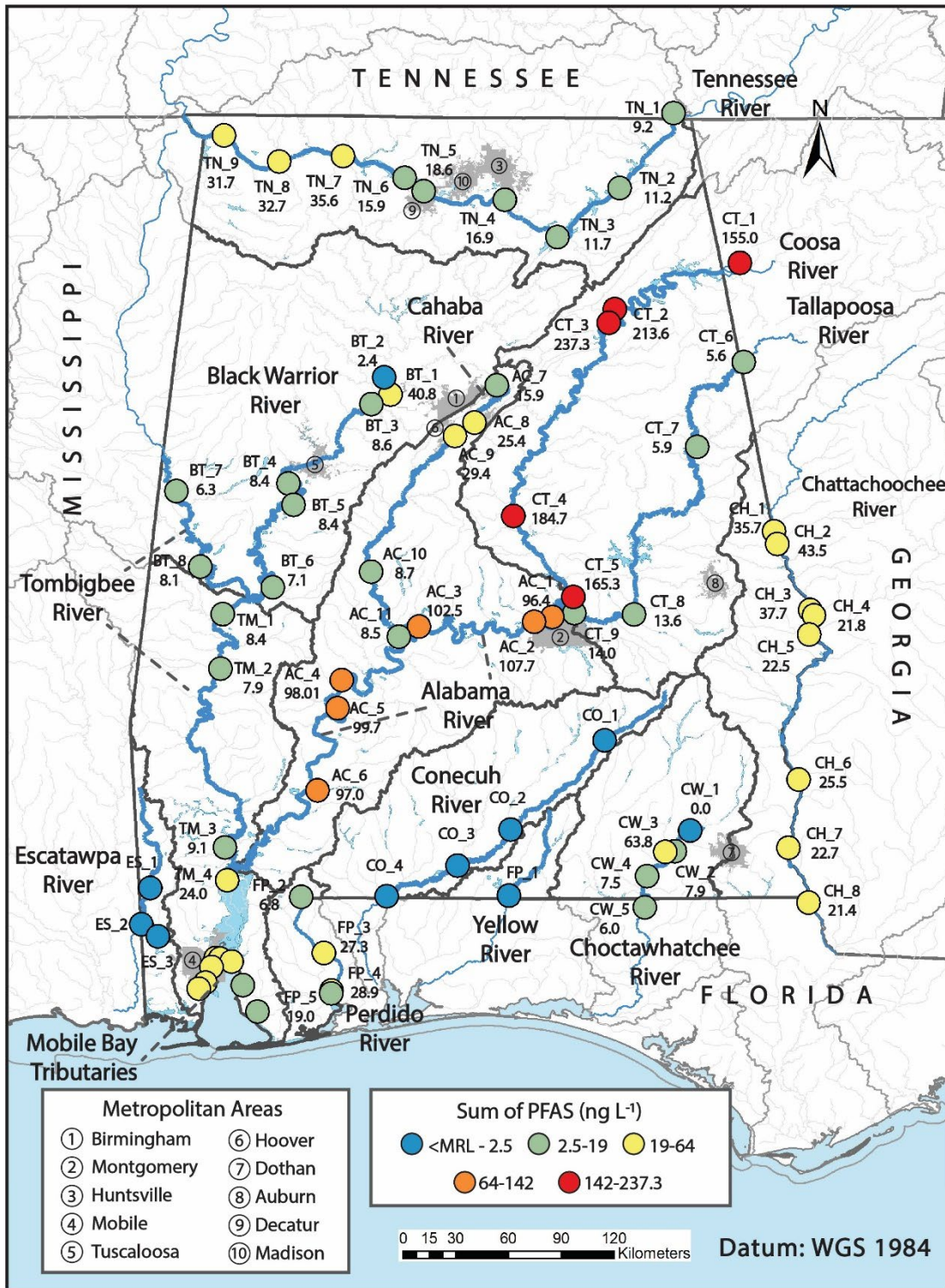


Figure 2.8 Spatial Distribution of PFAS in Alabama. \sum_6 PFAS concentrations (in ng/L) are displayed for sampling locations. The 10 largest metropolitan areas are highlighted for spatial reference (Vitcotski et al. 2022).

2.5 Conclusion

The method was developed and validated for measuring trace concentration of 17 PFAS, including prevalent subclasses (PFCAs and PFSAs) and a group of emerging ethers (PFECAs). A new set of MRM parameters was optimized for PFECAs (PF4OPeA, PF5OHxA and 3,6-OPFHpA) through the UHPLC-QqQ-MS/MS system using an Agilent JetStream ESI in negative mode for the first time. This method exhibits enhancements in peak shape, analytes separation, and significantly reduces the analysis time to 9 minutes, offering improvements over previously reported methods.

The data of Mobile Bay water samples offers a snapshot of the intricate patterns of PFAS distribution in Alabama's surface waters. Monitoring these patterns is the first step toward formulating effective environmental management and health protection strategies. As PFAS concerns grow globally, localized studies like this are crucial in detecting these persistent organic pollutants. This study also suggests a need for comprehensive monitoring and mitigation strategies for PFAS contamination. The recurrent presence of specific compounds in all sites underlines the importance of understanding contamination sources for each PFAS compound. A clear grasp of these contamination patterns forms the foundational step towards evolving effective environmental management and health protection strategies. Future studies focusing on source identification and hydrological modeling will further deepen our understanding of PFAS distribution and guide the formulation of efficient water quality management policies.

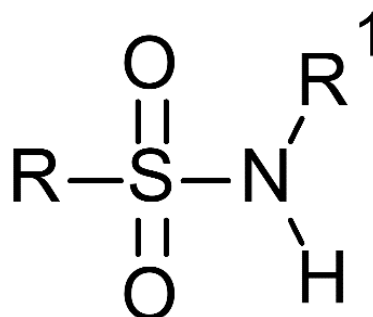
To gain a comprehensive understanding of the prevalence of per- and polyfluoroalkyl substances (PFAS) in river water samples, this quantitative method was employed in a total of 74 samples collected across Alabama. The significance of this research lies in its ability to shed light on the extent of PFAS contamination, which has become a growing concern for environmental and

public health organizations. By regularly monitoring contamination levels in surface waters, it can aid in clearer understanding of the impact of these potentially hazardous substances on both the environment and human health.

Chapter 3. A Quantitative UHPLC-MS/MS Method for the Analysis of Perfluoroalkyl Sulfonamides (FASAs) in the Environment

3.1 Introduction

Perfluoroalkane sulfonamides (FASAs) are a subclass of PFAS, which contain a fully fluorinated carbon backbone ($F_{2n+1}C_n$) and a sulfonamide functional group ($-SO_2NRR^1$). Based on the structures of sulfonamide functional groups, sulfonamides are classified into linear and branched FASAs (Figure 3.1).



Perfluoroalkane Sulfonamide (FASAs): $R = F_{2n+1}C_n$, $R^1 = H$

N-Methyl-Perfluoroalkane Sulfonamide (NMeFASAs): $R = F_{2n+1}C_n$, $R^1 = CH_3$

N-Ethyl-Perfluoroalkane Sulfonamide (NEtFASAs): $R = F_{2n+1}C_n$, $R^1 = CH_2CH_3$

N-Butyl-Perfluoroalkane Sulfonamide (NBuFASAs): $R = F_{2n+1}C_n$, $R^1 = CH_2CH_2CH_2CH_3$

Figure 3.1 Structure of Perfluoroalkane sulfonamides (FASAs).

Since the 1950s, FASAs have been manufactured and used in a wide range of commercial products and industrial applications. FOSA and N-alkyl homologues were the most extensively used sulfonamides prior to 2002, which were ingredients in 3M's Scotchgard products (Chu & Letcher, 2014) and fire-fighting foams formula (QldGov, 2018). Moreover, sulfluramid, an NEtFOSA-containing pesticide, is widely used in tropical areas for controlling termites, cockroaches, and other insects. NEtFOSA is both surfactant and active ingredient of the pesticide

sulfluramid, which plays an important part in the agriculture of South America since 1989 (Löfstedt Gilljam et al., 2016; Zabaleta et al., 2018). FASAs are also used as surfactants in the electronics and semiconductor industries because of their low surface tension property. Short-chain sulfonamides (C3-C6) and their N-alkyl derivatives are preferred surfactants and have been patented by 3M in 2004 for use in buffered acid etch solution. Etch solution with fluorinated surfactants has a wide application, such as using in the etching of silicon oxide-containing materials in semiconductor chip fabrication (Michael J. Parent, 2004). In addition to being the critical ingredient in commercial products, FASAs are also used as building blocks or intermediates in the production of other perfluorochemicals for use in surface protection (Buck et al., 2011). For instance, N-Alkyl FOSA is the intermediate chemicals in the process of synthesizing N-Alkyl perfluoroalkane sulfonamido ethanols (N-Alkyl FOSEs) and perfluoroalkane sulfonamido acetic acids (N-Alkyl FOSAAs). N-ethyl FOSE was commercialized and used in paper and packaging product lines since the late 1960s, including both food contact and non-food contact applications. NEtFOSE was also used for textile and carpet surface treatments, such as 3M's Scotchgard products and DuPont's Capstone products. Similarly, N-ethyl FOSAA was an important ingredient in cleaning agents, floor polishes and car polishes (Bogdan, 2019).

Continuous production and unregulated discharge of PFAS is the origination of these sulfonamides to input into the environment. FASAs and their sulfonamido derivatives are synthesized from perfluoroalkane sulfonyl fluorides (PASFs) through the ECF process. Before 2002, perfluorooctane sulfonyl fluoride (POSF) was the major raw material for manufacturing PFOS, and their derivative sulfonamides (FOSAs), sulfonamido ethanols (FOSEs) and sulfonamido acetic acids (FOSAAs). Figure 3.2 represents the ECF process for manufacturing PFOS, (N-Alkyl) FOSA and their derivatives. Decades of mass production released a large

quantity of POSF-related chemicals into the environment, which include an uncertain amount of FASAs and their precursors (FASEs and FASAAs). According to a study by Paul et al, the global production of POSF between 1970-2002 was estimated to be 12250 tons (including unusable side-products), approximately 36.9% of them released into environment (Paul et al., 2009). Due to the bioaccumulation risks posed by long-chain PFAS, they were phased out in the United States since 2002, and the production of PFAS transferred to short-chain alternatives. The annual global production of POSF significantly decreased from 3838 ton/yr in 1995-2002 to 488 ton/yr in 2003-2010 (Bogdan, 2019). Perfluorobutane sulfonyl fluoride (PBSF) based compounds become one of the substitutes for POSF-related chemicals. The global production of PBSF has gradually increased in recent years, from 287 tonnes in 2011 to 317 tonnes in 2015. Among the PBSF consumption of 2015, the major application of it was for production of surfactants, pesticides and flame retardants, which counted for 55%, 28% and 14 %, separately (Lassen & Brinch, 2017). PBSF is the raw material for synthesizing perfluorobutane sulfonate (PFBS), perfluorobutane sulfonamide (FBSA) and their sulfonamido derivatives. A portion of the PBSF consumption has been used for the manufacturing of FBSA and N-alkyl FBSA. Hence, the elevating production of PBSF leads to the increasing release of these short-chain sulfonamides into the environment. In addition, PFBS, as the substitute for PFOS, is the principal product of most PBSF production lines. During the synthesis process of PFBS and other related chemicals, the release of sulfonamide side products is unavoidable as well, which causes a large amount of sulfonamide wastes to be released into the environment.

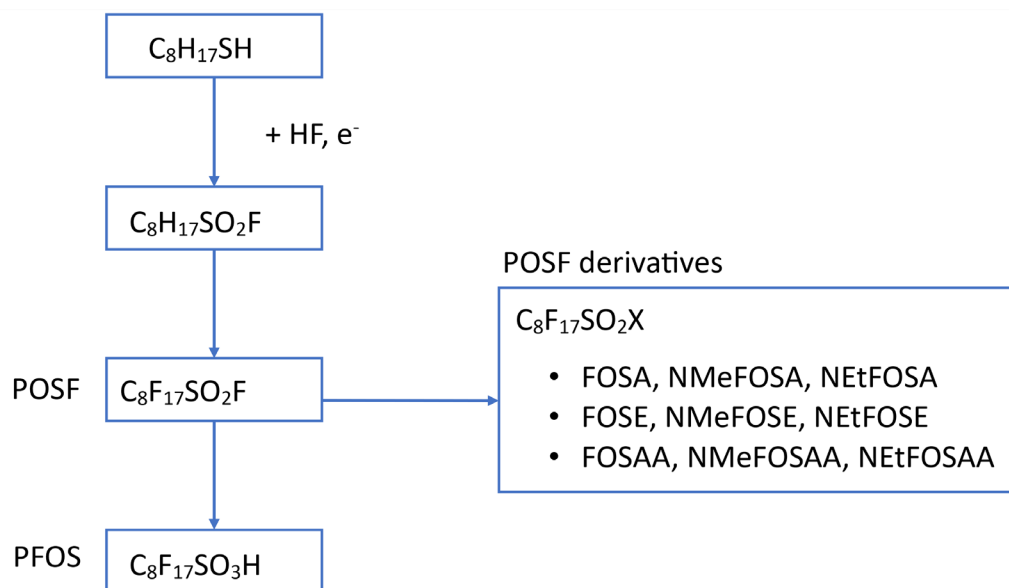


Figure 3.2 ECF process for manufacturing PFOS and derivatives.

The transformation of PFAS in the environment is a complicated process, which largely increases the abundance and variety of PFAS species in the environmental system. FASAs can degrade into lower molecular weight PFAS intermediates, and finally convert to persistent PFASs. In a study investigating the biodegradation of sulfluramid in soil-carrot mesocosms, FOSAA, FOSA and PFOS were found that could be transformed from NEtFOSA (Zabaleta et al., 2018). Two possible degradation pathways were proposed by Zhao et al. (2018), in which FOSAA and FOSA are the intermediates. One pathway is the deethylation of NEtFOSA to form FOSA, and then deamination to transform into PFOS. Another is that NEtFOSA is first oxidized to FOSAA, and then dealkylated to form FOSA, and finally deaminated to produce PFOS (Zhao et al., 2018). However, in the natural environment, the transformation and interaction of PFAS is much more complicated than under laboratory conditions. A large number of PFAS from different subclasses could be involved in the degradation process. In the biotransformation process of FOSAs, the degradation of their precursors, such as N-Alkyl FOSE and N-alkyl FOSAA, could increase the

uncertainty and complexity of the situation. NEtFOSE, a precursor of FASAs, can transform into multiple intermediates (FOSE, NEtFOSAA, NEtFOSA, FOSAA, FOSA) under ambient biotic or abiotic conditions, and ultimately degrade to persistent PFOS. Figure 3.3 demonstrates the possible metabolic pathways for the biotransformation of NEtFOSE in environmental media and biota (Zhang et al., 2020). FASAs, as important industrial chemicals, have been produced on a large scale over decades. The degradation of these chemicals in the environment leads to the continuous release of persistent PFASs. One of their degradation products, PFOS, is the most well-studied PFAS, which has been reported to associate with a series of diseases, including high cholesterol, thyroid disorders, pregnancy-induced hypertension, testicular and kidney cancers and endocrine disruption (Cooke, 2017). The toxicity of short-chain PFASs, such as PFBS, has been evaluated in many human and animal studies as well. PFBS poses comparable health effects with long-chains on the thyroid, reproductive systems, development, kidneys, livers and lipid and lipoprotein of humans and animals (USEPA, 2018). The emission of FASAs elevates the risks of exposure to PFASs for humans and wildlife.

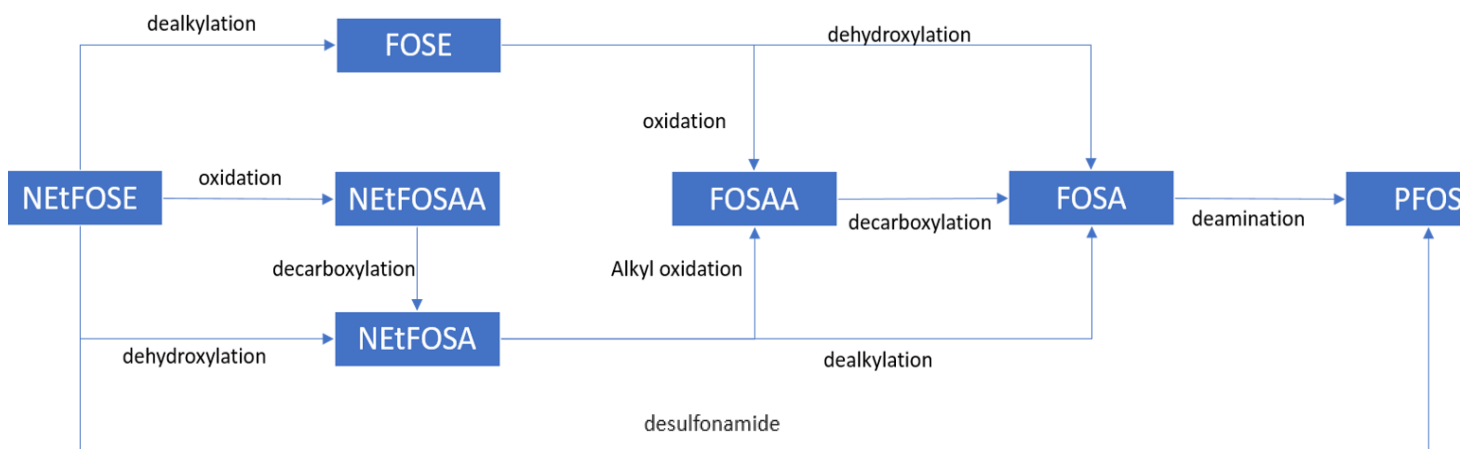


Figure 3.3 Metabolic Pathways for the biotransformation of NEtFOSE.

In addition to the health concerns from their degradation products, some FASAs, on their own, are considered to have toxicity and bioaccumulation potential. In a study on the developmental neurotoxicity of PFAS to cells, FOSA was found to have the most adverse effects on neurodevelopment compared with PFOS, PFOA and PFBS (Slotkin et al., 2008). FOSA has also been reported to have impacts on gene expression in mice and humans, which is involved in lipid metabolism, energy homeostasis and cell differentiation. Animals and humans exposed to a high level of FOSA could induce hepatocellular adenoma formation (Shipley et al., 2004). Studies on perfluorochemical-induced mitochondrial dysfunction suggest that some sulfonamides with protonated nitrogen atoms, including FOSA and NEtFOSA can protonophoric uncoupling the mitochondrial respiration to disrupt the metabolism and bioenergetics of animal cells (Schnellmann & Manning, 1990; Starkov & Wallace, 2002).

In the long run, FASAs would degrade into PFASAs with extremely stable structures under environmental conditions. Nevertheless, due to the continuous release from manufacturing plants and incomplete degradation under some complex environmental conditions, these precursors have been found in varying environmental media and living biota, such as atmosphere (Haug et al., 2011), global aqua systems (Boulanger et al., 2004; Cai, Yang, et al., 2012), sediments/soils (Nascimento et al., 2018; Zhao et al., 2015), as well as in the tissues and blood of wildlife (Asher et al., 2012; Nakata et al., 2006) and humans (Bonefeld-Jørgensen et al., 2014).

FOSA is the FASA most frequently identified in the world, having been discovered on six continents: Asia, Europe, Australia, North America, South America, and Antarctica. For example, FOAS was found in surface water at the concentration of <0.03-0.36ng/L in Yellow Sea, China (Z. Zhao et al., 2017), 0.44-8.9ng/L in Elbe River and North Sea, Germany (Ahrens, Plassmann, et al., 2009), 0.2-0.8ng/L in Stony Creek, Australia (Marchiandi et al., 2021), 0.023-0.08ng/L at

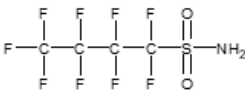
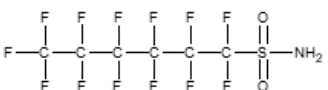
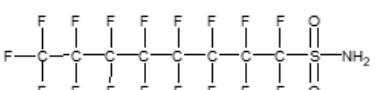
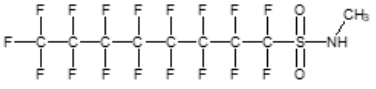
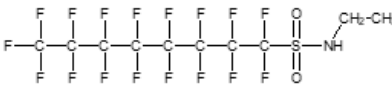
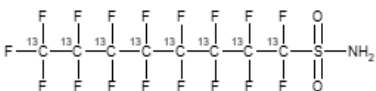
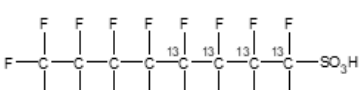
St. Lawrence Estuary and Gulf, Canada (Picard et al., 2021), <0.014–3.362ng/L at Todos os Santos Bay, Brazil (Löfstedt Gilljam et al., 2016) and <0.0403-0.0464ng/L at Fildes Peninsula, Antarctica (Cai, Yang, et al., 2012). FOSA also has been detected in drinking waters of many countries, including tap waters from Canada, USA, and China, as well as bottled waters from the Ivory Coast. One of the major pathways for PFAS entering the human body is via drinking PFAS-containing water. FOSA poses a direct threat to people exposed to this contaminated drinking water. According to several surveys of perfluoroalkyl chemicals in pooled serum samples from different countries, FOSA was detected in the blood serum of the general population from Australia, and women from Sweden and the USA (Gebbinck et al., 2015; Hurley et al., 2018; Toms et al., 2009).

Other than FOSA, their N-alkyl homologues and some short-chain FASAs, such as NMeFOSA, NEtFOSA, FBSA and FHxSA, have been found in environmental water and soils of different countries at a level of ng/L as well (Hua et al., 2019; Marchiandi et al., 2021; Munoz et al., 2018). However, FASAs in municipal and military wastewater are usually found at a high level that can reach 1000~10000-fold higher than in general environment waters. In a study of investigating 17 municipal wastewater treatment plants (WWTP) in China, the highest concentration of FBSA in WWTP influent was as high as 2203.61ng/L (Wang et al., 2020). Military wastewater could have even higher levels and more species of FASAs, since the periodic firefighting training activities at military bases. The AFFF formula consists of a mixture of chemicals, in which the PFAS content accounts for approximately 1kg per liter of firefighting foams. A study of Dauchy (2019) reported a high level of FOSA, NMeFOSA and NEtFOSA in the wastewater drained from a firefighting training area, among them, the highest level of FOSA was up to 49937ng/L (Dauchy et al., 2019). At WWTP surrounding area and AFFF-impact sites, the concentration of these sulfonamides in water and soils usually stayed at a high level as well

(Dauchy et al., 2019; Houtz et al., 2013), since current wastewater treatment plants do not have the capacity to remove most of the FASAs, as well as the direct input of FASA-containing wastewater with stormwater runoff into environment, such as AFFF wastewater.

Current studies primarily concentrate on persistent PFAAs, particularly PFSA and PFCA, and there is noticeable gap in research regarding their sulfonamide precursors, FASA. Existing methods used to include FASAs are typically time-consuming and designed to target a broad range of PFAS, potentially reducing the detection sensitivity for individual target analytes. To date, there are no expedient methods exclusively focusing on FASA reported in the literature. Determining the distribution of these precursor chemicals in the environment is crucial for understanding their complex transformations and fate, as well as tracing the origins of their product PFAS, such as PFBS, PFHxS and PFOS. This study aims to establish a rapid and validated analytical method for detecting and quantifying FASA in the environmental water samples. To achieve this, an ultra-high performance liquid chromatography coupled with a triple quadrupole mass spectrometry (UHPLC-MS/MS) was used under optimized conditions, resulting in highly sensitive and swift analysis for target analytes. The developed method will allow for rapid analysis and prompt response in the assessment of samples from contamination sources. Additionally, this method can process and analyze a large number of samples within a short time frame, hence improving efficiency.

Table 3.1 CAS, molecular weight, and structure of the target FASAs, internal standard and surrogate standard in this study.

Chemicals	Acronym	CAS	Molecular Weight (g/mol)	Molecular Formula
Perfluoroalkane sulfonamides (FASAs)				
Perfluorobutane sulfonamide	FBSA	30334-69-1	299.111	
Perfluorohexane sulfonamide	FHxSA	41997-13-1	399.13	
Perfluorooctane sulfonamide	FOSA	754-91-6	499.15	
N-Methyl perfluorooctane sulfonamide	NMeFOSA	31506-32-8	513.17	
N-Ethyl perfluorooctane sulfonamide	NEtFOSA	4151-50-2	527.2	
Mass-labeled Internal Standard				
Perfluoro[¹³ C ₈]octanesulfonamide	M8FOSA	1365803-60-6	507.09	
Mass-labeled surrogate Standard				
Sodium perfluoro-1-[1,2,3,4- ¹³ C ₄]octane sulfonate	MPFOS	960315-53-1	526.08	

3.2 Method

3.2.1 Chemical, Reagents and Materials

The high-purity analytical standards (purity > 98%) were used in this study, including five target analytes, one internal standard (IS) and one surrogate standard (SS). These comprise perfluoro-1-butanefulfonamide (FBSA), perfluoro-1-hexanesulfonamide (FHxSA), perfluoro-1-

octanesulfonamide (FOSA), N-methylperfluoro-1-octanesulfonamide (N-MeFOSA), N-ethylperfluoro-1-octanesulfonamide (N-EtFOSA), mass-labeled perfluoro-1-[¹²C₈]octanesulfonamide (M8FOSA, IS) and perfluoro-1-[1,2,3,4-¹³C₄]octane sulfonate (MPFOS, SS). These standards were produced from Wellington Laboratories (Ontario, Canada). LC grade solvents (acetonitrile, methanol, and water), ACS Grade Ammonium Hydroxide and ammonium acetate (purity>99%) were supplied by VWR International (Suwanee, GA). The UHPLC analytical columns (ZORBAX RRHD Eclipse Plus C18, 2.1 ×50 mm, 1.8 μm, Part No. 959757-902 and ZORBAX RRHD Eclipse Plus C18, 2.1 ×100 mm, 1.8 μm, Part No. 959758-902) and a guard column (Agilent ZORBAX Eclipse Plus C18, 2.1 × 5 mm, 1.8 μm, p/n 821725-901) were used for target analytes separation experiments. The columns, as well as 5M ammonium formate solution (Purity = 98.1%) and Captiva premium syringe layered filters (glass fiber/nylon, 0.2 μm) were obtained from Agilent Technologies. In addition, Whatman glass microfiber filters GF/C (47mm) for sample preliminary filtration were purchased from Sigma Aldrich (St. Louis, MO). Oasis WAX and HLB Prime extraction cartridges (6cc, 200mg), and a 20-Position vacuum manifold were provided by Waters Corporation (Milford, MA, USA).

3.2.2 Stock Solution and Calibration Solution Preparation

Stock solutions were prepared by diluting high-purity analytical standards of each target analytes using a solvent comprising methanol and water in a ratio of 9:1 (v/v). Independent stock solutions of 0.1μg/mL and 0.01μg/mL for each target PFAS were prepared, intended for conducting preliminary chromatographic experiments. A composite stock solution of 0.01μg/mL containing the five compounds was utilized to optimize UHPLC-MS/MS parameters. The surrogate and internal standard solutions were prepared in the working solution to achieve concentrations of 0.1μg/mL and 0.25 μg/mL, respectively. A calibration stock solution, a mixture

of the five target analytes and surrogate standard, was also prepared in the working solution to attain a concentration of 0.1 µg/mL. This calibration stock solution was subsequently diluted to a series level for calibration curve development.

3.2.3 Instrumental Conditions

The analysis of PFAS was conducted using an Agilent Technologies UHPLC-MS/MS system, which comprises a 1290 Infinity II UHPLC system coupled to a 6460 Triple Quadrupole MS and a Jet Stream electrospray ionization (ESI) source (Agilent Technologies, CA, USA). Data quantitation and analysis used Agilent MassHunter Qualitative Analysis 10.2 software.

The optimization of chromatographic separation was achieved by assessing various mobile phase solvents combinations (acetonitrile, methanol, and water) and several analytical C18 columns (ZORBAX RRHD Eclipse Plus C18, 2.1 ×50 mm, 1.8 µm, Part No. 959757-902 and ZORBAX RRHD Eclipse Plus C18, 2.1 ×100 mm, 1.8 µm, Part No. 959758-902). The selection of mobile phase solutions and modifiers was based on the properties of the target analytes. The inclusion of a modifier in the mobile phase solvents can provide a preferring pH environment for the analyte, thereby enhancing separation. Given that the target PFAS in this study are ionic compounds and tend to form anionic molecules in aqueous solutions, an acidic modifier was added to adjust the pH within the analytical column. Various concentrations (1-10mM) of modifiers (ammonium formate, ammonium acetate) were added into the aqueous mobile phase or organic mobile phases. Multiple combinations of mobile phases with the modifier were evaluated, as detailed in Table 3.2.

Two C18 analytical columns, 50mm and 100mm in length, were used to separate target compounds and improve the separation performance via adjustment of the mobile phase inflow percentage. A compatible guard column was installed upstream of the analytical column to

eliminate impurities and protect the analytical column. Chromatographic performances for the target analytes were further optimized by testing different flow rates (0.2-0.3mL/min), injection volumes (2-10 μ L) and column temperatures (40-60°C).

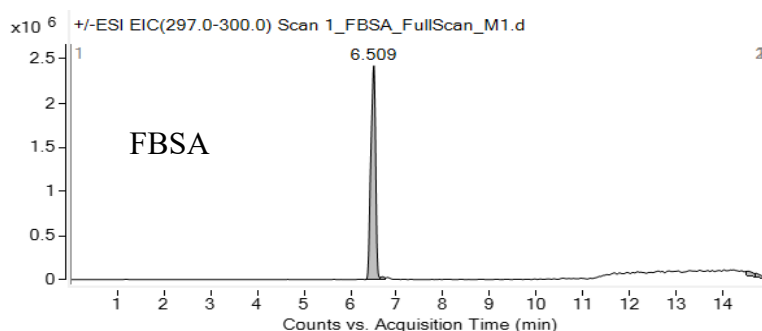
Table 3.2 Mobile phases and modifier combination tested for chromatographic separation.

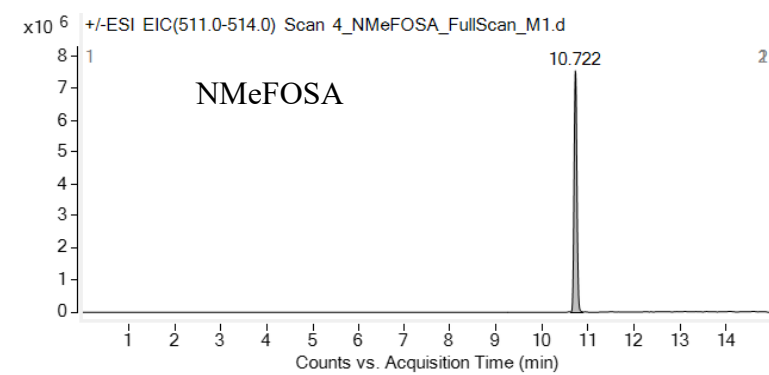
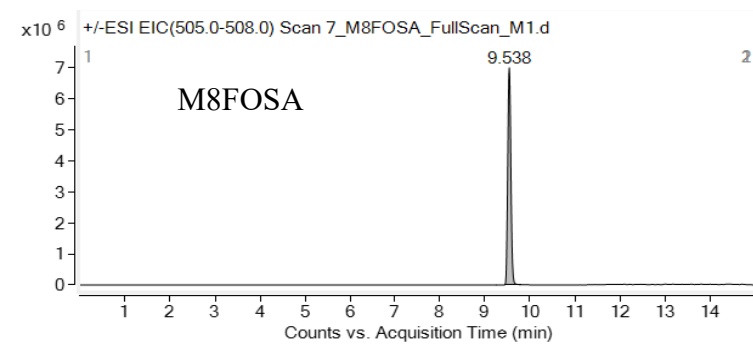
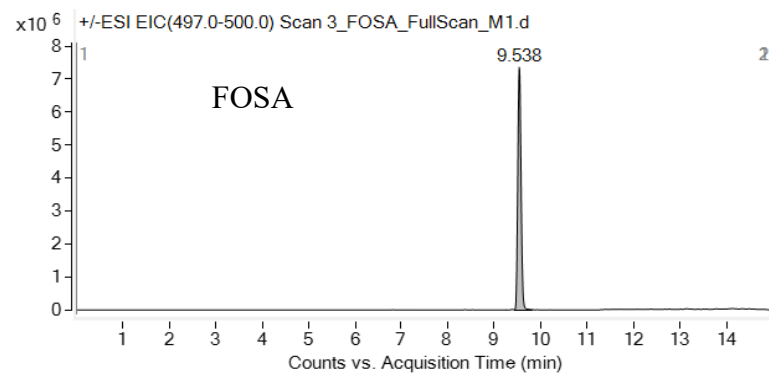
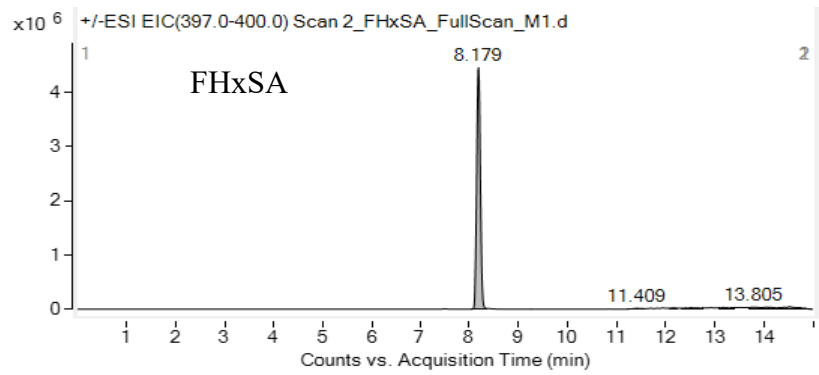
	A (Aqueous mobile phase)	B (Organic mobile phase)
1	1mM ammonium formate in 95% water and 5% acetonitrile	95% acetonitrile and 5% water
2	3mM ammonium formate in 95% water and 5% acetonitrile	95% acetonitrile and 5% water
3	5mM ammonium formate in 95% water and 5% acetonitrile	95% acetonitrile and 5% water
4	10 mM ammonium formate in 95% water and 5% acetonitrile	95% acetonitrile and 5% water
5	1mM ammonium acetate in 95% water and 5% acetonitrile	95% acetonitrile and 5% water
6	3mM ammonium acetate in 95% water and 5% acetonitrile	95% acetonitrile and 5% water
7	5mM ammonium acetate in 95% water and 5% acetonitrile	95% acetonitrile and 5% water
8	10 mM ammonium acetate in 95% water and 5% acetonitrile	95% acetonitrile and 5% water
9	5mM ammonium formate in 95% water and 5% acetonitrile	5mM ammonium formate in 95% acetonitrile and 5% water
10	5mM ammonium formate in 95% water and 5% methanol	5mM ammonium formate in 95% methanol and 5% water
11	5mM ammonium formate in 95% water and 5% methanol	95% methanol and 5% water
12	5mM ammonium formate in 95% water, 2.5% methanol and 2.5% acetonitrile	47.5% methanol, 47.5% acetonitrile and 5% water
13	5mM ammonium formate in 95% water, 4% acetonitrile and 1% methanol	76% acetonitrile, 19% methanol and 5% water

Mass spectrometry conditions and source parameters were optimized through full (MS2) scan, single ion monitoring (SIM) scan, product ion (PI) scan and multiple reaction monitoring

(MRM) experiments, under the appropriate ionization source condition. Optimum collision cell energy, fragmentor voltage for each target PFAS, as well as their cell accelerator voltage, delta EMV, and source parameters (gas temperature and flow, sheath gas temperature and flow, nebulizer pressure, capillary voltage, and nozzle voltage) were determined.

Full scan, SIM scan and PI scan experiments were performed independently for each target PFAS using the 0.1 µg/mL stock solution. During the full (MS2) scan, each analytical solution was scanned in a range of 50-600amu under both positive and negative modes of ionization source, separately, to preliminary determine the precursor ion (Figure 3.4). In the SIM scan analysis, fragmentor voltages for each chemical were evaluated in a range of 80-130V to optimize peak-shape of chromatography. The selection of optimal fragmentor voltage based on the peak height and area of the chromatogram for each compound (Figure 3.5 and Table 3.3). Information regarding precursor ions and their detention times were confirmed in a narrow scan window during the SIM scan. In the PI scan, collision energy optimization experiments (0-60eV) were conducted to identify all major product ions of each target PFAS (Figure 3.6). The MRM analysis experiments were carried out by integrating the optimized conditions from the full SIM and PI scan. These experiments were performed to evaluate different cell accelerator voltages (4-7V), delta EMV (200-400V) and source parameters [gas temperature (225-325°C), gas flow (5-11L/min), sheath gas temperature (250-350°C), sheath gas flow (8-12 L/min), nebulizer pressure (30-45psi), capillary voltage (1500-3500V) and nozzle voltage (0-2000V)].





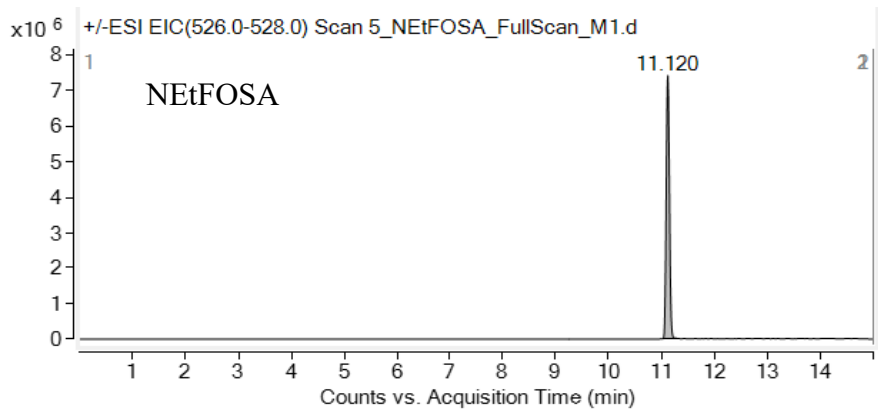
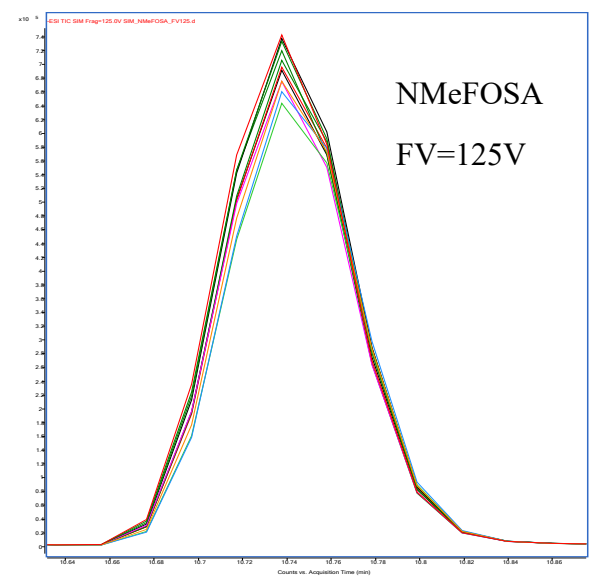
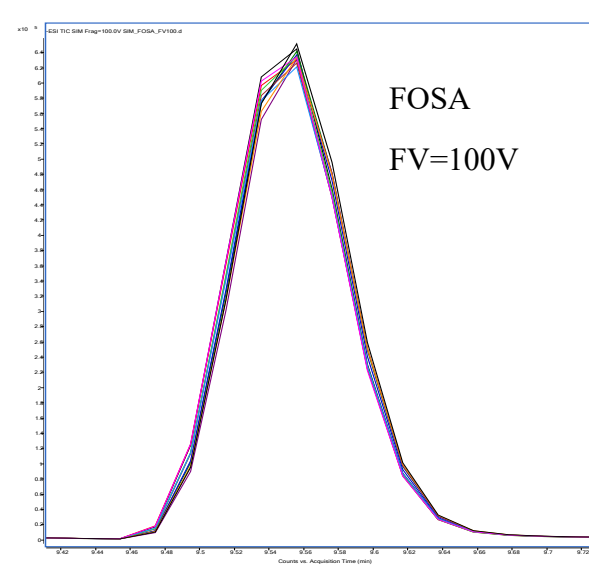
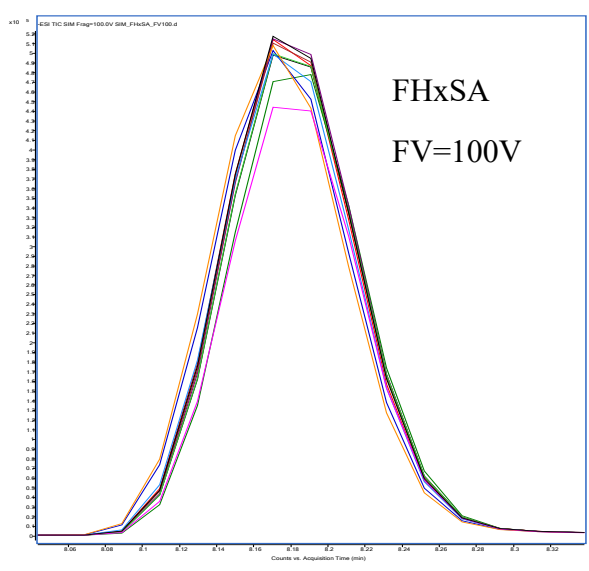
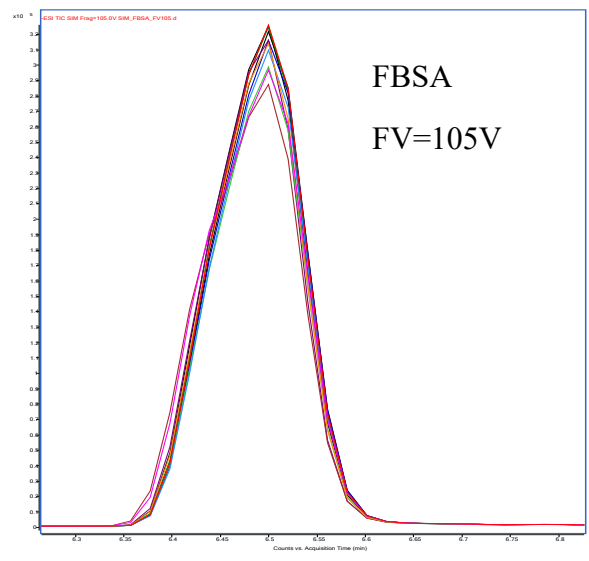


Figure 3.4 Full Scan Analysis for Target Analytes.



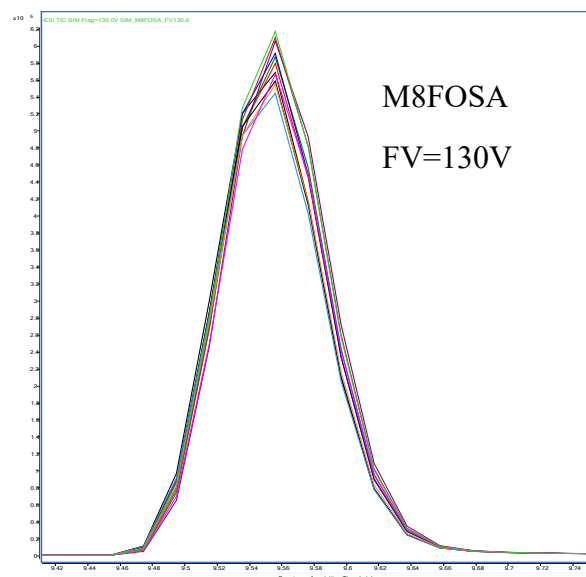
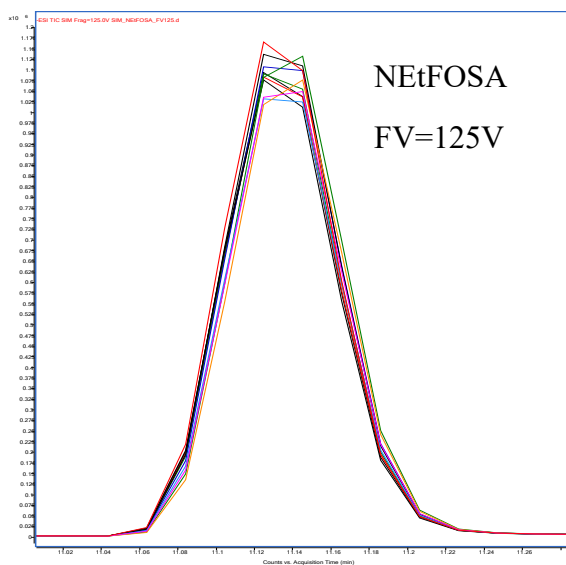


Figure 3.5 SIM Scan Analysis and Optimal Fragmentor Voltage Selection for Target Analytes.

Fragmentor Voltage (V)	Peak Area					
	FBSA	FHxSA	FOSA	NMeFOSA	NEtFOSA	M8FOSA
80	2043723	2622212	3040843	2727580	4561396	2634196
85	2078173	2655219	3063804	2796779	4657602	2667519
90	2118761	2355986	3117296	2847276	4639564	2700422
95	2139333	2630300	3166129	2835198	4645129	2684797
100	2161939	2703388	3126208	2901925	4755104	2749977
105	2167254	2678173	3108030	2924241	4754978	2772080
110	2154832	2508653	3098668	2968563	4773984	2803623
115	2102337	2655892	3073809	3016228	4909846	2831294
120	2095958	2696691	3017959	3092130	4994982	2874217
125	2037751	2682765	3042614	3112922	5037233	2902442
130	1981034	2635551	3081594	3079497	4931179	2943681

Table 3.3 The Peak Area of each Target FASAs under Various Fragmentor Voltages.

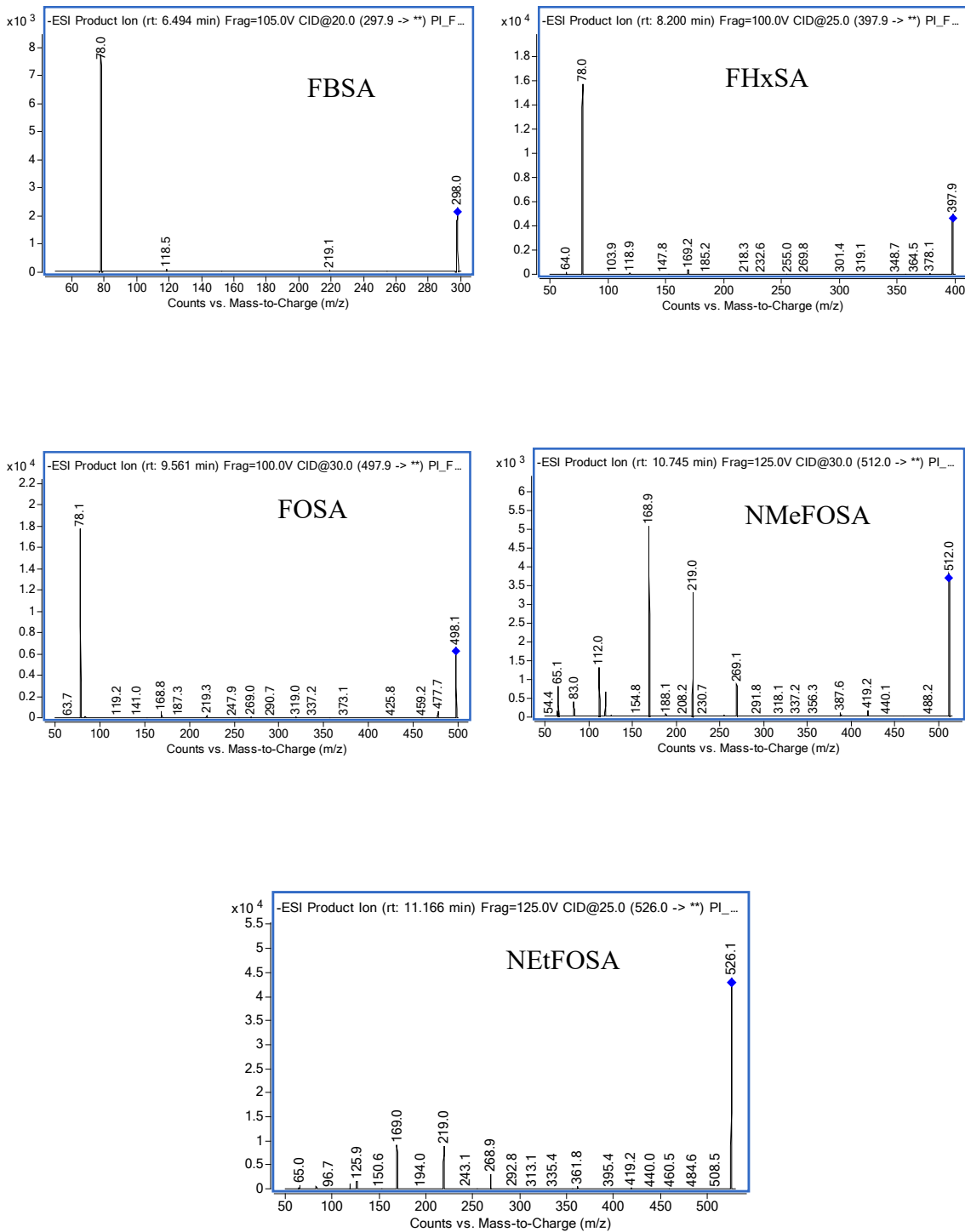


Figure 3.6 PI Scan Analysis for Target Analytes.

3.2.4 Extraction Method Selection

Two PFAS solid phase extraction (SPE) protocols were implemented to evaluate the recovery rate of target analytes using Oasis WAX and HLB Prime extraction cartridges. Two concentrations (10ng/sample and 50ng/sample) of target PFAS mixtures were added into LC grade water (200mL for each sample, 5 replicates each), and subjected to the two different extraction methods, while other procedures remained consistent. The extraction protocols are detailed below.

Protocol 1: Oasis WAX cartridges were preconditioned with 4mL of 1% NH₄OH in methanol, followed by 4mL of methanol, and finally 4mL of water, in order to activate the internal polymer. The samples were then loaded onto the cartridges. To ensure the full capture of all target chemicals from the samples, the sample container was rinsed with 10mL of LC water and added to the same cartridge. Once all sample was loaded, 10mL of 25mM ammonium acetate in water buffer solution was added to each cartridge to adjust the pH and remove water-soluble impurities. After drying out the cartridges, the target analytes trapped in the polymer were eluted using organic solvents (5mL of methanol followed by 5mL of 1% NH₄OH in methanol).

Protocol 2: Oasis HLB Prime cartridges were tested in this protocol. The samples were directly loaded onto the cartridges without preconditioning. LC water (10mL) was also used to rinse the sample containers. Before the elution of target PFAS, 4mL of LC water was used to clean the cartridges. The final elution solvent used was 10mL of methanol.

After the SPE cleanup procedure, all eluates (10mL) were evaporated using a rotary evaporator (Rotavapor R-300, Buchi) under specified conditions: a 45 °C water bath, 75rpm rotation, and 150mbar vacuum pressure. The target analytes were extracted with a 2.5mL solution

of a methanol-water mixture (95:5, v/v). Each sample was then spiked with 5ng/mL of IS and subjected to analysis via the UHPLC-LC/MS system.

The recovery rate of each target analyte was calculated using the following equation:

$$\text{Recovery (\%)} = [(\text{Response of the Spiked Sample}) / (\text{Response of the Neat Standard})] \times 100$$

3.2.5 Method Validation and Quality Control

Calibration Curve Development

The calibration stock solution (100 ng/mL) was diluted into a series level of concentrations, including 20 ng/mL, 10 ng/mL, 5 ng/mL, 2 ng/mL, 1 ng/mL, 0.5 ng/mL, 0.2ng/mL. The internal standard was spiked at a concentration of 5ng/mL in these calibrations. The calibration curve experiments were conducted using these seven solutions on the UHPLC-MS/MS system. The Agilent Masshunter software QQQ Quantitative Analysis 10.2 was employed to process the calibration data and construct a seven-point calibration curve for each target analyte. These calibration curves were developed for quantifying the unknown concentrations of target analytes in samples. To ensure the reliability of the results, the accuracy and linearity of calibration curves were evaluated.

Method Precision

Quality control samples at three concentrations (1,5,20ng/mL) were prepared by diluting the calibration stock solution in the working solutions, with the internal standard spiked at a concentration of 5ng/mL in each sample. These three quality control samples were run in the same experiment bath every 48 hours (day 1, day 3 and day 5). The related standard deviation (%RSD) of each quality control sample across the three days was determined to assess the precision of the method. The formula for the related standard deviation is as follows:

%RSD = 100× the sample standard deviation/ sample mean

Matrix Effect Experiment

Water samples (200mL) were spiked with standard sulfonamide solutions at a concentration of 10ng and processed through the solid-phase extraction (SPE) method using Oasis Wax cartridges. Following extraction, samples were concentrated to 1mL using a mixture of methanol and water at a ratio of 95:5 (v/v) and analyzed. The results of our analysis are displayed in Table 3.4. Compounds FBSA, FHxSA, and FOSA had recoveries ranging from 93.3% to 117.4%, while the recoveries for alkylated sulfonamides, NMeFOSA, and NEtFOSA were between 42.1% and 54.9%. These values are summarized in Table 3.4.

Here is the percent recovery (%R) equation: $\%R = \frac{(A-B)}{C} \times 100$

A = measured concentration in the fortified sample,

B = measured concentration in the unfortified sample, and

C = fortification concentration

Table 3.4 Recovery Rate (% recovery) of Matrix Effect Experiment.

	FBSA	FHxSA	FOSA	NMeFOSA	NEtFOSA
Sample 1	113.1	115.4	99.1	54.9	54.4
Sample 2	107.0	117.4	93.3	42.5	42.1
Sample 3	107.5	114.9	109.0	43.2	43.6

3.3 Results and Discussion

3.3.1 Optimum UHPLC-MS/MS Conditions

The ZORBAX RRHD Eclipse Plus C18 analytical column (2.1 ×50 mm, 1.8 μm, Part No. 959757-902) achieved the optimal separation for target sulfonamides. Among all mobile phase

solvent combinations tested, 5mM ammonium formate in water/methanol (95/5, v/v) (A) and 5mM ammonium formate in methanol/water (95/5, v/v) (B) were selected as the mobile phases. The mobile phase mixture was conveyed through the column at 0.2mL/min, adhering to the following gradient: 0min (50%B); 0.2min (50%B); 0.5 min (80%B); 1 min (90%); 2.5 min (99%); 4.5 min (99%); 5 min (50%). Separation was accomplished within 5 minutes, followed by a 2-minute post-run time. The temperature of the analytical column was maintained at 50 °C. In each run, a 10 µL volume of the sample was injected into the system for analysis, followed by a wash with a solvent mixture of methanol, acetonitrile and water (40/40/20, v/v). The optimal conditions of UHPLC system are present in Table 3.5.

Table 3.5 Optimal conditions for UHPLC.

Optimal UHPLC Conditions			
Agilent Infinity 1290	II model G7120A		
Analytical column	ZORBAX RRHD Eclipse Plus C18, 2.1 × 50 mm, 1.8 µm, Part No. 959757-902		
Guard column	Agilent ZORBAX Eclipse Plus C18 (2.1 × 5 mm, 1.8 µm, p/n 821725-901)		
Mobile phase	A. 5mM ammonium formate in water/methanol (95/5, v/v) B. 5mM ammonium formate in methanol/water (95/5, v/v)		
Gradient method conditions	Time	A%	B%
	0	50	50
	0.2	50	50
	0.5	20	80
	1.0	10	90
	2.5	1	99
	4.5	1	99
	5.0	50	50
	Post run: 2 min		
Flow rate	0.2mL/min		
Total runtime	5 min		
Column temperature	50 °C		
Injection volume	10 µL		
Injection wash solvent	Methanol/acetonitrile/water (40/40/20, v/v)		

The JetStream Electrospray Ionization Source operated in the negative mode, a state where the solvent evaporated, and target analytes were subsequently ionized. These ionized chemicals were then directed to the triple quadrupole mass spectrometer for quantification. The optimized ionization source parameters, along with the MRM conditions, are summarized in Table 3.6 and Table 3.7. The chromatogram of each target sulfonamide with the optimum separation and peak shape is presented in Figure 3.7.

Table 3.6 Optimal conditions for Ionization Source and Mass Spectrometer (MS).

MS and Ionization Source Conditions	
Ionization Source	JetStream Electrospray Ionization Source (Negative mode)
Mass Spectrometer	Agilent G6460C
Gas temperature	275 °C
Gas flow	7 L/min
Nebulizer	45 Psi
Sheath gas temperature	375 °C
Sheath gas flow	10 L/min
Capillary voltage	3500V
Nozzle voltage	0V
Delta EMV	200
MS1 and MS2 resolution	Unit

Table 3.7 MRM Conditions for Each Target FASAs.

Target Analytes	Retention Time (Rt. Min)	Precursor Ion (m/z)	Product Ion (m/z)	Fragmentor Voltage (V)	Collision Energy (eV)	Cell Accelerator Voltage (V)
1 FBSA	1.981	297.9	78	105	20	5
2 FHxSA	2.304	397.9	78	100	25	5
3 FOSA	2.636	498	78	100	30	5
4 NMeFOSA	2.990	512	169/219	125	30	5
5 NEtFOSA	3.150	526	169/219	125	25	5
SS MPFOS	2.221	503	99/80	180/150	48/55	4
IS M8FOSA	2.636	506	78	160	30	5

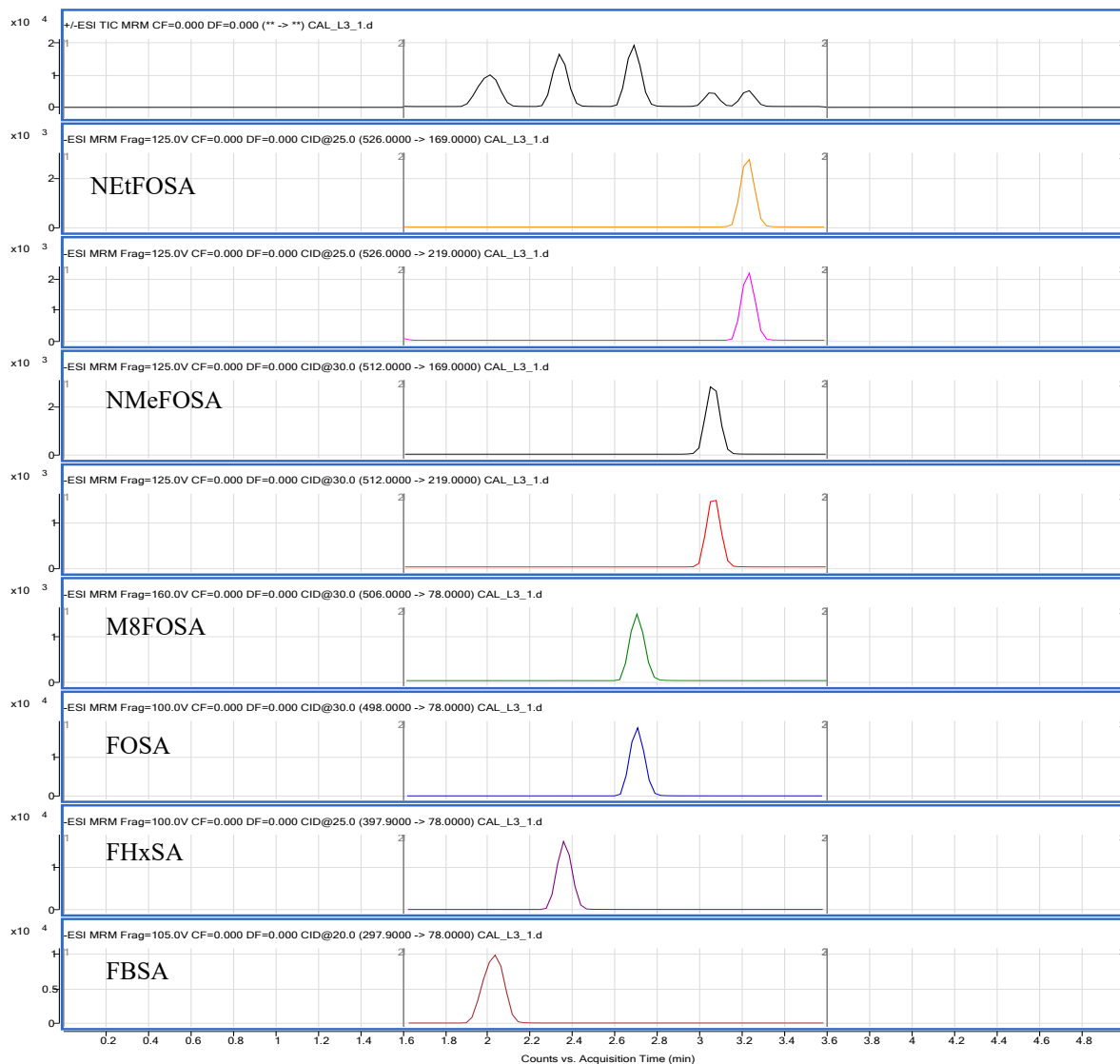


Figure 3.7 The optimal Chromograms for Each Target FASAs.

3.3.2 Sample Extraction Method Selection

The comparison of the two sample extraction protocols is illustrated in Table 3.8, Figure 3.8, and Figure 3.9. These exhibit the average percent recovery rate of the five replicated samples. Upon comparison of the recovery rates for each analyte, the results using the WAX cartridge (Protocol 1) demonstrated superior recovery rates. The recovery rate using the WAX cartridge was

between -1.9% and 21.1% higher than that of the HLB cartridge for the target analytes. Consequently, the SPE protocol using the WAX cartridge was selected for the subsequent sample preparation procedures.

Table 3.8 Percent recovery rate (Unit: %) of the two extraction protocols for each target PFAS. (Mean \pm Standard deviation)

Analytes	(P1) WAX		(P2) HLB		Difference (%WAX-%HLB)	
	10ng/sample	50ng/sample	10ng/sample	50ng/sample	10ng/sample	50ng/sample
FBSA	86.2 \pm 11.6	72.8 \pm 4.7	73.0 \pm 5.4	66.3 \pm 6.8	13.2	6.5
FHxSA	97.6 \pm 15.3	83.6 \pm 4.6	76.5 \pm 6.7	73.5 \pm 8.8	21.1	10.1
FOSA	82.0 \pm 9.9	84.1 \pm 4.1	65.2 \pm 5.7	72.6 \pm 6.9	16.8	11.5
NMeFOSA	40.5 \pm 11.3	23.2 \pm 1.9	28.4 \pm 7.3	25.1 \pm 5.6	12.2	-1.9
NEtFOSA	42.2 \pm 11.1	24.4 \pm 1.8	30.1 \pm 7.3	25.9 \pm 5.3	12.1	-1.5
MPFOS	92.9 \pm 2.5	98.0 \pm 4.2	92.2 \pm 4.0	98.2 \pm 3.7	0.7	-0.3

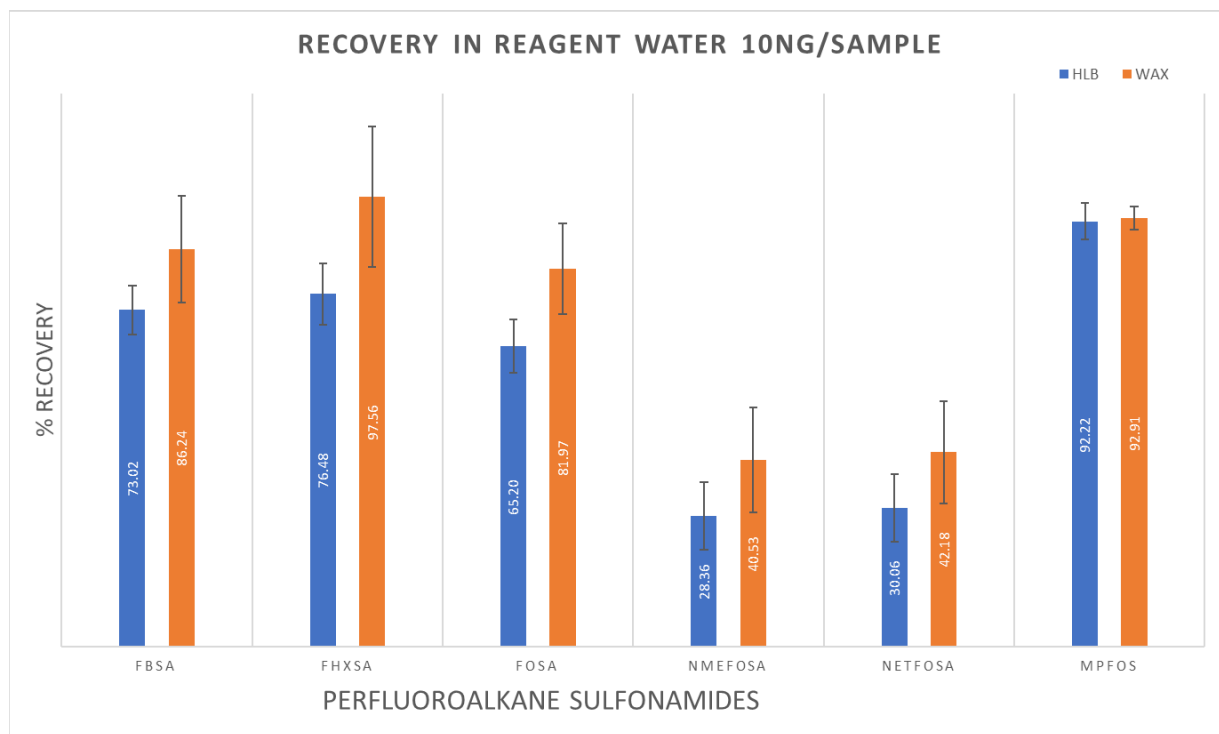


Figure 3.8 Recovery Rate and standard deviation of each Target Analyte in Reagent Water (10ng/Sample).

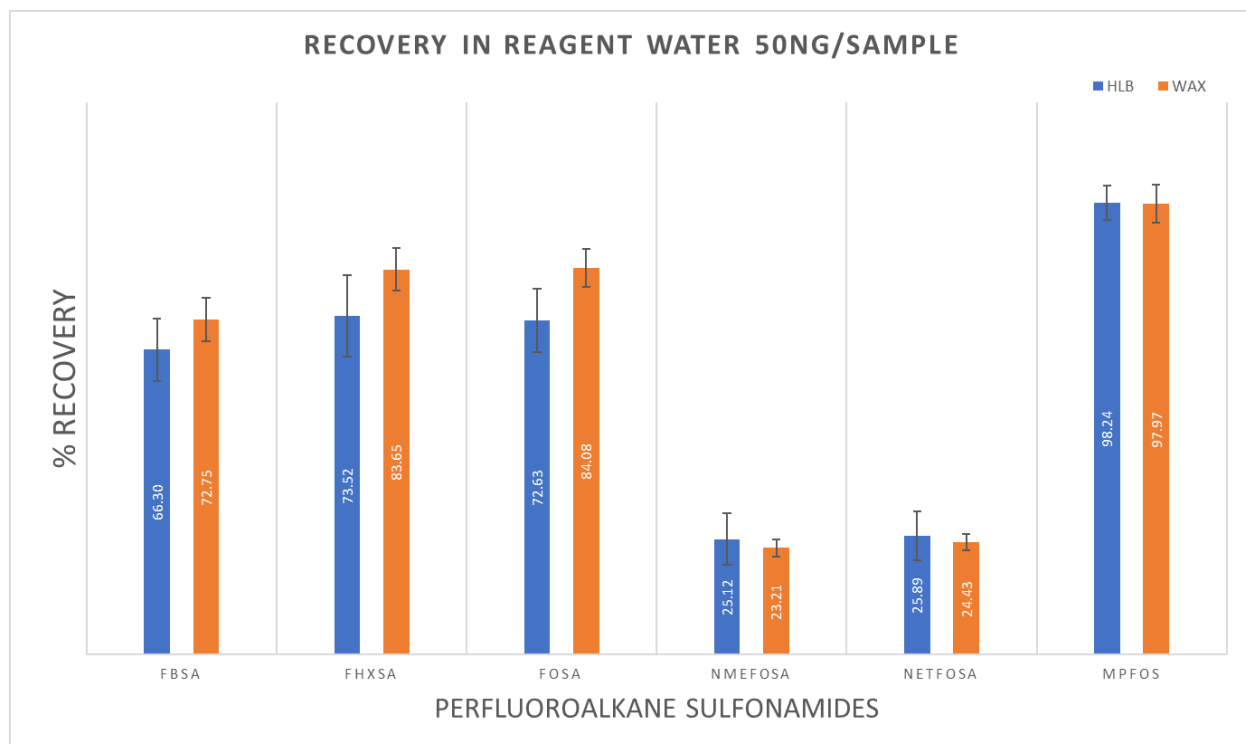


Figure 3.9 Recovery Rate and standard deviation of each Target Analyte in Reagent Water (50ng/Sample).

3.3.3 Result of Method Validation and Quality Control

Calibration Curve

A seven-point calibration curve was developed (0.2-20ng/mL) for each target FASA and MPFOS, as depicted in Figure 3.10. The linearities (r^2) for all calibration curves are greater than 0.999, suggesting a substantial positive correlation between the concentration of target analytes and their peak response in the mass spectrometer. The accuracy data for each analyte is summarized in Table 3.9. The acceptable accuracy range for quality control is 70-130% of the true value. The lowest concentration level (0.2ng/mL) for FBSA, NMeFOSA and NEtFOSA surpassed this acceptable criterion. However, all other six levels complied with the acceptable range. For FHxSA and FOSA, all seven concentration levels complied with the acceptable range. As a result, the calibration curve for FBSA, NMeFOSA and NEtFOSA were derived from the six

concentration levels. Meanwhile, all seven concentration levels were used for FHxSA and FOSA to construct the calibration curves.

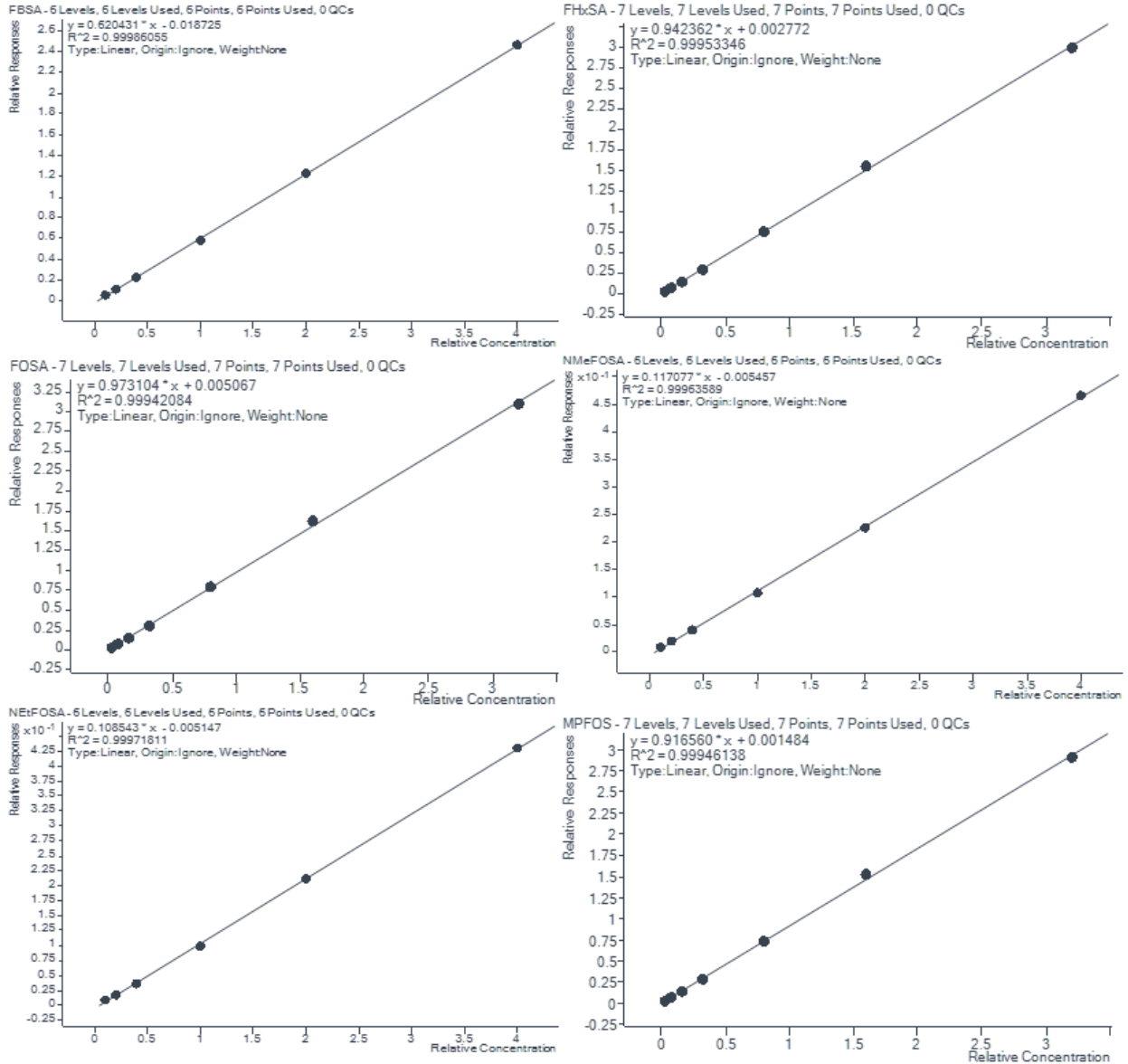


Figure 3.10 Calibration Curves for Target FASAs.

Table 3.9 The Accuracy of the Calibrations.

Concentration ng/mL	Calibration Curve Accuracy (%)					
	FBSA	FHxSA	FOSA	NMeFOSA	NEtFOSA	MPFOS (SS)
0.2	148.6	81.9	76.4	175.8	175.8	83.3
0.2	148.0	83.5	73.6	175.0	186.4	79.4
0.2	147.3	86.6	79.4	176.7	174.3	80.4
0.5	112.4	91.2	87.5	122.3	129.4	92.1
0.5	113.1	93.5	87.5	125.0	117.9	96.1
0.5	112.4	93.8	88.8	117.3	117.8	91.4
1	99.5	92.9	93.2	102.0	106.0	91.6
1	102.4	94.5	92.4	104.8	104.9	93.7
1	100.2	95.7	93.7	105.6	97.0	98.2
2	97.9	95.9	98.7	94.9	96.7	95.8
2	98.1	97.7	97.7	96.6	91.8	96.7
2	98.6	99.2	98.1	100.9	95.4	99.0
5	96.6	99.6	100.8	95.0	95.7	97.3
5	95.4	99.4	99.9	97.4	95.6	98.4
5	96.7	100.6	100.8	94.4	94.2	103.6
10	101.0	103.1	103.8	98.7	99.5	104.4
10	100.5	103.9	104.4	99.5	100.8	103.7
10	99.1	103.2	102.9	96.8	99.1	102.8
20	100.2	99.1	99.3	101.0	102.1	100.9
20	100.2	98.9	99.0	100.2	99.6	97.2
20	100.2	99.6	99.0	100.8	99.4	99.3

Method Precision

The precision of the method for each target analyte across three different concentrations is detailed in Table 3.10. The percentage related standard deviations (%RSD) were calculated from all data (5 replicates each) collected over three days. The %RSD for the concentrations of replicate analyses should not exceed 20% for all method analytes (Rosenblum & Wendelken, 2019). Remarkably, in this method, the %RSD for all target compounds fell within a range of 0.61% to 4.37%, highlighting the high precision of this method.

Table 3.10 Results of Precision Experiment (ng/mL).

		FBSA	FHxSA	FOSA	NMeFOSA	NEtFOSA	MPFOS	
1ng/mL	Day1	0.85	0.78	0.76	0.82	0.85	0.74	
		0.85	0.76	0.74	0.90	0.90	0.79	
		0.83	0.77	0.74	0.91	0.84	0.71	
		0.82	0.76	0.78	0.87	0.86	0.71	
		0.86	0.77	0.75	0.89	0.88	0.77	
	Day2	0.82	0.73	0.74	0.84	0.86	0.79	
		0.83	0.73	0.74	0.87	0.84	0.80	
		0.84	0.73	0.73	0.83	0.89	0.78	
		0.83	0.75	0.70	0.83	0.87	0.80	
		0.83	0.73	0.73	0.83	0.86	0.82	
	Day3	0.83	0.78	0.75	0.85	0.83	0.79	
		0.84	0.78	0.73	0.84	0.80	0.81	
		0.85	0.76	0.74	0.83	0.86	0.75	
		0.84	0.77	0.73	0.82	0.85	0.79	
		0.83	0.79	0.76	0.85	0.83	0.82	
		Mean	0.84	0.76	0.74	0.85	0.85	0.78
		SD	0.01	0.02	0.02	0.03	0.03	0.03
		%RSD	1.51	2.61	2.35	3.54	2.96	4.37
5ng/mL	Day1	4.09	4.27	4.26	4.09	4.07	4.13	
		4.11	4.27	4.21	4.00	4.03	4.21	
		4.08	4.27	4.29	4.03	3.98	4.19	
		4.13	4.23	4.27	4.03	4.11	4.16	
		4.10	4.27	4.24	3.98	4.00	4.28	
	Day2	4.14	4.29	4.24	3.97	4.09	4.23	
		4.15	4.23	4.26	4.03	3.89	4.20	
		4.08	4.24	4.22	4.15	3.99	4.31	
		4.06	4.14	4.22	3.82	3.97	4.14	
		4.11	4.21	4.22	4.11	4.08	4.19	
	Day3	4.16	4.22	4.22	3.97	3.99	4.15	
		4.15	4.18	4.20	4.03	3.96	4.18	
		4.21	4.28	4.25	4.00	4.05	4.23	
		4.13	4.29	4.26	3.99	4.11	4.32	
		4.16	4.24	4.21	4.04	4.12	4.10	
		Mean	4.12	4.24	4.24	4.02	4.03	4.20
		SD	0.04	0.04	0.03	0.07	0.07	0.07
		%RSD	0.91	0.98	0.61	1.85	1.68	1.55
20ng/mL	Day1	18.30	18.26	18.11	18.03	18.36	18.33	
		18.19	17.91	17.85	17.85	18.28	18.17	

	18.15	17.97	17.95	18.12	18.29	18.00
	18.31	18.08	18.06	18.24	18.41	18.07
	18.11	18.11	18.00	18.39	18.38	17.82
Day2	18.23	17.98	17.78	18.32	17.74	18.12
	18.43	18.20	18.23	18.32	18.21	18.29
	18.40	18.18	18.16	18.47	18.32	17.97
	18.42	18.15	18.00	18.23	18.08	18.38
	18.20	17.91	17.89	17.87	18.15	18.11
Day3	18.51	18.26	18.13	18.29	18.11	18.21
	18.22	17.69	18.06	18.62	18.56	18.74
	18.14	17.73	18.11	18.62	18.26	18.47
	18.04	17.92	17.96	18.59	18.46	18.23
	18.04	17.82	17.97	18.26	18.28	18.29
Mean	18.25	18.01	18.02	18.28	18.26	18.21
SD	0.15	0.18	0.12	0.24	0.19	0.22
%RSD	0.80	1.02	0.68	1.33	1.06	1.23

3.4 Application to Surface Water Samples

3.4.1 Sample Collection

A total of 46 surface water samples were collected in the Chattooga River watershed on August 9, 2022, at 23 sampling locations, and duplicate samples were collected at each location (refer to Figure 3.11 for the detailed location). The sampling sites were located along the Chattooga River and several of its tributary creeks, in proximity to potential contamination sources. These sources include wastewater treatment plant (WWTP), chemical production facilities, and industrials manufacturing PFAS-containing products (Appendix B.3). Detailed information about each site can be found in Table 3.11.

Samples were collected in high-density polyethylene (HDPE) containers and kept in a cooler with ice during transportation to the laboratory. Prior to the collection process, each container was meticulously rinsed with deionized (DI) water. A field blank, consisting of DI water,

was prepared in the lab, transported to the field, and subjected to the same processing procedure as the surface water samples to ensure consistent treatment.

Table 3.11 Details of Sampling Locations.

Sample ID	Long	Lat	Details
1	-85.2861	34.6980	Chattooga River Headwaters - upstream of WWTP
2	-85.2815	34.6984	Town Creek - upstream of WWTP
3	-85.2935	34.6787	Chattooga River - Downstream from Lafayette
4	-85.3000	34.6667	Chattooga River - Downstream of Industries in Lafayette
5	-85.3277	34.6110	Chattooga River - Upstream of Duck Creek
6	-85.3470	34.6190	Duck Creek
7	-85.3520	34.5823	Chattooga River - Upstream of Spring and Teloga Creeks
8	-85.3770	34.5548	Teloga Creek
9	-85.3355	34.5622	Chattooga River - Upstream from Sources
10	-85.3106	34.5607	Cane Creek
11	-85.3098	34.5447	Chattooga River - Downstream from Mt Vernon
12	-85.2986	34.5464	Chappel Creek
13	-85.3008	34.5395	Chattooga River - Downstream from WWTP
14	-85.3012	34.5196	Chattooga River - Downstream from WWTP
15	-85.3350	34.4678	Chattooga River - Upstream Summerville
16	-85.3626	34.4449	Chattooga River - Downstream from Summerville Ind
17	-85.3795	34.4404	Racoon Creek
18	-85.3959	34.4021	Chattooga River - Downstream from Raccoon Creek + Mohawk Ind
19	-85.3944	34.3784	Taliaferro Creek
20	-85.4456	34.3357	Chattooga R. - Downstream from Hinton C., Upstream from AL
21	-85.5096	34.2959	Mills Creek
22	-85.5092	34.2902	Chattooga River - Downstream of Mills Creek
23	-85.5600	34.2635	Chattooga River - Upstream of Lake

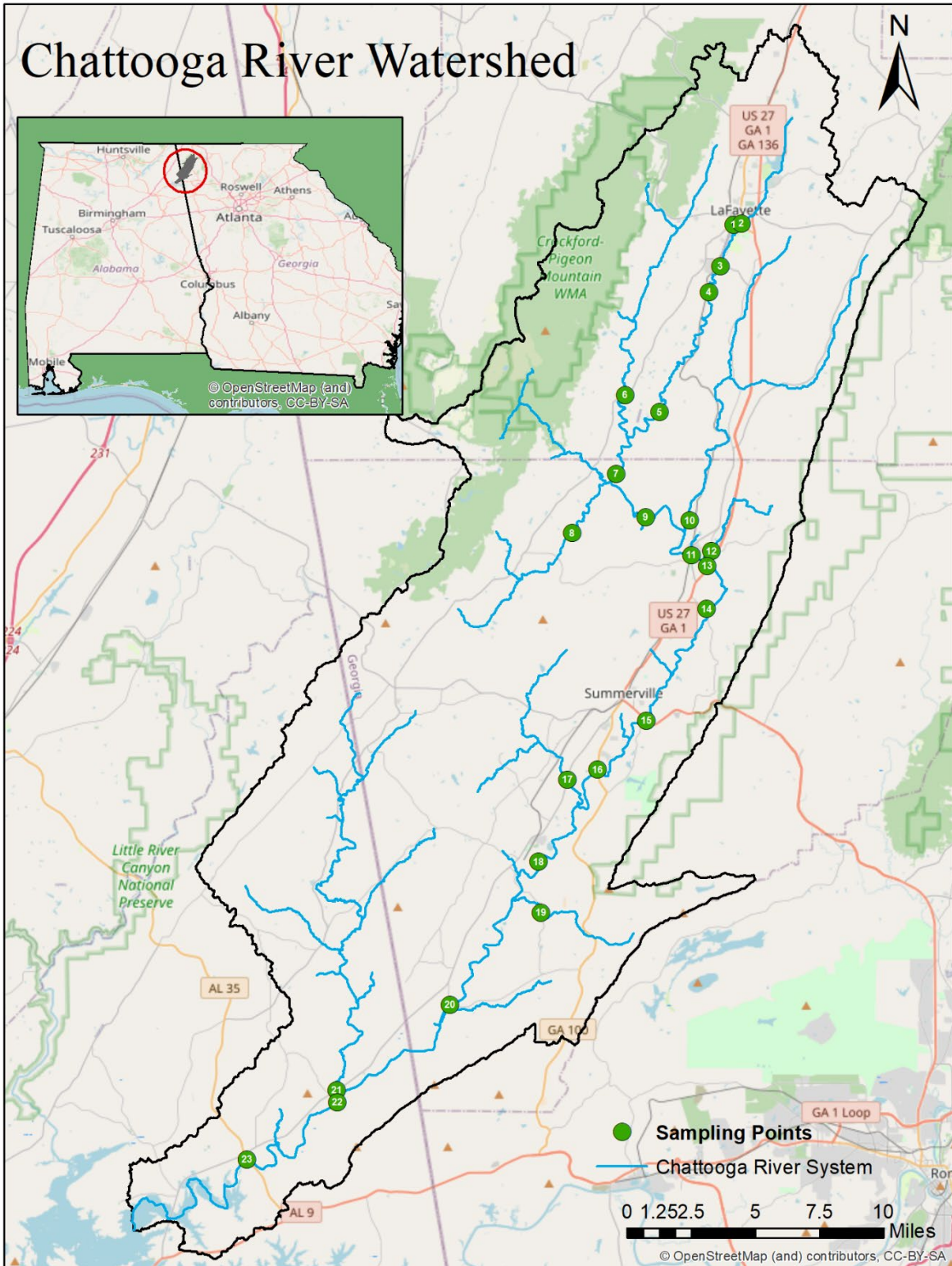


Figure 3.11 Sample Sites in Chattooga Watershed.

3.4.2 Sample Preparation

Surface water samples were initially filtered through Whatman glass microfiber filters (0.7 μ m) using a vacuum-assisted microfiltration assembly to remove any suspended solid matter. The pH of the filtered water samples was adjusted to 6.5. Subsequently, sample extraction was executed for each sample, utilizing Waters Oasis WAX (weak anion exchange) cartridges (150mg, 6cc) arranged on a 20-position vacuum manifold. Before the SPE cleanup, surface water samples were spiked with 12.5ng of surrogate standards (MPFOS) per sample (400mL). Two cartridges were used for each sample to process 200mL of water sample. The cartridges were first conditioned sequentially with 4mL of 1% ammonium hydroxide in methanol, 4mL of methanol solvent, and 4mL of water. Thereafter, the samples were loaded into the cartridges at an elution flow rate of one drop per second. Upon completing the 200mL sample passage through each cartridge, 10mL of water was used to thoroughly rinse the respective sample containers and subsequently loaded into the same cartridges. Next, 10mL of ammonium acetate (25mM) in water buffer (pH 4) solution were added into the cartridges to adjust the pH and eliminate the water-soluble impurities. Once the cartridges were dried, the target compounds retained within the cartridge polymers were eluted using 5mL of methanol and 5mL of 1% ammonium hydroxide in methanol. The fractions of the same sample were combined and concentrated using a rotary evaporator (Rotavapor R-300, Buchi) under specified conditions: a 45°C water bath, 75rpm rotation, and 150mbar vacuum pressure. The target compounds were subsequently extracted with a 2mL solvent mixture of methanol and water (95:5, v/v). Lastly, each water sample extraction was spiked with internal standard at 5ng/mL and analyzed via the UHPLC-MS/MS.

3.4.3 Quality Control

To ensure the integrity and reliability of the data, stringent quality control measures were incorporated. These included the preparation of field blanks and a quality control sample processed along with the surface water samples. Duplicate samples were prepared for all locations, and each of these duplicates was run 5 times through the UHPLC-MS/MS system. In all field blanks, no target analytes were detected, suggesting there was no cross contamination in the sample processing workflow. The recovery rate for each FASA in the quality control samples fell within the acceptable range of 70-130%. The recovery rate of the five target analytes in the quality control are 80.4% (PFBA), 84.9% (PFH_xSA), 85.1% (FOSA), 80.0% (NMeFOSA), 79.8% (NEtFOSA). The surrogate standard (MPFOS), which was spiked before the SPE process, was also recovered within the sample acceptable range. The recovery of surrogate standard MPFOS in each sample and quality control are presented in Table 3.12.

Table 3.12 The Recovery Rate of Surrogate Standard MPFOS in Surface Water Samples and Quality Control.

Sample ID	MPFOS Recovery	Sample ID	MPFOS Recovery
1	82.1%	13	75.7%
2	79.9%	14	72.7%
3	100.5%	15	87.7%
4	87.1%	16	86.1%
5	113.0%	17	81.0%
6	90.3%	18	84.8%
7	89.0%	19	87.7%
8	86.0%	20	82.8%
9	94.4%	21	89.0%
10	92.7%	22	86.6%
11	97.2%	23	86.6%
12	73.9%	Quality Control	85.4%

3.4.4 Target PFAS in Water Samples

In the analysis of five target FASAs, only three compounds were detected in Chattooga River watershed, including FBSA, FHxSA and FOSA. Neither of the methyl nor ethyl derivatives (NMeFOSA, NEtFOSA) were present in any of the collected samples. The total FASA concentrations ranged from 0.5 to 123.2ng/L, with FBSA being the most abundant. A comprehensive summary of the concentrations, mean (\pm standard deviation), and total FASA concentrations at each sampling site is presented in Table 3.13.

FBSA was the most frequently detected analyte, found in 93% (n=43) of the samples, and represented a substantial portion of the total FASA concentrations. The mean concentrations of FBSA ranged from non-detectable to 125.8ng/L, with a median concentration of 6.9ng/L. Since

2002, when the PBSF-based production process replaced the traditional POSF-based process, the production of FBSA has increased significantly, as either a major or side product. Two previous studies have reported ubiquitous detection (100%) of FBSA in surface water from Melbourne, Australia (0.5-4.8ng/L) (Marchiandi et al., 2021), and from St. Lawrence Estuary and Gulf, Canada (0.005-0.12ng/L) (Picard et al., 2021). Besides its widespread presence in environmental water systems, FBSA is occasionally found in tap water and its sources (Kaboré et al., 2018). However, the concentration of FBSA detected in the Chattooga watershed is notably higher than in previous studies, suggesting potential contamination sources of FBSA in the area. The highest concentration was identified at sampling site 8, with the mean concentration of 123.2ng/L. This high concentration at site 8, substantially higher than at other locations, hints at substantial FBSA input from nearby contamination sources. Sample 8 was collected from Teloga Creek, situated downstream of a fire station, which could be a major source of FBSA. In recent 20 years, FBSA and its short-chain precursors have been commonly used in aqueous film forming foam (AFFF), the primary type of firefighting foam stored and utilized in fire stations. Activities related to firefighting training or unintentional releases of AFFF could be potential sources of high FBSA concentrations in the Teloga Creek tributary. With cropland and rangeland making up the majority of the Teloga Creek catchment area, the use of pesticides, which often contain FBSA, could be another source of contamination. Water from the Teloga Creek tributary flows into the Chattooga River, and the FBSA concentration at the subsequent location (site 9) is the second highest, with the mean concentration of 19.7ng/L. This concentration is significantly diluted due to the confluence of several tributary creeks into the Chattooga River in this area.

Compared to FBSA, the detection rates of FHxSA and FOSA were significantly lower, found only in 4% (n=2) and 22% (n=10) of the samples, respectively. FHxSA was only detected

at one sampling site, presenting a mean concentration of 3.2ng/L. Similar FHxSA concentrations have been observed in surface water gathered from AFFF-impacted area, such as Merette and Resolute Lakes in Italy (1.2-3.6ng/L), and downstream of the Welland River in Canada (1.0-4.2ng/L). FOSA, on the other hand, was detected in 22% of the samples from the Chattooga watershed, with a range from non-detectable to 43.1ng/L. At four out of the five sampling sites, FOSA was found at lower concentrations, with a range from non-detectable to 5.1ng/L. Previous studies have highlighted FOSA as one of the most frequently detected FASA globally, usually found at lower concentrations in surface water. Examples include findings from Stony Creek in Australia (0.2-0.8ng/L) (Marchiandi et al., 2021), Elbe River and North Sea in Germany (0.44-8.9ng/L) (Ahrens, Plassmann, et al., 2009), Todos os Santos Bay in Brazil (<0.014-3.362 ng/L) (Löfstedt Gilljam et al., 2016), Yellow Sea in China (<0.03-0.36 ng/L) (Z. Zhao et al., 2017), and even as remote as Fildes Peninsula in Antarctica (<0.04-0.12ng/L) (Cai, Yang, et al., 2012). However, in contrast with other locations, FOSA was detected at a higher concentration at sampling site 5, with the mean concentration of 41.4ng/L. Site 5 is located at the downstream of Lafayette city, receiving water that flow through various facilities such as manufacturing plants, fire stations and a Wastewater Treatment Plant (WWTP). The high concentration of FOSA at this site suggests potential contamination sources in the vicinity.

Table 3.13 Results of Surrogate Standard Recovery, Quality Control Recovery and FASAs in Chattooga Surface Water (Unit: ng/L).

Sample ID	FBSA			FHxSA			FOSA			ΣFASAs
	A	B	Mean	A	B	Mean	A	B	Mean	Mean
1	12.6 ±0.1	11.1 ±0.1	11.9 ±0.1	5.0 ±0.1	1.5 ±0	3.2 ±0.1	5.1 ±0.1	1.7 ±0	3.4 ±0.1	18.5
2	2.7 ±0	2.8 ±0.1	2.8 ±0.1	nd	nd	nd	nd	nd	nd	2.8
3	3.3 ±0	3.3 ±0.1	3.3 ±0	nd	nd	nd	nd	nd	nd	3.3
4	3.0 ±0.1	2.9 ±0	2.9 ±0.1	nd	nd	nd	0.9 ±0	0.9 ±0	0.9 ±0	3.9
5	2.6 ±0.1	2.6 ±0	2.6 ±0.1	nd	nd	nd	39.7 ±0.6	43.1 ±0.3	41.4 ±0.4	44.0
6	nd	nd	nd	nd	nd	nd	1.6 ±0	0.7 ±0.4	1.2 ±0.3	1.2
7	1.7 ±0	1.7 ±0	1.7 ±0	nd	nd	nd	0.8 ±0	0.5 ±0	0.6 ±0	2.4
8	120.6 ±0.9	125.8 ±0.9	123.2 ±0.9	nd	nd	nd	nd	nd	nd	123.2
9	20.2 ±0.1	19.2 ±0.2	19.7 ±0.1	nd	nd	nd	nd	nd	nd	19.7
10	1.0 ±0	1.5 ±0	1.3 ±0	nd	nd	nd	nd	nd	nd	1.3
11	10.4 ±0.1	11.0 ±0.2	10.7 ±0.1	nd	nd	nd	nd	nd	nd	10.7
12	4.6 ±0.1	1.1 ±0	2.8 ±0.1	nd	nd	nd	nd	nd	nd	2.8
13	10.6 ±0.1	10.3 ±0.1	10.5 ±0.1	nd	nd	nd	nd	nd	nd	10.5
14	10.2 ±0.1	8.4 ±0.1	9.3 ±0.1	nd	nd	nd	nd	nd	nd	9.3
15	9.9 ±0.2	8.4 ±0.1	9.2 ±0.1	nd	nd	nd	nd	nd	nd	9.2
16	8.0 ±0.1	7.7 ±0.1	7.9 ±0.1	nd	nd	nd	nd	nd	nd	7.9
17	2.1 ±0	1.0 ±0	1.5 ±0	nd	nd	nd	nd	nd	nd	1.5
18	7.9 ±0.2	7.9 ±0.1	7.9 ±0.1	nd	nd	nd	nd	nd	nd	7.9
19	1.5 ±0	0.9 ±0	1.2 ±0	nd	nd	nd	nd	nd	nd	1.2
20	8.1 ±0.1	7.2 ±0.1	7.6 ±0.1	nd	nd	nd	nd	nd	nd	7.6
21	0.9 ±0	nd	0.5 ±0	nd	nd	nd	nd	nd	nd	0.5
22	6.1 ±0.1	6.3 ±0.1	6.2 ±0.1	nd	nd	nd	nd	nd	nd	6.2
23	8.8 ±0.1	8.9 ±0.1	8.9 ±0.1	nd	nd	nd	nd	nd	nd	8.9

3.5 Conclusion

A rapid, sensitive, and selective method was validated and applied to the surface waters to analyze five FASA. The sample processing procedure has been optimized for the target analytes, resulting in superior recovery rates. Optimal UHPLC and MS conditions were identified, ensuring high sensitivity, superior separation, and peak resolution in a short run time. The total run time of this method is only 5 minutes, with the separation for target compounds completed within 2 minutes. In contrast to previously reported extensive and time-consuming methods, this method provides the notable advantages of handling and analyzing a substantial number of samples in a short timeframe, providing the accurate detection and monitoring FASA in environmental water samples. This efficiency enables quick screening and prompt response in assessing samples from contamination sources, thus resulting in significant time and cost savings.

The optimized sample processing procedure and analytical method were applied to the surface water samples collected from the Chattooga watershed. FBSA was detected ubiquitously in 94% of the samples, with the maximum mean concentration level reaching up to 123.2ng/L. This wide distribution of the FBSA could potentially pose risks to local wildlife, as well as indirectly impact humans through drinking waters, especially considering that the Chattooga River serves as a water supply for several cities.

Chapter 4. Qualitative Profiling of PFOA and PFOS isomers -Method Development

4.1 Introduction

Isomers are chemicals with identical molecular formulas but distinct structural arrangement. The carbon backbone arrangement of PFAS can be linear or branched, and that can

cause differences in their properties, toxicity, and behaviors. Theoretically, PFAS with longer chain length have more structural isomers. A study by Rayne et al. indicated the number of potential isomers increases rapidly for C4 to C8 PFAS (including alkyl sulfonated, carboxylates, telomere alcohols, olefins and acids and their derivatives), which has 4, 8, 17, 39 and 89 congeners separately (Rayne et al., 2008). PFOA and PFOS are two of the most well studied eight-carbon PFAS, and their branched isomers are more frequently found in the environment than other PFAS. Branched isomeric PFOA/PFOS include monomethyl substituted, and dimethyl substituted branched isomers, on a carbon of their backbones, where one or two fluorine atoms were substituted by trifluoromethyl groups.

Due to a large number of potential structural arrangements, branched isomers of long-chain PFAS are the most widely distributed in environment, such as PFOA, PFOS and PFHxS (Schulz et al., 2020). The primary source of these long-chain PFAS, especially PFOA and PFOS, is from the massive production using traditional electrochemical fluorination (ECF) process in 1956-2002. Linear long-chain PFAS were the target products of manufacturing process and desirable materials to use in producing PFAS- related industrial and commercial products. However, the ECF is a crude process, and the breakage and rearrangement of carbon chains occurs during the reaction, yielding only 70-80% desired linear PFOS, 80-85% desired linear PFOA and around 95% desired linear PFHxS (Schulz et al., 2020). The branched byproducts, along with linear PFAS, were produced, used in products, and eventually released to the environment. The long-term and large-scale use of the ECF process led to the accumulation of branched PFAS in the environment last century. To improve the purity of the synthetic chemicals, the telomerization process, a linear PFAS manufacturing technique, was developed since the 1970s and gradually replaced the ECF process (Cheremisinoff, 2016). Due to the increasing concerns of long-chain PFAS, major

manufacturers in the United States started to phase out the long-chain PFAS and discontinued using ECF process after the 2000s. They transferred their production to short-chain alternatives and applied the telomerization process as a substituted producing technique. Although the production of branched byproducts rapidly decreased after the manufacturing technique shifted, legacy isomeric PFAS still persist in the environment and are not eliminated under natural environmental conditions. In addition, the impure ECF process is regulated and banned only in some countries, and it is still in use in a number of Asian and European countries (De Voogt, 2010). Thus, the number of manufacturers worldwide that still use the ECF process is unclear, and the amount of isomeric PFAS is possibly still ever-increasing in the environment.

Isomeric long-chain PFAS have been found in surface water, groundwater and soils worldwide, as well as in the blood of wildlife and humans (Schulz et al., 2020; L. Zhao et al., 2017). Similar to PFAS with straight carbon chains, branched isomers are persistent in the environment and bioaccumulative in animals. The same molecular weight and carbon-fluorine chemical bonds are the identical properties of linear PFAS, while the varying structures make the isomers present partially distinct chemical and physical characteristics, leading to differences on their profiles and behaviors in the environment and organisms.

Multiple studies reported that the branched PFOS/PFOA detected in environment waters usually differ from the typical isomer composition of the ECF process (20-30% branched isomers). High percentages of branched PFOS are frequently found in surface water, such as the proportion of branched PFOS accounting for 51.9% in Mississippi River, USA (Benskin et al., 2010), 44-57% in Lake Ontario, Canada (Houde et al., 2008), 56.8% in Liao River, China, and 59.8% in Taihu River, China (Chen et al., 2015). The authors indicated the high percentage of branched PFOS in the surface water is largely affected by the preferential sorption of sediments to linear

PFAS isomers. The same tendency occurs in the liquid chromatography separation process, where all branched isomers elute earlier than linear PFOS on both the C18 column and the FluoroSep-rPOctyl columns, indicating that the branched isomers have lower hydrophobicity than the linear isomers (Chen et al., 2015). These studies provide evidence that linear isomers are inclined to partition to the solid phase, while branched isomers tend to stay in the liquid phase. In addition, the degradation of precursors is another source to affect the isomeric profiles of PFOS in different environmental media. Li et al. compared the FOSA content, a precursor of PFOS, in Hai River Basin, China with commercial ECF standards. He found the ratio of branched FOSA and linear FOSA in surface water was significantly lower than that in commercial ECF standards, which implied that branched FOSA is more inclined to degrade than linear FOSA in the environment (Li et al., 2020). Due to the preferential bonding of linear PFOS to sediment, the branched portion in environmental soils and sediments was found to be much lower than the linear portion. In the study of Liao River and Taihu River, the percentage of branched isomers detected in sediment samples and suspended particulate matter samples only accounts for 28.6-30% and 14.7-16.2%, respectively, which is much less than the ratio of branched isomers in water samples (Chen et al., 2015). In the sediment of Lake Ontario, the branched PFOS have a lower proportion than that in the water samples as well, only accounting for 11-19% of total PFOS (Houde et al., 2008). However, branched PFOA exhibits significantly different behaviors in the environment compared to branched PFOS, with linear PFOA typically predominating in surface water. Benskin et al. investigated surface waters from three continents (North America, Asia and Europe) and found that the branched PFOA takes 14.2-19.6% of the total PFOA, and branched PFOA proportions are comparable with or less than that in 3M ECF PFOA standards (~18%) (Benskin et al., 2010). The content of branched PFOA in sediments is variable, spanning a broad range. For instance, the

proportions of branched PFOA in the sediments of Taihu River, China, were estimated to be between 1.1% and 27.3% (Chen et al., 2015). In theory, the preferential sorption to solid phases also occurs with linear PFOA in environmental media due to its greater hydrophobicity than branched PFOA; however, the impacts of other factors make PFOA have distinct profiles. One of the primary reasons causing the higher linear PFOA proportion in environmental water is the presence of additional sources, such as the production of linear PFOA through the telomerization process. Different from the single manufacture source (ECF process) of PFOS, PFOA was massively produced from both the ECF and the telomerization process. Thus, the PFOA-containing contaminants released from manufacturing plants have a higher percentage of the linear form, which caused the increasing distribution of linear PFOA in environmental systems.

Due to the wide distribution of isomeric PFAS in the environment across the world, branched isomers of PFAS have been detected at varying levels in different animal species as well, including birds, aquatic organisms and mammals (Greaves & Letcher, 2013; Houde et al., 2008; Wang et al., 2018). Schulz et al. conducted a review of various studies and observed that animals tend to bioaccumulate the linear PFOS isomer preferentially. In contrast, humans show a preference for bioaccumulating the branched forms. This observation was made through comparisons with the isomeric contents found in ECF products, which consist of 20-30% branched isomers (Schulz et al., 2020). For instance, in a study of isomeric PFOS bioaccumulation potential in the chicken embryos, an increase in the linear PFOS proportion was found in the incubated chicken embryos mixture (83.7% linear isomer) compared to the standard mixture (62.7% linear isomer) that was injected into the eggs (O'Brien et al., 2011). The high percentages of linear PFOS were also detected in chicken eggs (~91.8% linear PFOS) around a fluorochemical facility (Wang et al., 2019) and in aquatic organisms (~85.5% linear PFOS) of environmental water (Taihu Lake,

China) (Chen et al., 2018). However, branched PFOS shows the opposite accumulation preference in blood serum of humans. According to several studies targeting populations with different ages, branched PFOS were often detected at a higher percentage in human blood than in ECF standards. For example, infants in the Swedish POPUP (Persistent Organic Pollutants in Uppsala Primiparas) Survey were found to have approximately 36% branched PFOS (Gyllenhammar et al., 2018). Similarly, about 32.9% branched PFOS was detected in the blood of 3-11-year-old children participating in the U.S. NHANES (National Health and Nutrition Examination Survey) (Ye et al., 2018). Additionally, adults from the C8 Health Project in China showed around 50.2% branched PFOS in their blood (Tian et al., 2019). Nevertheless, the bioaccumulation preference of isomers is not consistent all the time. In current studies, high percentages of branched PFOS were also reported in animal samples. For example, a high percentage of branched PFOS (70.2%) was found in the eggs of barnacle geese of Norway (Hitchcock et al., 2019). Many uncertainties could affect the behavior and fate of PFAS isomers in organisms. Due to the limited number of related studies, existing evidence is insufficient to derive an accurate isomer behavior pattern in animals and humans.

A number of studies provided evidence that PFOA and PFOS have acute toxicity and bioaccumulation potential on wildlife and humans, especially when exposed to high levels of contaminants. However, the majority of these studies analyzed the health effect and toxicity of linear PFOA/PFOS or total PFOA/PFOS in organisms, and only a few studies distinguished the varying toxic profiles of their isomers in humans and wildlife. Studies on PFAS exposure and health effects in a Chinese population (Shenyang, China) have reported the association between serum PFAS isomer concentration and a number of diseases, including liver and kidney dysfunction. Both branched PFOA and branched PFOS were found to positively associate with

serum uric acid level in adults, where a high level of uric acid could cause hyperuricemia and a series of kidney disease (Zeng et al., 2019). Another study also reported branched PFOS could increase in alanine aminotransferase (ALT) level in serum, which associates liver function biomarker disorders (Nian et al., 2019). In addition, studies targeting the US populations also found PFAS isomers exposure has effect on serum biochemistry profiles, including glucose homeostasis, serum protein/lipid profiles and components of metabolic syndrome (Liu et al., 2018).

An effective analytical method is necessary to systematically understand the profile and fate of PFOA/PFOS isomers in the environment and organisms. For isomers of each chemical, which have the same mass, the most challenging task is effectively separating and identifying the branched isomers. In this study, a validated analytical method was developed for PFOA/PFOS isomers identification and quantification using ultrahigh-performance liquid chromatography-tandem mass spectrometry (UHPLC-MS/MS) with electrospray ionization (ESI). UHPLC-MS/MS is a powerful tool for chemical analysis. Target analytes in the environmental samples can be effectively separated in UHPLC and analyzed in short running time in MS/MS detector. With the method developed, PFOA/PFOS isomers can be accurately identified and quantified from environmental and biological samples. This advancement aids in the tracing and routine monitoring of these isomers, enhancing our understanding of their profiles.

4.2 Method Development

4.2.1 Chemicals, Reagents and Materials

In this study, the target compounds include linear perfluorooctanoic acid (L-PFOA) and six branched isomers of PFOA; linear perfluorooctane sulfonate (L-PFOS) and seven branched

isomers of PFOS. Detailed information on all target analytes is provided in Table 4.1. High-purity standards (purity > 98%) were provided by Wellington Laboratories (Ontario, Canada). LC grade solvents, including methanol, acetonitrile and water were procured from VWR International (Suwanee, GA). The analytical column (Waters CORTECS UPLC C18, 1.6 μ m, 2.1 \times 150mm, p/n 186007096) and guard column (Waters CORTECS UPLC C18 VanGuard Pre-Column (1.6 μ m, 2.1 \times 5mm, p/n 186007123) were provided by Waters Corporation (Milford, MA, USA).

Table 4.1 Molecular weight, and structures of the target PFAS and isomers, and internal standard in this study.

Chemicals	Acronym	Weight (g/mol)	Molecular Structures
PFOA isomers			
n-Perfluorooctanoic acid	L-PFOA	413.9	$ \begin{array}{cccccccc} & \text{F} & \text{F} & \text{F} & \text{F} & \text{F} & \text{F} & \text{F} \\ & & & & & & & \\ \text{F} & -\text{C} & -\text{C} & -\text{C} & -\text{C} & -\text{C} & -\text{C} & -\text{C}-\text{COOH} \\ & & & & & & & \\ & \text{F} & \text{F} & \text{F} & \text{F} & \text{F} & \text{F} & \text{F} \end{array} $
Perfluoro-3-methylheptanoic acid	3-PFOA	413.9	$ \begin{array}{ccccccc} & \text{F} & \text{F} & \text{F} & \text{F} & \text{CF}_3 & \text{F} \\ & & & & & & \\ \text{F} & -\text{C} & -\text{C} & -\text{C} & -\text{C} & -\text{C} & -\text{C}-\text{COOH} \\ & & & & & & \\ & \text{F} & \text{F} & \text{F} & \text{F} & \text{F} & \text{F} \end{array} $
Perfluoro-4-methylheptanoic acid	4-PFOA	413.9	$ \begin{array}{ccccccc} & \text{F} & \text{F} & \text{F} & \text{CF}_3 & \text{F} & \text{F} \\ & & & & & & \\ \text{F} & -\text{C} & -\text{C} & -\text{C} & -\text{C} & -\text{C} & -\text{C}-\text{COOH} \\ & & & & & & \\ & \text{F} & \text{F} & \text{F} & \text{F} & \text{F} & \text{F} \end{array} $
Perfluoro-5-methylheptanoic acid	5-PFOA	413.9	$ \begin{array}{ccccccc} & \text{F} & \text{F} & \text{CF}_3 & \text{F} & \text{F} & \text{F} \\ & & & & & & \\ \text{F} & -\text{C} & -\text{C} & -\text{C} & -\text{C} & -\text{C} & -\text{C}-\text{COOH} \\ & & & & & & \\ & \text{F} & \text{F} & \text{F} & \text{F} & \text{F} & \text{F} \end{array} $
Perfluoro-6-methylheptanoic acid	6-PFOA	413.9	$ \begin{array}{ccccccc} & \text{F} & \text{CF}_3 & \text{F} & \text{F} & \text{F} & \text{F} \\ & & & & & & \\ \text{F} & -\text{C} & -\text{C} & -\text{C} & -\text{C} & -\text{C} & -\text{C}-\text{COOH} \\ & & & & & & \\ & \text{F} & \text{F} & \text{F} & \text{F} & \text{F} & \text{F} \end{array} $

Perfluoro-4,5-dimethyl-hexane sulfonate	4,5-PFOS	499.9	
---	----------	-------	--

Mass-labeled Internal Standard

Sodium perfluoro-1-[1,2,3,4- ¹³ C ₄]octane sulfonate	MPFOS	526.08	
---	-------	--------	--

4.2.2 Standard Preparation

Stock solution of 0.1µg/mL for each target PFAS were diluted in the solvent mixture (methanol: water 9:1) independently for full scan, SIM scan and PI scan analysis. A composite stock solution of 0.01µg/mL compressing all target compounds was prepared to conduct MRM experiments.

4.2.3 UHPLC-MS/MS Method Development

A chiral column, Waters CORTECS UPLC C18, 1.6µm, 2.1×150mm, p/n 186007096, was used for the separation of the isomers. A matched guard column (Waters CORTECS UPLC C18 VanGuard Pre-Column, 1.6µm, 2.1×5mm, p/n 186007123) was installed upstream of the analytical column to pre-filter the impurities. The mobile phase combination is (A) 5mM ammonium formate in water/acetonitrile/methanol (95/2.5/2.5, v/v/v) and (B) 5mM ammonium formate in water/acetonitrile/methanol (30/35/35, v/v/v), using a gradient method: 0 min (55%B); 1 min (55%B); 2 min (65%B); 17 min (75%); 18 min (80%); 30 min (90%); 32 min (95%); 33 min (99%B); 34 min (99%B); 35 min (55%). The total run time of this method is 35 minutes, with a post run of 2 minutes. Samples were injected into the system at 5µL injection volume, and carried by mobile phase solutions flow into the stationary phase column at a flow rate of 0.15mL/min,

with the column temperature of 40 °C. The ionization source parameters and MS conditions were optimized through full scan, SIM scan, PI scan and MRM experiments.

Table 4.2 Optimal conditions for UHPLC-MS/MS.

UHPLC Conditions			
Pump	Agilent Infinity 1290 II		
Analytical column	Waters CORTECS UPLC C18 (1.6µm, 2.1×150mm, p/n 186007096)		
Guard column	Waters CORTECS UPLC C18 VanGuard Pre-Column (1.6µm, 2.1×5mm, p/n 186007123)		
Mobile phase	A. 5mM ammonium formate in water/acetonitrile/methanol (95/2.5/2.5, v/v/v) B. 5mM ammonium formate in water/acetonitrile/methanol (30/35/35, v/v/v)		
Gradient method conditions	Time	A%	B%
	0	45	55
	1	45	55
	2	35	65
	17	25	75
	18	20	80
	30	10	90
	32	5	95
	33	1	99
	34	1	99
	35	45	55
	Post run: 2 min		
Flow rate	0.15mL/min		
Total runtime	35 min		
Column temperature	40 °C		
Injection volume	5 µL		
Injection wash solvent	Methanol/acetonitrile/water (40/40/20, v/v)		
MS/MS Condition			
Gas temperature	225 °C		
Gas flow	10 L/min		
Nebulizer	45 Psi		
Sheath gas temperature	350 °C		
Sheath gas flow	11 L/min		
Capillary voltage	3600V		
Nozzle voltage	1500V		

Delta EMV	400
Cell acceleration voltage	4
MS1 and MS2 resolution	Wide

Table 4.3 MRM Conditions for each target isomers.

	Target Analytes	Precursor Ion (m/z)	Product Ion (m/z)	Fragmentor Voltage (V)	Collision Energy (eV)
1	L-PFOS	499	99/80	70	50/50
2	P1-PFOS	499	419/219/169/99	70	30/30/30/40
3	P45-PFOS	499	330/280/230/180/130/80	70	40/40/40/40/40/50
4	P4-PFOS	499	330/230/180/130/80	70	40/40/40/40/50
5	P6-PFOS	499	330/280/230/169/99/80	70	40/40/40/40/40/50
6	P3-PFOS	499	319/280/169/130/80	70	40/40/40/50/50
7	P55-PFOS	499	280/230/130/80	70	40/40/50/50
8	P5-PFOS	499	280/230/180/130/80	70	40/40/40/50/50
9	L-PFOA	413	369/219/169/119	70	10/20/20/30
10	P3-PFOA	413	369/219/169/119	70	10/20/20/20
11	P4-PFOA	413	369/169/119	70	10/20/25
12	P5-PFOA	413	369/219/119	70	10/10/10
13	P6-PFOA	413	369/169	70	10/10
14	P45-PFOA	413	369/269/219/169/119	70	10/20/20/10/20
15	P55-PFOA	413	219	70	10

4.3 Results and Discussion

In this study, a qualitative method has been introduced for profiling both linear and branched isomers of PFOA and PFOS, which are perfluoroalkyl substances (PFAS) types. The method is based on ultra-high-performance liquid chromatography-tandem mass spectrometry (UHPLC-MS/MS), a highly sensitive analytical technique capable of separating and identifying even the most complex mixtures of chemicals. In implementing this method, pure stock solutions were prepared for each of the isomers, and a series of experiments were conducted using UHPLC-MS/MS to separate and identify each isomer with its specific retention times and MS/MS transitions.

4.3.1 Optimizing Chromatographic Separation of PFOA and PFOS Isomers

When performing chromatography, it is essential to conduct experiments with various columns and solvent systems to determine the ideal conditions for optimal separation and resolution of the target analytes. Before attempting chromatography, the PFOA and PFOS isomers stock solution was prepared in a methanol and water solvent mixture (9:1, v/v) to obtain a working concentration of 0.1 $\mu\text{g/mL}$ and 0.01 $\mu\text{g/mL}$. The analytical separation and identification of target isomers require careful consideration of experimental conditions and a thorough understanding of the sample preparation. This study used an ultra-high-performance liquid chromatography method to separate and identify linear and branched PFOA and PFOS isomers. Specific retention times of each isomer were identified using individual isomer standards. Multiple transitions were used to identify each isomer with structural certainty. Using a Waters CORTECS UPLC C18 column, peak separation was achieved for each isomeric compound. The column is designed for its high efficiency and excellent selectivity, making it an ideal choice for isomeric compound separation. To achieve the best possible separation between the components of a mixture, a gradient binary mobile phase solvent system was utilized. This mobile phase system was selected by blending an appropriate mixture of various solvents. By varying the composition of the mobile phase over time, a better separation of the isomers was achieved. The gradient mobile phase solvent transitioned smoothly from low to high elution strength, allowing for better separation of PFOA and PFOS isomers. The mobile phase composition, flow rate, and column temperature were also adjusted to enhance the separation process further. The analytical column was maintained at optimal thermal conditions of 40°C, with an injection volume of 5 μL and a flow rate of 0.15 mL/min. To further improve the performance of the analytical column and reduce baseline noise, a Waters CORTECS UPLC C18 VanGuard Pre-Column was incorporated upstream of the analytical column. This pre-column acted as a guard column, preventing unwanted particles from entering the analytical

column and reducing the frequency of column maintenance. Excellent separation for all the linear and branched PFOA and PFOS was accomplished within analysis time of 2 to 4 min and 7 to 10 min, respectively, as shown in Figures 4.1a and 4.1b. The optimized UHPLC conditions for each target analyte were summarized in Table 4.2, and Figures 4.1a and 4.1b illustrate the effective peak separation achieved for the monitored transitions of each isomer.

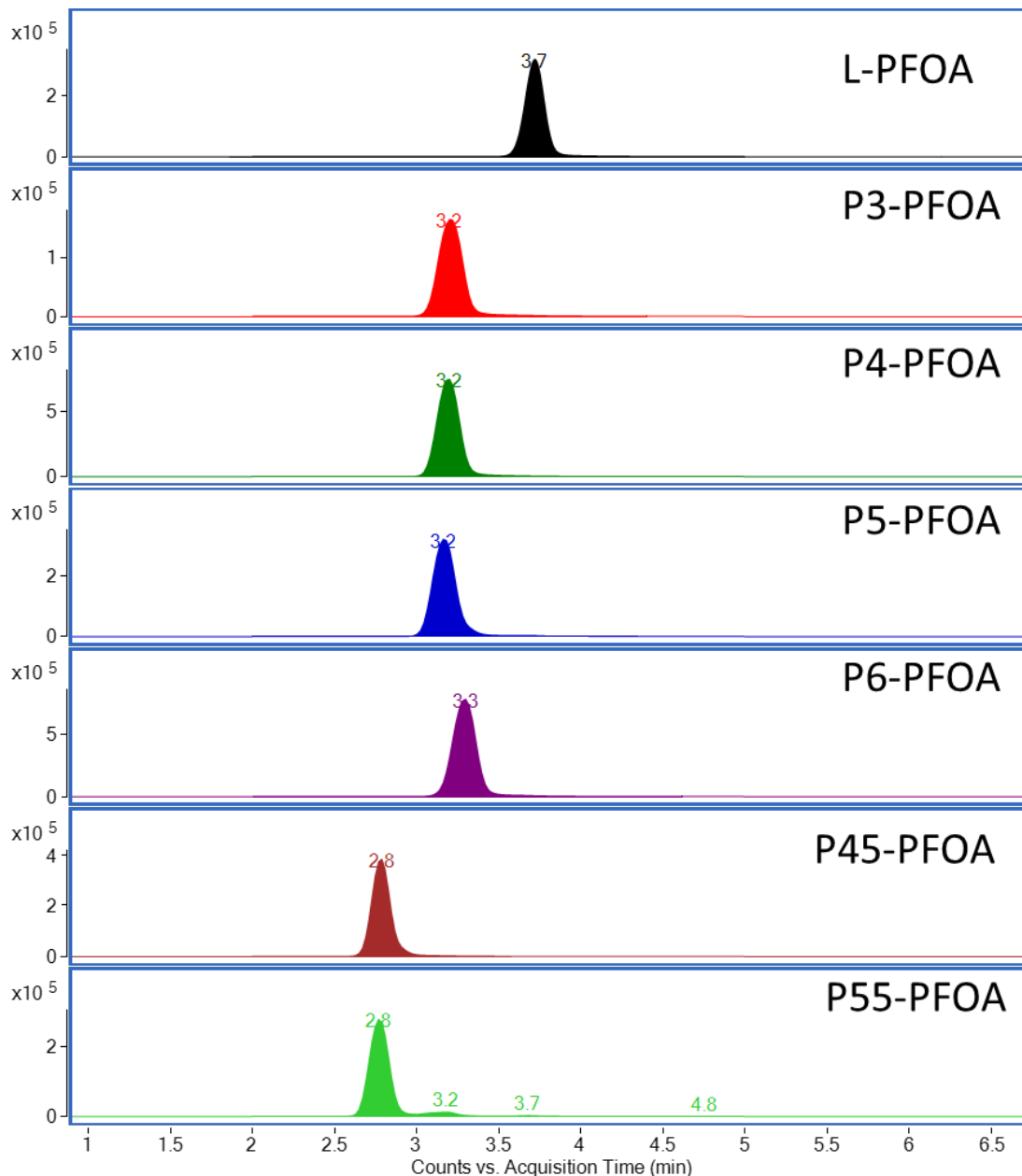


Figure 4.1a The Optimal Chromograms for Each Target Isomer.

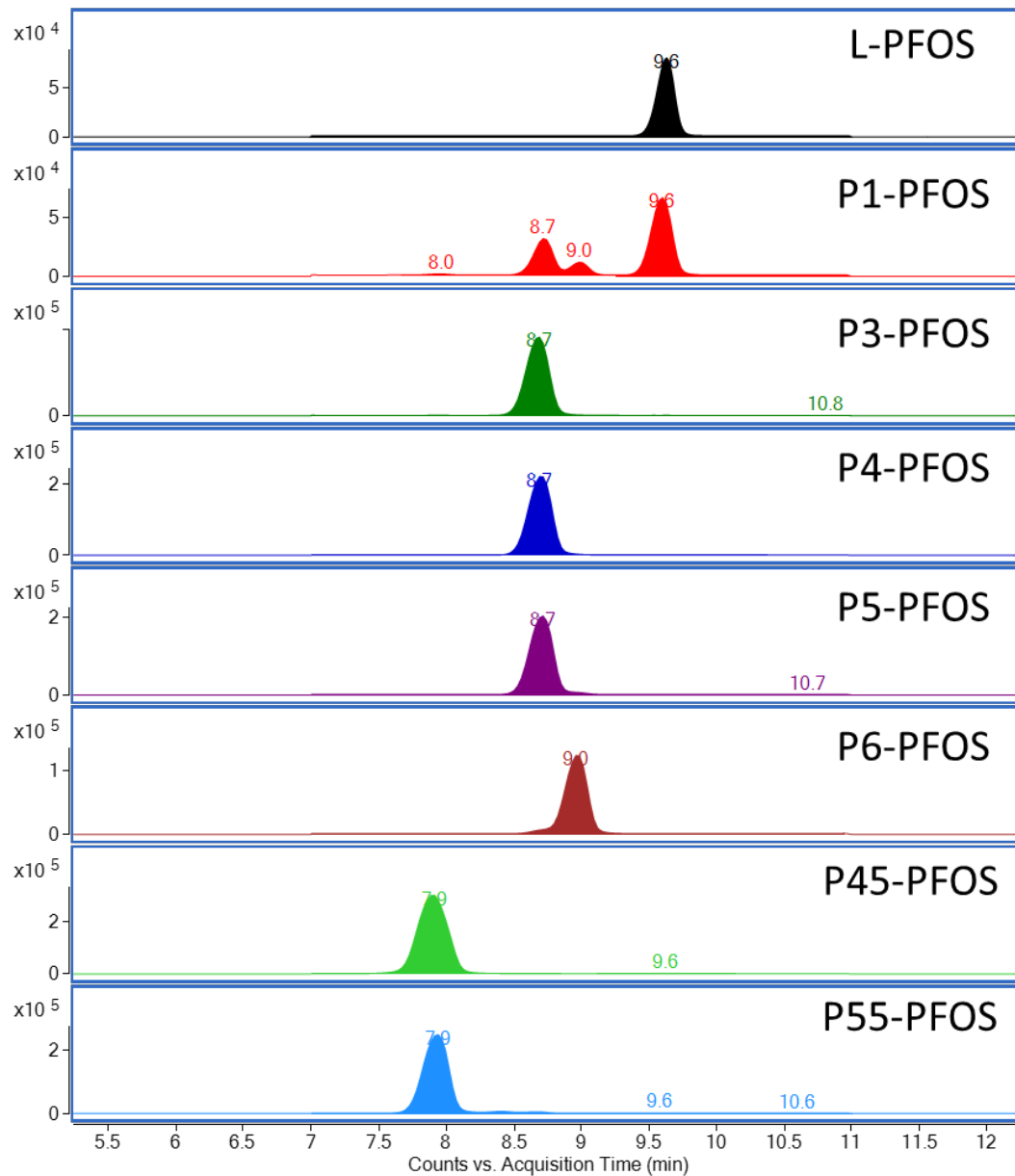


Figure 4.1b The Optimal Chromograms for Each Target Isomer. (continued)

Table 4.4 Optimal conditions for UHPLC-MS/MS.

UHPLC Conditions			
Pump	Agilent Infinity 1290 II		
Analytical column	Waters CORTECS UPLC C18 (1.6 μ m, 2.1 \times 150mm, p/n 186007096)		
Guard column	Waters CORTECS UPLC C18 VanGuard Pre-Column (1.6 μ m, 2.1 \times 5mm, p/n 186007123)		
Mobile phase	A. 5mM ammonium formate in water/acetonitrile/methanol (95/2.5/2.5, v/v/v) B. 5mM ammonium formate in water/acetonitrile/methanol (30/35/35, v/v/v)		
Gradient method conditions	Time	A%	B%
	0	45	55
	1	45	55
	2	35	65
	17	25	75
	18	20	80
	30	10	90
	32	5	95
	33	1	99
	34	1	99
	35	45	55
	Post run: 2 min		
Flow rate	0.15mL/min		
Total runtime	35 min		
Column temperature	40 °C		
Injection volume	5 μ L		
Injection wash solvent	Methanol/acetonitrile/water (40/40/20, v/v)		
MS/MS Condition			
Gas temperature	225 °C		
Gas flow	10 L/min		
Nebulizer	45 Psi		
Sheath gas temperature	350 °C		
Sheath gas flow	11 L/min		
Capillary voltage	3600V		
Nozzle voltage	1500V		
Delta EMV	400		
Cell acceleration voltage	4		
MS1 and MS2 resolution	Wide		

4.3.2 Optimization of MS and MS/MS Conditions

Four different experiments were conducted to optimize the conditions for mass spectrometry analysis of linear and branched PFOA and PFOS isomers. These included full (MS2) scan, single ion monitoring (SIM) scan, product ion (PI) scan, and multiple reaction monitoring (MRM) experiments. Each experiment was conducted under different ionization source conditions to ensure the best outcomes. The optimization process involved a thorough analysis of various parameters, such as collision cell energy, fragmentor voltage, cell accelerator voltage, delta EMV, and source parameters like gas temperature and flow, sheath gas temperature and flow, nebulizer pressure, capillary voltage, and nozzle voltage. These MS/MS conditions and parameters were determined for each target isomer, and the results are summarized in Tables 4.2 and 4.3. The full (MS2) scan is an essential experiment in mass spectrometry analysis. In this experiment, each analytical solution was scanned in a range of 50-550 amu in negative ionization mode to preliminarily determine the precursor ion for each isomer tested. This information was used to optimize the SIM and PI scans. The SIM scan analysis evaluated fragmentor voltages for each isomer, and the optimal voltage was 70 V (Table 4.3). The optimal fragmentor voltage was selected based on the peak height and area of the chromatogram for each compound. In addition, information regarding precursor ions and their detection times were confirmed in a narrow scan window during the SIM scan. The PI scan experiments were conducted after identifying each isomer's selective precursor ion and fragmentor voltage. These experiments involved collision cell energies ranging from 0 to 60 eV to identify all significant product ions of each target PFOA and PFOS isomer. Fragmentation patterns were analyzed, and all major product ions were identified for each compound. Finally, the MRM analysis experiments were carried out by integrating the optimized conditions from the full, SIM and PI scan. These experiments were performed to evaluate different cell accelerator voltages (4-7V), delta EMV (200-400V), and source parameters,

including gas temperature (225-325°C), gas flow (5-11L/min), sheath gas temperature (250-350°C), sheath gas flow (8-12 L/min), nebulizer pressure (30-45psi), capillary voltage (1500-3600V), and nozzle voltage (0-2000V). The optimization process involved comprehensively analyzing each parameter and experiment to ensure the most accurate and reliable results. The optimal MS and MS/MS parameters achieved for the target analytes are given in Table 4.3. This detailed optimization process has resulted in a sensitive and selective qualitative analysis of PFOA and PFOS isomers, which is critical for identifying and profiling these contaminants in environmental samples.

Table 4.5 MRM Conditions for each target isomers.

Target Analytes	Precursor Ion (m/z)	Product Ion (m/z)	Fragmentor Voltage (V)	Collision Energy (eV)
1 L-PFOS	499	99/80	70	50/50
2 P1-PFOS	499	419/219/169/99	70	30/30/30/40
3 P45-PFOS	499	330/280/230/180/130/80	70	40/40/40/40/40/50
4 P4-PFOS	499	330/230/180/130/80	70	40/40/40/40/50
5 P6-PFOS	499	330/280/230/169/99/80	70	40/40/40/40/40/50
6 P3-PFOS	499	319/280/169/130/80	70	40/40/40/50/50
7 P55-PFOS	499	280/230/130/80	70	40/40/50/50
8 P5-PFOS	499	280/230/180/130/80	70	40/40/40/50/50
9 L-PFOA	413	369/219/169/119	70	10/20/20/30
10 P3-PFOA	413	369/219/169/119	70	10/20/20/20
11 P4-PFOA	413	369/169/119	70	10/20/25
12 P5-PFOA	413	369/219/119	70	10/10/10
13 P6-PFOA	413	369/169	70	10/10
14 P45-PFOA	413	369/269/219/169/119	70	10/20/20/10/20
15 P55-PFOA	413	219	70	10

4.3.3 Identification of PFOA and PFOS Isomers

Ultra-high-performance liquid chromatography coupled with triple quadrupole mass spectrometry (UHPLC-MS/MS) is a powerful analytical technique to separate and identify isomeric compounds. This study developed a method for high-resolution separation of different PFOA and PFOS isomers. These isomers' physical and chemical properties vary significantly, making it crucial to identify them accurately. The MS/MS conditions were optimized to provide susceptible and specific detection, enabling the characterization of these isomers with structural certainty. All the isomers tested in this method were characterized based on their UHPLC retention times and MS/MS parameters specific to each analyte (Figures 4.1a and 4.1b, Table 4.3). In addition to separating isomers, this method can also characterize linear and branched isomers using multiple product ions, which makes it more specific in its structural characterization. The structural characterization of these isomers is crucial since they have different physical and chemical properties. The UHPLC-MS/MS analysis of linear and branched PFOA and PFOS isomer standards was conducted on multiple days, and it was found that there was no variation in their retention time or peak shape, indicating that the method is reproducible. This method helps in qualitative profiling and identification of these compounds, which is essential for environmental monitoring and analysis. To understand the prevalence and distribution of contaminants in environmental samples, it is crucial to establish a quantitative method for analysis. This method should undergo proper validation before being applied to quantify PFOA and PFOS isomers in the environmental samples. The validation process would ensure that the method is accurate, reliable, and precise and can detect these compounds at their relevant concentrations in the environmental matrices.

4.4. Conclusions

In conclusion, the qualitative method developed in this project can profile both linear and branched isomers of PFOA and PFOS. The method development for the target PFAS and isomers was finalized, including preparing standard solutions, solvents, column selection, and optimization of UHPLC and MS conditions. While separating these isomers in reverse-phase columns can be complex, multiple columns were tested and selective reverse-phase columns with a chiral nature were found that can effectively separate isomeric compounds. This separation is crucial in identifying and tracking sources of PFAS contamination more efficiently. However, it is essential to note that this method is still in its preliminary stage and requires further investigation to test the repeatability of qualitative profiling of isomers in actual environmental samples. The quantification of these isomers in the environment is aimed to be optimized by measuring isomeric patterns and their respective ratios. By doing so, the accuracy and sensitivity of this method can be further improved. In future work, more extensive validation studies are required to demonstrate the reproducibility and accuracy of this method. Additionally, this method will be applied to actual environmental samples to assess its effectiveness in identifying and tracking sources of PFAS contamination. The use of this method in studying the degradation and transformation of PFAS in the environment will be the following step for investigating.

Chapter 5. A Summary of Scientific Contributions

5.1 Summary

This research focused on developing advanced methods for detecting per- and polyfluoroalkyl substances (PFAS) in environmental samples. An Ultrahigh-performance liquid chromatography-triple quadrupole mass spectrometry (UHPLC-QqQ-MS/MS) coupled with JetStream electrospray ionization source was utilized in this study. This technique is notable for its high resolution and sensitivity, crucial for identifying PFAS, typically present at low environmental concentrations. Including JetStream electrospray ionization source enhances ionization efficiency, thereby improving the detection limits and accuracy of PFAS analysis. The study analyzed various classes of PFAS, including perfluorocarboxylic acids (PFCAs), perfluorosulfonic acids (PFSAs), perfluoroether carboxylic acids (PFECAs), fluorinated alkyl sulfonic acids (FASAs), and isomers of PFOA and PFOS. This broad range of PFAS analysis is essential for understanding their prevalence and environmental impact. The methods developed in this study were thoroughly validated for calibration accuracy, sensitivity, selectivity, and repeatability, ensuring that the results are reliable and can be replicated in future studies. This validation process is critical for establishing a reliable framework for consistent and comparable PFAS research. Per- and polyfluoroalkyl substances (PFAS) are a group of synthetic compounds that have been widely used in industrial and consumer products. Efficient analysis of PFAS in complex environmental samples of water, sediment, and biota is crucial due to their persistence and potential health hazards. Various sample processing methods have been optimized, such as solid-phase extraction, liquid-liquid extraction, and solid-phase microextraction, to monitor their distribution and assess their potential risks. These methods have been successfully applied to

extract and analyze PFAS from environmental matrices, enabling their accurate quantification and identification using UHPLC-MS/MS. The optimization of sample processing methods has led to significant improvements in the sensitivity, accuracy, and reliability of PFAS analysis, providing a valuable tool for environmental monitoring and risk assessment. Also, this research's enhanced ability to detect and differentiate various PFAS compounds was significant. The optimized protocols developed enable effective separation and identification of these compounds, including the differentiation of isomers of PFOS and PFOA. Such methods are vital for assessing source tracking of PFAS contamination in environmental media. Application of the validated methods developed in this research may contribute significantly to monitoring PFAS distribution, and this knowledge is crucial for assessing the risks posed by these substances to ecosystems and human health. The data generated from this research can provide a foundation for more informed policy decisions and public health advisories concerning PFAS. The advanced techniques and detailed analysis offer valuable insights for future studies and regulatory approaches to effectively manage PFAS use and address contaminated sites. In summary, the study presents a significant advancement in environmental analysis, providing new tools and insights for addressing the complex challenge of PFAS contamination. The methodological robustness and comprehensive approach highlight the importance of protecting public health and the environment from synthetic contaminants and their potential implications for future research and policy.

5.2 Research Novelty and Contribution

Chapter 2 presents a reliable analytical method developed for analyzing 17 common PFAS in the surface water of Mobile Bay, AL. The method targeted two groups of persistent and frequently detected PFAS, and a group of emerging substances used as substitutes for legacy PFAS. The method achieved remarkable improvements in peak response and analyte separation

and reduced analysis time to 9 minutes, making it an advancement over prior reported methods in the literature. This validated method was applied to a large batch of surface water samples collected across Alabama, facilitating a comprehensive understanding of PFAS distribution and environmental impacts. The method was subsequently applied for diverse collaborative projects, including an investigation of the effects of PFOS on unionid mussels, an assessment of PFAS bioaccumulation in oysters, an analysis of seasonal variations of PFAS in oysters from Mobile Bay, an evaluation of the efficacy of the Algae Turf Scrubber technique for PFAS remediation, and experimentation with various biochars for the treatment of PFAS-contaminated water. Through the analysis of diverse sample types, the method demonstrated robustness and repeatability, improving the efficiency of routinely monitoring efforts targeting these PFAS in multiple environmental and biological matrices.

Chapter 3 introduces a rapid method developed and validated for qualitative and quantitative analysis of FASA, a group of precursor compounds. While existing methods encompass a broad range of PFAS, including several sulfonamides, there are no expedient methods exclusively focusing on FASA analysis. This method offers a high sensitivity and selectivity analysis of FASA in an ultra-short runtime. The total duration is 5 minutes, and the separation of target compounds is accomplished within 2 minutes. This novel approach provides the notable advantages of handling and analyzing a substantial number of samples within a condensed timeframe. Such efficiency results in significant time and cost savings, providing rapid screening and expedient response in evaluating samples from potential contamination sources.

Chapter 4 presents a qualitative method for linear and branched isomers of PFOA and PFOS. PFOA and PFOS are the most extensively utilized and commonly distributed PFAS in the environment, and high-purity reference standards are available. However, separating and

analyzing isomeric PFAS, which have identical molecular formulas and similar physical and chemical properties, is a considerable challenge for the scientific community. Previous methods for assessing PFOA and PFOS isomers were limited and often involved lengthy analysis times. This study used a chiral analytical column, enabling the separation of isomers within shorter run time analysis. This chemical profiling method provides valuable information that can aid in a better understanding of the sources and pathways of these PFAS in the environment.

In addition to the method development and validation, a number of sample preparation methods were designed and improved for target compound isolation from solids, sediments, biota, and algae. The development and optimization of sample preparation and cleanup strategies ensure comprehensive PFAS analysis across diverse sample types. These refined protocols encompass a broad range of sample categories, offering extensive insights and recommendations for conducting PFAS analysis using advanced mass spectrometry techniques.

Overall, these analytical methods have the potential to greatly assist in the monitoring and management of PFAS contamination, providing environmental scientists with the tools they need to accurately detect and quantify these compounds in environmental media. This information can help guide decision-making processes and ultimately contribute to protecting and conserving our environment.

5.3 Research Limitation and Future Work

PFAS consists of over 6000 substances, and this study specifically focuses on 35 selected PFAS and 13 isomeric PFAS identification and analysis using UHPLC-MS/MS. All the compounds were quantified in this study by plotting calibration curves developed with pure PFAS analytical standards. However, unknown PFAS detection is also very important for understanding this widespread class of PFAS using non-target analytical approaches, as well as in assessing their

complete environmental impact. So tandem mass spectrometry techniques specifically designed to conduct non-target analysis need to be developed. These methods will offer a broader perspective on the PFAS analysis landscape and are becoming increasingly important for environmental researchers.

The method developed in Chapter 2 was tested on a large number of environmental samples, including water, sediment, and biological samples, confirming its robustness and long-term reliability. Whereas the method developed in Chapter 3 only used water samples for its development and validation process. To ensure the method's applicability to various sample types, including sediment and biological samples, future work should focus on conducting sample preparation experiments for various sample types such as sediments and biota.

Chapter 4 outlines a method for identifying and profiling linear and branched PFOA and PFOS isomers. This method is crucial in predicting the source tracking of PFOA and PFOS isomers in environmental samples. By identifying the sources of contamination, it is possible to take preventive measures to minimize further contamination and mitigate the adverse effects of isomers on human health and the environment. However, to accurately quantify the concentration of isomers and assess their environmental risk, the complete quantitative method development and validation, including sample preparation techniques, is essential. This development will help in determining the exact concentration of these chemicals in environmental samples and assessing their potential risk to the environment and human health. The tools that are developed through this process will play a significant role in environmental protection efforts. As the number of new PFAS in the environment continues to grow, new and improved analytical methods that overcome PFAS analysis challenges are necessary to identify and monitor them effectively. Overall, the

continued improvement and refinement of analytical methods will help us stay ahead of the challenges posed by new and emerging PFAS and other harmful substances.

Appendix

Appendix A: Supplementary information for Chapter 2

Table A. 1: Concentrations for target PFAS in global surface water reported in literature.

Compound	Location	Concentration	Reference
PFBA	Coastal Areas, Korea	nd - 9.55 ng/L	(Naile et al., 2010)
	Mississippi River Basin, USA	nd-458ng/L	(Nakayama et al., 2010)
	Jucar River, Spain	5.21-644 ng/L	(Campo et al., 2016)
	Ganges River Basin, India	<0.01-1 ng/L	(Sharma et al., 2016)
	Beihu Gulf, China	252-1771 pg/L	(Pan et al., 2019)
	Bohai Bay, China	3.58-18.2 ng/L	(Yunqing Liu et al., 2019)
	New Jersey, USA	<0.9-10.0 ng/L	(Goodrow et al., 2020)
	Bohai Sea, China	<0.37-8.69 ng/L	(Zhao et al., 2020)
	Surrounding Rivers of Bohai sea, China	<0.37-531 ng/L	(Zhao et al., 2020)
PFBS	Coastal Areas, Korea	nd - 39.8 ng/L	(Naile et al., 2010)
	Taihu Lake, China	0.64–6.71ng/L	(Zhu et al., 2016)
	Orge River, France	4.4ng/L	(Labadie & Chevreuil, 2011)
	Mississippi River Basin, USA	nd-84.1ng/L	(Nakayama et al., 2010)
	Danube River and its tributaries, Europe	<0.55-3.7 ng/L	(Loos et al., 2017)
	Vietnam Riverine Area	<0.10-8.28 ng/L	(Lam et al., 2017)
	Ganges River Basin, India	<1.1145-10.19 ng/L	(Sharma et al., 2016)
	Beihu Gulf, China	41-1764 pg/L	(Pan et al., 2019)

	Bohai Bay, China	0.610-30.9 ng/L	(Yunqing Liu et al., 2019)
	Near A Fluoropolymer Manufacturing Plant, Netherlands	2.5-11 ng/g ww	(Brandsma et al., 2019)
	Coastal Areas, Korea	<0.04-3.87 ng/L	(J. Lee et al., 2020)
	New Jersey, USA	<1.8-6.6 ng/L	(Goodrow et al., 2020)
	Bohai Sea, China	<0.41-6.59 ng/L	(Zhao et al., 2020)
	Surrounding Rivers of Bohai Sea, China	<0.41-281 ng/L	(Zhao et al., 2020)
	Perdido Bay, USA	0.72-2.75ng/L	(Mulabagal et al., 2018)
PFPeA	Taihu Lake, China	nd-6.17ng/L	(Zhu et al., 2016)
	Orge River, France	8.9ng/L	(Labadie & Chevreuil, 2011)
	Mississippi River Basin, USA	nd-31.5ng/L	(Nakayama et al., 2010)
	Songhua River, China	nd-<0.132 ng/L	(Dong et al., 2018)
	Jucar River, Spain	0.08-2.82 ng/L	(Campo et al., 2016)
	Ganges River Basin, India	<0.443-2.97 ng/L	(Sharma et al., 2016)
	Beihu Gulf, China	49-2968 pg/L	(Pan et al., 2019)
	Bohai Bay, China	1.70-8.94 ng/L	(Yunqing Liu et al., 2019)
	Costal Area, Korea	<0.2-2.20 ng/L	(J. Lee et al., 2020)
	New Jersey, USA	1.0-17.7 ng/L	(Goodrow et al., 2020)
	Bohai Sea, China	<0.02-34.4 ng/L	(Zhao et al., 2020)
	Surrounding Rivers of Bohai Sea, China	<0.02-479 ng/L	(Zhao et al., 2020)
PFHxA	Coastal Areas, Korea	nd - 47 ng/L	(Naile et al., 2010)

	Taihu Lake, China	12.48-63.06ng/L	(Zhu et al., 2016)
	Orge River, France	11.3ng/L	(Labadie & Chevreuil, 2011)
	Mississippi River Basin, USA	nd-53.4ng/L	(Nakayama et al., 2010)
	Downstream of Fluoropolymer Manufacturing Facilities, France	<4-188 ng/L	(Bach et al., 2017)
	Danube River and its tributaries, Europe	<1.10-8.5 ng/L	(Loos et al., 2017)
	Songhua River, China	nd-0.213 ng/L	(Dong et al., 2018)
	Jucar River, Spain	1.44-18.7 ng/L	(Campo et al., 2016)
	Vietnam Riverine Area	<0.07-4.26 ng/L	(Lam et al., 2017)
	Ganges River Basin, India	0.37-4.73 ng/L	(Sharma et al., 2016)
	Beihu Gulf, China	33-1001 pg/L	(Pan et al., 2019)
	Bohai Bay, China	0.58-11.5 ng/L	(Yunqing Liu et al., 2019)
	Costal Area, Korea	<0.04-2.18 ng/L	(J. Lee et al., 2020)
	New Jersey, USA	<1.1-26.0 ng/L	(Goodrow et al., 2020)
	Bohai Sea, China	0.89-33.4 ng/L	(Zhao et al., 2020)
	Surrounding Rivers of Bohai sea, China	0.13-1985 ng/L	(Zhao et al., 2020)
	Perdido Bay, USA	0.45-3.22ng/L	(Mulabagal et al., 2018)
PFHxS	Coastal Areas, Korea	0.38-41.8 ng/L	(Naile et al., 2010)
	Taihu Lake, China	9.47-83.08ng/L	(Zhu et al., 2016)
	Orge River, France	13.6ng/L	(Labadie & Chevreuil, 2011)
	Mississippi River Basin, USA	nd-169ng/L	(Nakayama et al., 2010)
	Songhua River, China	nd-<0.042 ng/L	(Dong et al., 2018)
	Jucar River, Spain	12.07-36.7ng/L	(Campo et al., 2016)

	Vietnam Riverine Area	<0.03-5.98 ng/L	(Lam et al., 2017)
	Ganges River Basin, India	<0.017-0.3 ng/L	(Sharma et al., 2016)
	Beihu Gulf, China	nd-247 pg/L	(Pan et al., 2019)
	Bohai Bay, China	0.139-17.4 ng/L	(Yunqing Liu et al., 2019)
	Near A Fluoropolymer Manufacturing Plant, Netherlands	<0.5-1.3 ng/g ww	(Brandsma et al., 2019)
	Costal Area, Korea	<0.1-8.84 ng/L	(J. Lee et al., 2020)
	New Jersey, USA	<2.0-95.9 ng/L	(Goodrow et al., 2020)
	Bohai Sea, China	<0.13-3.62 ng/L	(Zhao et al., 2020)
	Surrounding Rivers of Bohai Sea, China	<0.13-305 ng/L	(Zhao et al., 2020)
	Perdido Bay, USA	0.64-3.36ng/L	(Mulabagal et al., 2018)
PFHpA	Piedmont, Italy	<10-73ng/L	(Gosetti et al., 2010)
	Coastal Areas, Korea	nd - 47.2 ng/L	(Naile et al., 2010)
	Taihu Lake, China	nd-4.5ng/L	(Zhu et al., 2016)
	Orge River, France	4.5ng/L	(Labadie & Chevreuil, 2011)
	Mississippi River Basin, USA	nd-90.2ng/L	(Nakayama et al., 2010)
	Downstream of Fluoropolymer Manufacturing Facilities, France	<4-20ng/L	(Bach et al., 2017)
	Danube River and its tributaries, Europe	<3.20-19 ng/L	(Loos et al., 2017)
	Songhua River, China	nd-0.213 ng/L	(Dong et al., 2018)
	Jucar River, Spain	0.64-20.1 ng/L	(Campo et al., 2016)
	Vietnam Riverine Area	<0.05-7.81 ng/L	(Lam et al., 2017)
	Ganges River Basin, India	0.34-3.27 ng/L	(Sharma et al., 2016)

	Beihu Gulf, China	62-390 pg/L	(Pan et al., 2019)
		0.73-10.42	
	Bohai Bay, China	ng/L	(Yunqing Liu et al., 2019)
	Costal Area, Korea	<0.1-1.50 ng/L	(J. Lee et al., 2020)
	New Jersey, USA	1.1-14.6 ng/L	(Goodrow et al., 2020)
	Bohai sea, China	<0.71-22 ng/L	(Zhao et al., 2020)
	Surrounding Rivers of Bohai sea, China	<0.71-2663 ng/L	(Zhao et al., 2020)
	Perdido Bay, USA	0.18-2.83ng/L	(Mulabagal et al., 2018)
PFHpS	Orge River, France	0.65ng/L	(Labadie & Chevreuil, 2011)
		<0.004-0.04	
	Ganges River Basin, India	ng/L	(Sharma et al., 2016)
PFOA	Piedmont, Italy	<10ng/L	(Gosetti et al., 2010)
	Coastal Areas, Korea	2.95-68.6 ng/L	(Naile et al., 2010)
		20.81-	
	Taihu Lake, China	43.19ng/L	(Zhu et al., 2016)
	Orge River, France	9.4ng/L	(Labadie & Chevreuil, 2011)
	Mississippi River Basin, USA	nd-125ng/L	(Nakayama et al., 2010)
	Downstream of Fluoropolymer Manufacturing Facilities, France	<4-57 ng/L	(Bach et al., 2017)
	Danube River and its tributaries, Europe	<1.07-37 ng/L	(Loos et al., 2017)
		<0.121-0.678	
	Songhua River, China	ng/L	(Dong et al., 2018)
	Jucar River, Spain	0.07-52.2 ng/L	(Campo et al., 2016)
		<0.13-53.5	
	Vietnam Riverine Area	ng/L	(Lam et al., 2017)
	Ganges River Basin, India	0.08-1.18 ng/L	(Sharma et al., 2016)
	Beihu Gulf, China	132-1046 pg/L	(Pan et al., 2019)

	Bohai Bay, China	3.64-629ng/L	(Yunqing Liu et al., 2019)
		0.210-16.5	
	Costal Area, Korea	ng/L	(J. Lee et al., 2020)
	New Jersey, USA	1.9-33.9 ng/L	(Goodrow et al., 2020)
	Bohai Sea, China	3.20-845 ng/L	(Zhao et al., 2020)
	Surrounding rivers of Bohai sea, China	0.96-7335 ng/L	(Zhao et al., 2020)
	Perdido Bay, USA	0.83-4.33ng/L	(Mulabagal et al., 2018)
PFOS	Piedmont, Italy	nd - <50ng/L	(Gosetti et al., 2010)
	Coastal Areas, Korea	4.11-450 ng/L	(Naile et al., 2010)
	Taihu Lake, China	7.23-44.34ng/L	(Zhu et al., 2016)
	Orge River, France	17.4ng/L	(Labadie & Chevreuil, 2011)
	Mississippi River Basin, USA	nd-245ng/L	(Nakayama et al., 2010)
	Downstream of Fluoropolymer Manufacturing Facilities, France	<4-8 ng/L	(Bach et al., 2017)
	Danube River and its tributaries, Europe	<1.09-26 ng/L	(Loos et al., 2017)
		0.0367-0.271	
	Songhua River, China	ng/L	(Dong et al., 2018)
	Jucar River, Spain	0.01-128 ng/L	(Campo et al., 2016)
		<0.03-40.2	
	Vietnam Riverine Area	ng/L	(Lam et al., 2017)
		<0.01-1.73	
	Ganges River Basin, India	ng/L	(Sharma et al., 2016)
	Beihu Gulf, China	nd-487 pg/L	(Pan et al., 2019)
		0.951-14.3	
	Bohai Bay, China	ng/L	(Yunqing Liu et al., 2019)
		<0.04-1.92	
	Korea Costal Area, Korea	ng/L	(J. Lee et al., 2020)

	New Jersey, USA	<2.0-102.0 ng/L	(Goodrow et al., 2020)
	Bohai Sea, China	<0.29-2.91 ng/L	(Zhao et al., 2020)
	Surrounding Rivers of Bohai Sea, China	<0.29-71.8 ng/L	(Zhao et al., 2020)
	Perdido Bay, USA	0.71-10.31ng/L	(Mulabagal et al., 2018)
HFPO-DA	Bohai Bay, China	nd-3.99 ng/L	(Yunqing Liu et al., 2019)
(GenX)	Bohai Sea, China	<0.02-6.87 ng/L	(Zhao et al., 2020)
	Surrounding Rivers of Bohai Sea, China	<0.02-663 ng/L	(Zhao et al., 2020)
	Xiaoqing River, China	1.04-4340ng/L	(Yao et al., 2021)
ADONA	Bohai Sea, China	<0.02-0.05 ng/L	(Zhao et al., 2020)
	Surrounding Rivers of Bohai Sea, China	<0.02-0.044 ng/L	(Zhao et al., 2020)
PF4OPeA	Xiaoqing River, China	nd-114ng/L	(Yao et al., 2021)
PF5OHxA	Xiaoqing River, China	nd-37.2ng/L	(Yao et al., 2021)

Appendix B: Supplementary information for Chapter 3

Figure B. 1: Concentrations for FASAs in global aqua media reported in literature.

Studies	Media	Sulfonamides	Concentration (ng/L)	Location
(Marchiandi et al., 2021)	surface water	FBSA	0.5-4.8	Stony Creek, Melbourne, Australia (close to firefighting training area)
		FOSA	0.2-0.8	
		NMeFOSA	<0.2	
(Taniyasu et al., 2005)	surface water	NEtFOSA	<0.1	Tokyo Bay
		NEtFOSA	<0.3	Tomakomai Bay
(Loganathan et al., 2007)	WWTP influent	FOSA	<0.5-0.8	Georgia
	WWTP effluent	FOSA	<0.5-0.92	
	WWTP influent	FOSA	<0.5-1.9	Kentucky
	WWTP effluent	FOSA	1.7-2.5	
(Wang et al., 2020)	WWTP influent	FBSA	nd-2203.61	17 WWTP in China
	WWTP effluent	FBSA	0.08-7.18	
	groundwater	FOSA	nd-0.17	
(Picard et al., 2021)	surface water	FBSA	0.005-0.12	St. Lawrence Estuary and Gulf, Canada
		FHxSA	0.001-0.03	
		FOSA	0.023-0.08	
(Bossi et al., 2008)	WWTP influent	FOSA	<0.2-1	6 WWTP in Denmark
	WWTP effluent	FOSA	<0.2-2.1	
(Cai, Zhao, et al., 2012)	surface water	NEtFOSA	<0.0236-0.279	From East (Shanghai) to South China Sea (Shenzhen)
(Cai, Yang, et al., 2012)	seawater	FOSA	<0.0403-0.0464	Fildes Peninsula, King George Island, Antarctica
	snow	FOSA	<0.0403	
	lake water	FOSA	<0.0403	

	surface runoff	FOSA	0.12	
(Arvaniti et al., 2012)	WWTP influent	FOSA	<0.16-14	2 WWTP in Greek
	WWTP effluent	FOSA	<0.16-7.1	
	WWTP influent	NMeFOSA	<0.29	
	WWTP effluent	NMeFOSA	<0.29	
	WWTP influent	NEtFOSA	<0.52	
	WWTP effluent	NEtFOSA	<0.52	
(Zhou et al., 2021)	groundwater	FOSA	0.0087	Loess Plateau, China
(Houtz et al., 2013)	AFFF-impacted groundwater	FHxSA	nd-53000	Ellsworth Air Force Base, Piedmont, SD.
(Ahrens, Plassmann, et al., 2009)	surface water	FOSA	0.44-8.9	Elbe River and North Sea, Germany
(D'Agostino & Mabury, 2017)	surface water	FHxSA	nd-19	Hamilton, Ontario, Canada
		FOSA	nd-1.6	
		FHxSA	1.2-3.6	Kartell, Noviglio, Italy
		FOSA	nd	
(Hua et al., 2019)	surface water	NEtFOSA	<LOQ-0.67	Haihe River, China
		NMeFOSA	<0.1-0.80	
		FOSA	<LOQ-3.34	
		NEtFOSA	0.40-0.82	Dagu Drainage Canal, China
		NMeFOSA	0.43-1.27	
		FOSA	<LOQ	
(Schultz et al., 2006)	WWTP influent	FOSA	nd-5.5	10 municipal wastewater treatment plant, USA
	WWTP effluent	FOSA	nd-10	
(Fang et al., 2014)	surface water	FOSA	0.0456	Taihu Lake, China
(Ahrens, Barber, et al., 2009)	surface ocean water	FOSA	<17-307	North Atlantic Ocean
		FOSA	<17-60	Middle Atlantic Ocean

		FOSA	<17-53	South Atlantic Ocean
(Dauchy et al., 2019)	firefighting wastewater	FOSA	1217-49937	
		NMeFOSA	<1000 - <5000	
		NEtFOSA	<1000 - <5000	
	WWTP effluent	FOSA	<1000 - <10000	
		NMeFOSA	nd- <10000	
		NEtFOSA	nd- <10000	
(Löfstedt Gilljam et al., 2016)	surface water	FOSA	≤0.014–3.362	Todos os Santos Bay, Baihai State, Brazil
(Theobald et al., 2011)	seawater	FOSA	<0.003-0.314	German Bight, the North Sea and western Baltic Sea
(Nguyen et al., 2017)	river water	FOSA	0.032-0.46	Swedish coast, Northern Europe
	seawater	FOSA	0.019-0.051	Baltic Sea, Northern Europe
(Munoz et al., 2015)	surface water	FOSA	<0.06-0.73	
		NMeFOSA	<0.09-0.46	French
		NEtFOSA	<0.06-0.81	
	tap water	FOSA	nd- <0.07	Canada
		FOSA	nd- <0.07	USA
		FOSA	nd-0.31	China
	bottled water	FOSA	nd- <0.07	Ivory Coast
	Source water	FBSA	<0.02-0.15	Great Lakes/St. Lawrence River, Canada
		FHxSA	<0.02-0.09	
		FBSA	<0.02	Europe
		FHxSA	0.07	
		FBSA	<0.07	USA
		FHxSA	<0.02	
		FBSA	0.27	Chile

(Kaboré et al., 2018)		FHxSA	<0.02	
		FBSA	<0.02-0.09	Burkina Faso
		FHxSA	<0.02	
		FBSA	<0.07-0.38	Ivory Coast
		FHxSA	<0.02-0.15	
		FBSA	<0.02	China
	FHxSA	4		
(Ahrens, Felizeter, et al., 2009)	surface water	FOSA	nd-0.2	German Bight
(Pan et al., 2014)	surface water	FOSA	nd-0.62	Yangtze River, China
		FOSA	<0.03-0.05	Bohai Sea
(Z. Zhao et al., 2017)	surface water	FOSA	<0.03-0.36	Yellow Sea
		FOSA	<0.03-0.13	Yangtze River, China
(Munoz et al., 2017)	surface water	FOSA	nd-0.11	French Guiana, Guadeloupe, Martinique, Reunion and Mayotte

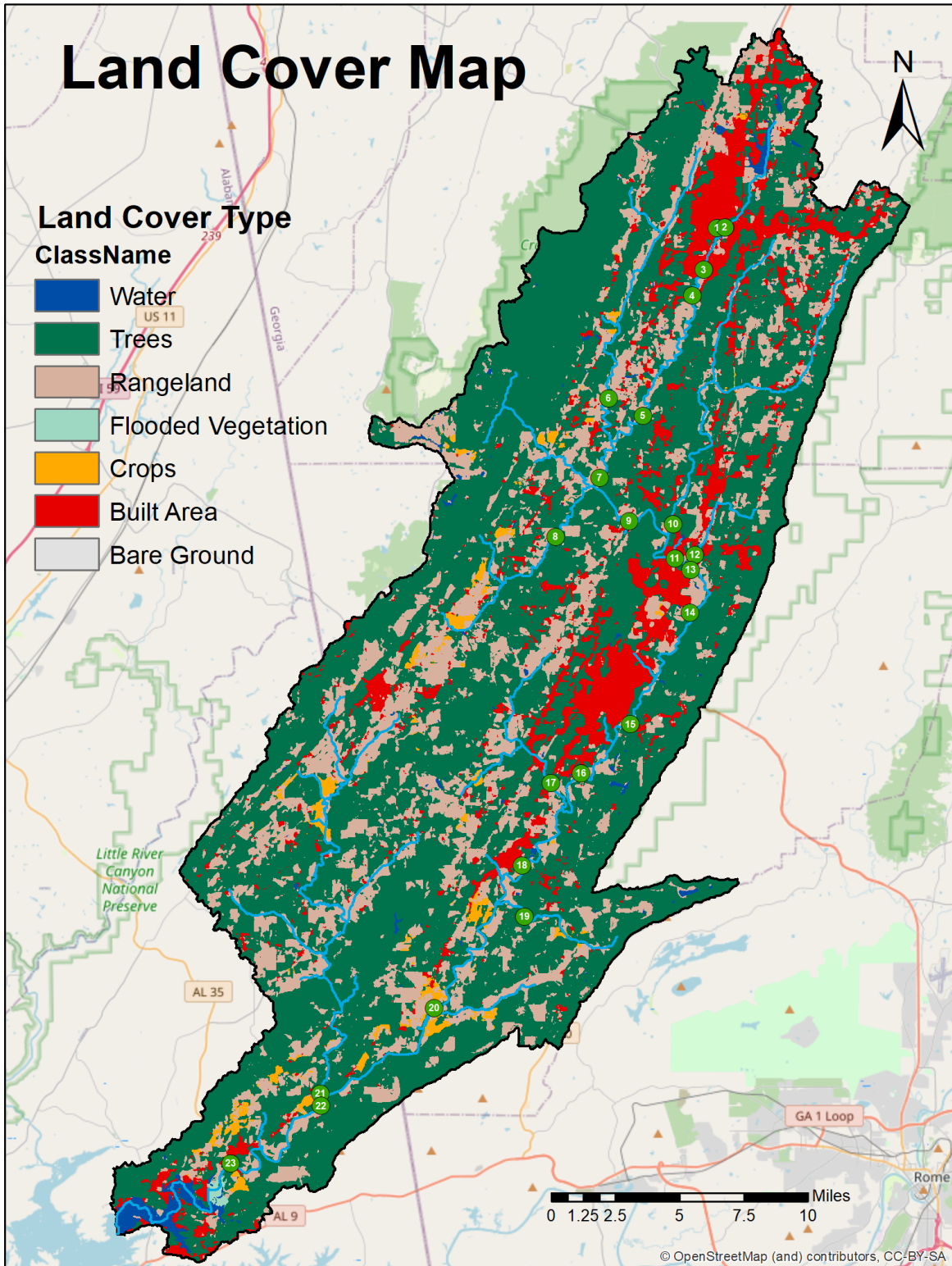


Figure B.2: Land Cover Map for Chattooga Watershed.

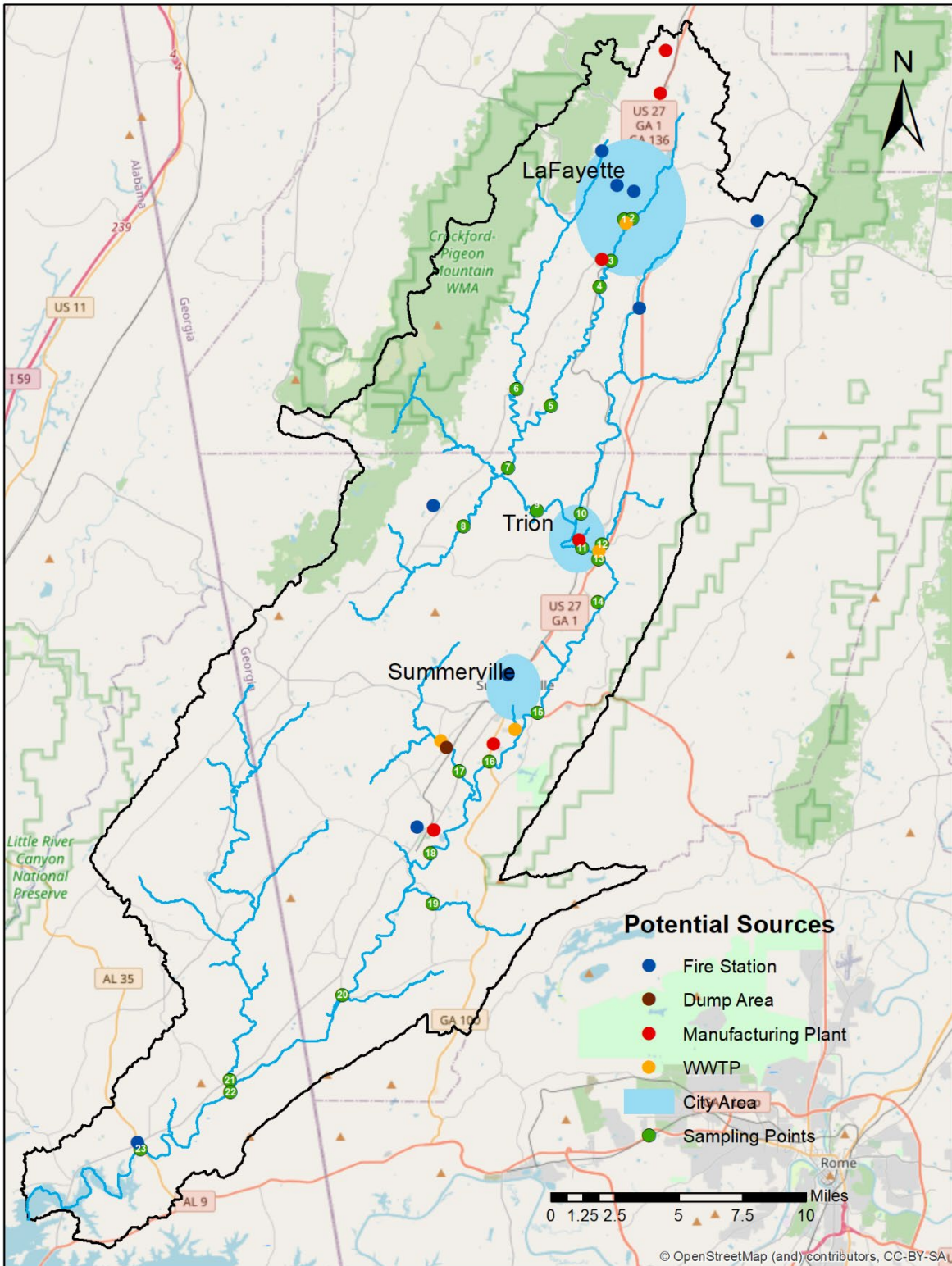


Figure B.3: Potential Point Contamination Sources in Chattooga Watershed.

Appendix C: Collaborative Research Projects

In conjunction with my doctoral research, I have engaged in collaborative endeavors with various research groups at Auburn University using the PAIR program. In such multidisciplinary projects, my primary focus has been on the development of methodologies, the processing of samples, and the implementation of analyses. We have scrutinized more than one thousand samples utilizing UHPLC-MS/MS. Our laboratory can investigate over forty PFAS and internal standards in surface water, sediment, biota (fish, oysters), and agricultural samples (plants & algae). Throughout these initiatives, we have established various sample preparation protocols, selected appropriate surrogate and internal standards, and optimized instrument conditions and analyses. Below, I have summarized a few key contributions to the group projects.

Project I: Exploring the Impact of Environmentally Relevant PFOS Concentrations on Unionid Mussels

Summary: This research examined the accumulation of PFOS in unionid mussels from Alabama waterways. The study aimed to determine if feeding habits and size of the unionids affected PFOS accumulation and the concentration of PFOS in surrounding sediments. Additionally, the research investigated if environmentally relevant PFOS levels could cause gene expression changes in unionids' gills and mantle tissue. In this project, various groups of mussel samples were processed and analyzed by the author to evaluate the impact of environmentally relevant PFOS concentrations on unionid mussels.

Project II: A study to evaluate the potential of PFAS bioaccumulation and its impacts on depuration in oysters.

Summary: This study examined whether oysters could depurate an ecologically relevant mixture of PFAS compounds. Oysters were tested in PFAS mixtures and evaluated for PFAS bioaccumulation potential, and their impacts on the oyster depuration were monitored over time. In both projects, various sample preparation and analytical methods were developed by the author and optimized for accurate analysis of PFAS in water and oyster tissues.

Project III: PFAS levels in Mobile Bay waters and studying their effects on oysters grown in various seasons, including their potential for bioaccumulation.

Summary: This project aimed to assess the impact of PFAS exposure on oysters cultivated under varying conditions and during different seasons. PFAS extraction method details are summarized below.

PFAS extraction from oyster tissue: To facilitate the ensuing analysis, tissue samples underwent a preparatory process that entailed being freeze-dried for 96 hours in separate HDPE containers and ground into a fine powder using a mortar and pestle. Following this, 3 grams of the ground and homogenized tissue sample were measured and carefully transferred into a 50mL HDPE vial. Each vial was then filled with 30mL of 0.05N KOH in methanol solution, and an internal standard MPFOS was spiked into the solution at a concentration of 1ng/mL. The samples were extracted using sonication at 60Hz for 1 hour, followed by agitation on an orbital shaker at 70rpm for 16 hours. After that, the supernatant from each sample was decanted and centrifuged at 13000 rpm and a temperature of 4 °C for 15 minutes. The resulting tissue sample extracts were filtered through

syringe filters (glass fiber/nylon, 0.45 μ m) to remove suspended solids. The filtered tissue supernatant was transferred into an HDPE bottle and diluted with 500 mL of DI water. Subsequently, an SPE cleanup procedure using Oasis WAX cartridges was performed. The cartridges were first conditioned with 4mL of 1% NH₄OH in methanol, 4mL of methanol, and 4mL of LC-grade water. Samples were then loaded onto the SPE cartridges, and 10mL of ammonium acetate (25mM) in water solution was used to neutralize the pH of the cartridge polymer. Target compounds were eluted using 4mL of methanol and 4mL of 1% NH₄OH in methanol. Following the SPE process, the sample extract was evaporated using a rotary evaporator and re-extracted with a 2.5 mL solvent mixture of methanol and water (95:5, v/v). Before analysis, each sample extract was spiked with 1ng/mL of the internal standards MPFOS and M2PFOA. Subsequently, the samples were analyzed via UHPLC-MS/MS.

PFAS extraction from sediment samples: A meticulous process was followed to analyze sediment samples. First, the samples were freeze-dried for 72 hours in individual HDPE containers and then pulverized into a fine powder. Afterward, 6 grams of each sediment sample were homogenized with 30 mL of 0.3% NH₄OH in methanol solution in an HDPE vial. The samples underwent sonication at 60Hz for 1 hour and were then shaken for 16 hours at 70rpm on an orbital shaker to ensure thorough extraction. Once the extraction process was complete, the supernatant for each sample was decanted and centrifuged at a specific speed and temperature (13000rpm and 4°C, respectively) for 15 minutes. The sediment sample extracts were passed through syringe filters (glass fiber/nylon, 0.45 μ m) to eliminate suspended sediments. The filtered sediment supernatant was transferred to an HDPE bottle and diluted with 500mL of DI water, after which it underwent a solid-phase extraction (SPE) cleanup procedure. The SPE was carried out using Oasis WAX cartridges, which were preconditioned with 1% NH₄OH in methanol (4mL), methanol (4mL), and

LC-grade water (4mL). After loading all samples, 10mL of ammonium acetate (25mM) in water solution was used to neutralize the pH of the cartridge polymer. Target compounds were eluted using 4mL of methanol and 4mL of 1% NH₄OH in methanol. After the SPE procedure, the sample extract was evaporated in the rotary evaporator and re-extracted with a 2.5 mL solvent mixture of methanol and water (95:5, v/v). Each sample extract was spiked with 2ng/mL of the internal standards (MPFOS, M2PFOA) and analyzed using the UHPLC-MS/MS system.

Project IV: Assessing the Efficiency of Using an Algae Turf Scrubber (ATS) Technique to Cleanup PFAS Contamination

Summary: The overall goal of this study was to evaluate the effectiveness of a laboratory-scale model ATSTM in removing a PFAS mixture comprised of PFOS, PFOA, HFPO-DA, and 3,6-OPFHpA from water. This work involved testing the effectiveness of the Algae Turf Scrubber (ATS) system in removing PFAS from water. The ATS system is commonly used for biomass production and pollutant removal, but its potential for PFAS remediation has not been explored. The study focused on four types of PFAS: PFOS, PFOA, PDHA, and HFPO-DA. A community of periphytic algae was cultured and exposed to a mixture of PFAS contaminants at a concentration of 2µg/L for 72 hours.

Sample preparation and analysis: In analyzing water samples, Oasis WAX cartridges (6cc, 150 mg; Waters Corporation, Milford, MA, U.S.) were utilized via the solid phase extraction (SPE) method. The cartridges were pre-conditioned before loading the samples, involving 4 mL of 0.1% ammonium hydroxide in methanol, 4 mL of methanol, and 4 mL of LC-grade water. The samples were then loaded onto the cartridges and eluted at a flow rate of 2 drops per second. Once eluted,

the cartridges were washed with 4 mL of 25 mM ammonium acetate buffer (pH 4.0) in LC-grade water and dried under vacuum. Finally, the target analytes were extracted with 4 mL of methanol and 4 mL of 0.1% ammonium hydroxide in methanol.

To analyze algal biomass samples, the samples were washed three times with 5% methanol in deionized (DI) water and centrifuged. The supernatant was then separated, assuming it contained PFAS adsorbed onto the algal biomass and processed through SPE. The solid portion of the biomass was freeze-dried at -80 °C for 24 hours and then extracted with 50 mL of a 95% methanol solution in water. The solution was sonicated at 60 Hz for 2 hours and centrifugation at 6000 rpm at 4 °C for 15 minutes. The supernatant extract was then concentrated through a BUCHI rotary evaporator and diluted with DI water. The algal extracts were then processed through the SPE approach, and extracted with 3 mL methanol, followed by 3 mL of 0.1% ammonium hydroxide in methanol. Method blanks and control samples were also processed alongside experimental samples through SPE. Target analytes were quantified in MRM mode, with a six-point calibration curve developed using concentrations ranging from 0.05 to 10 ng/mL. All calibration levels were spiked with an internal standard at 1 ng/mL, and a 5 µL sample was injected for analysis. Additionally, multiple solvent blanks were injected between each sample to avoid carryover of target analytes from sample to sample during analysis. The target PFAS mixture (5 ng/mL) was also subjected to a cleanup and analysis process and utilized as quality control in the analysis.

Project V: PFAS remediation-Assessing the Efficiency of different biochar for PFAS removal in experimental waters.

In this study, we tested the effectiveness of different types of biochar in removing PFAS from experimental water. We developed appropriate sample preparation procedures and optimized analytical methods for experimental samples. We analyzed over 300 samples and processed the data to evaluate the biochar's capability to remove PFAS.

Sample preparation: Water samples were taken after biochar treatment and mixed with extraction internal standards (MPFBA, MPFHxA, MPFPeA, M3PFBS, M3PFHxS, 18O2PFHxS, M8PFOS, 5ng/mL) before being processed using Oasis WAX (6CC, 150 mg) cartridges. The samples were loaded onto pre-conditioned SPE cartridges and eluted. These cartridges were washed with 10 mL of 25 mM ammonium acetate, and then dried under a vacuum. PFAS on the SPE column was extracted using 1% ammonium hydroxide in methanol (4 mL) and methanol (4 mL), and the resulting extracts were combined. A sample aliquot (1 mL) was transferred into an LC vial and injection standards (M2PFOA and MPFOS, 4ng/mL) were added. The mixture was then analyzed using a UHPLC-MS/MS system comprising a 1290 Infinity II high-speed pump (model G7120A), a triple quadrupole mass spectrometer, and a Jet Stream ESI source (Agilent Technologies Inc., Santa Clara, CA, USA). The stationary phase was a ZORBAX RRHD Eclipse Plus C18 (2.1 x 100 mm, 1.8 m, Part No. 959758-902), and a gradient elution method was used for the chromatographic experiments. The details of binary phase conditions are presented in Table C.1. MRM experiments were conducted in negative ionization mode, and several MS/MS conditions were optimized, including gas temperature and flow, sheath gas temperature and flow, fragment or voltage, collision cell energy, nebulizer pressure, nozzle voltage, and capillary voltage. For each target analyte, a calibration curve was developed by diluting calibration stock solutions to create

concentrations ranging from 0.4 to 50 ng/mL. Negative, positive, and quality control samples and solvent blanks were analyzed with every batch of experiments. MSMS conditions and MRM parameters are shown in Tables C.1 & C.2. Agilent Mass Hunter software version B. 07.1 was used to process qualitative and quantitative data. Chromatographic peak retention times and MRM parameters (specific qualifier and quantifier ions) were compared with analytical standards to identify target PFAS in experimental water samples. The optimal method parameters are listed below.

Table C.1: Optimized UHPLC-MRM Conditions for PFAS analysis.

Pump	Agilent Infinity 1290 II
Analytical column	Agilent RRHD Eclipse Plus C18 (2.1 × 100 mm, 1.8 μm, p/n 959758-902)
Guard column	Agilent ZORBAX Eclipse Plus C18 (2.1 × 5 mm, 1.8 μm, p/n 821725-901)
Mobile phase	A. 5mM ammonium formate in water/acetonitrile (95/5, v/v) B. acetonitrile/water (95/5, v/v)
Gradient method conditions	Time (min), B% 0 (20); 1 (20); 2 (50); 3 (60); 5 (70); 7 (80); 8 (90); 9 (99); 12 (99); 12.2 (20); 13 (20)
Post run	2 min
Flow rate	0.2mL/min
Total runtime	13 min
Column temperature	40 °C
Injection volume	10 μL
Injection wash solvent	Methanol/acetonitrile/water (40/40/20, v/v)
MS/MS Condition	
Gas temperature	225 °C
Gas flow	10 L/min
Nebulizer	45 Psi
Sheath gas temperature	350 °C
Sheath gas flow	11 L/min
Capillary voltage	3600V
Nozzle voltage	1500V
Delta EMV	400V
Cell acceleration voltage	4
MS1 and MS2 resolution	Unit
Ionization mode	Negative

Table C.2: MRM parameters.

Analytes	Precursor (m/z)	Quantification /Confirmation (m/z)	Relative response ratio	Fragmentor Voltage (V)	Collision Energy (eV)
PFBA	213	168.9	-	60	8
¹³ C ₄ -PFBA	217	172	-	60	8
PFBS	298.9	98.9/80	47.5	100	30/45
¹³ C ₃ -PFBS	302	80	-	130	44
PFPeA	263	219		70	5
¹³ C ₅ -PFPeA	268	223		60	8
PFPeS	348.9	98.9/80	51.2	135/130	40/45
¹⁸ O ₂ -PFH _x S	403	83.9		100	50
PFH _x A	313	268.9		70	8
¹³ C ₅ -PFH _x A	318	273		70	8
PFH _x S	398.9	99/80	43.5	100	45/50
¹³ C ₃ -PFH _x S	402	99/80	43.5	156/100	44/45
PFOA	413.1/413	169.1/369	10.1	70	15/5
¹³ C ₂ -PFOA	414.8	369.8/169	9.4	80	5/15
¹³ C ₄ -PFOA	417	172	-	-	-
PFOS	498.9	99/80	97.9	100/145	50/50
¹³ C ₈ -PFOS	507	99/80	-	148/100	50/52
¹³ C ₄ -PFOS	503	99/80	45.2	180/150	48/55

References

- 3M. (2000). *Phase-out plan for POSF-based products*. Retrieved 10/04/2023 from <https://www.regulations.gov/document/EPA-HQ-OPPT-2002-0051-0006>
- Agilent Technologies, I. (2023). *Jet stream technology ion source (AJS)*. Retrieved 10/04/2023 from <https://www.agilent.com/en/product/liquid-chromatography-mass-spectrometry-lc-ms/lc-ms-ion-sources/jet-stream-technology-ion-source-ajs>
- Ahmed, M., Johir, M., McLaughlan, R., Nguyen, L. N., Xu, B., & Nghiem, L. D. (2020). Per-and polyfluoroalkyl substances in soil and sediments: Occurrence, fate, remediation and future outlook. *Science of The Total Environment*, 748, 141251.
- Ahrens, L., Barber, J. L., Xie, Z., & Ebinghaus, R. (2009). Longitudinal and latitudinal distribution of perfluoroalkyl compounds in the surface water of the Atlantic Ocean. *Environmental Science & Technology*, 43(9), 3122-3127.
- Ahrens, L., Felizeter, S., & Ebinghaus, R. (2009). Spatial distribution of polyfluoroalkyl compounds in seawater of the German Bight. *Chemosphere*, 76(2), 179-184.
- Ahrens, L., Plassmann, M., Xie, Z., & Ebinghaus, R. (2009). Determination of polyfluoroalkyl compounds in water and suspended particulate matter in the river Elbe and North Sea, Germany. *Frontiers of Environmental Science & Engineering in China*, 3(2), 152-170.
- Al Amin, M., Sobhani, Z., Liu, Y., Dharmaraja, R., Chadalavada, S., Naidu, R., Chalker, J. M., & Fang, C. (2020). Recent advances in the analysis of per-and polyfluoroalkyl substances (PFAS)—A review. *Environmental Technology & Innovation*, 100879.
- Androulakakis, A., Alygizakis, N., Gkotsis, G., Nika, M.-C., Nikolopoulou, V., Bizani, E., Chadwick, E., Cincinelli, A., Claßen, D., & Danielsson, S. (2022). Determination of 56 per-and polyfluoroalkyl substances in top predators and their prey from Northern Europe by LC-MS/MS. *Chemosphere*, 287, 131775.
- Arvaniti, O. S., Ventouri, E. I., Stasinakis, A. S., & Thomaidis, N. S. (2012). Occurrence of different classes of perfluorinated compounds in Greek wastewater treatment plants and

- determination of their solid–water distribution coefficients. *Journal of hazardous materials*, 239, 24-31.
- Asher, B. J., Wang, Y., De Silva, A. O., Backus, S., Muir, D. C., Wong, C. S., & Martin, J. W. (2012). Enantiospecific perfluorooctane sulfonate (PFOS) analysis reveals evidence for the source contribution of PFOS-precursors to the Lake Ontario foodweb. *Environmental Science & Technology*, 46(14), 7653-7660.
- ATSDR. (2018). *ATSDR's minimal risk levels (MRLs) and environmental media evaluation guides (EMEGs) for PFAS*. Retrieved 10/04/2023 from <https://www.atsdr.cdc.gov/pfas/resources/mrl-pfas.html>
- AWWA. (2019). *Per- and polyfluoroalkyl substance (PFAS), overview and prevalence*. American Water Works Association. Retrieved 10/04/2023 from [https://www.awwa.org/Portals/0/AWWA/ETS/Resources/Per-andPolyfluoroalkylSubstances\(PFAS\)-OverviewandPrevalence.pdf?ver=2019-08-14-090234-873](https://www.awwa.org/Portals/0/AWWA/ETS/Resources/Per-andPolyfluoroalkylSubstances(PFAS)-OverviewandPrevalence.pdf?ver=2019-08-14-090234-873)
- Bach, C., Dauchy, X., Boiteux, V., Colin, A., Hemard, J., Sagres, V., Rosin, C., & Munoz, J.-F. (2017). The impact of two fluoropolymer manufacturing facilities on downstream contamination of a river and drinking water resources with per-and polyfluoroalkyl substances. *Environmental Science and Pollution Research*, 24(5), 4916-4925.
- Banks, R. E., Smart, B. E., & Tatlow, J. (2013). *Organofluorine chemistry: principles and commercial applications*. Springer Science & Business Media.
- Barzen-Hanson, K. A., Roberts, S. C., Choyke, S., Oetjen, K., McAlees, A., Riddell, N., McCrindle, R., Ferguson, P. L., Higgins, C. P., Field, J. A. J. E. s., & technology. (2017). Discovery of 40 classes of per-and polyfluoroalkyl substances in historical aqueous film-forming foams (AFFFs) and AFFF-impacted groundwater. 51(4), 2047-2057.
- Benskin, J. P., Yeung, L. W., Yamashita, N., Taniyasu, S., Lam, P. K., & Martin, J. W. (2010). Perfluorinated acid isomer profiling in water and quantitative assessment of manufacturing source. *Environmental Science & Technology*, 44(23), 9049-9054.
- Bentel, M. J., Yu, Y., Xu, L., Kwon, H., Li, Z., Wong, B. M., Men, Y., & Liu, J. (2020). Degradation of perfluoroalkyl ether carboxylic acids with hydrated electrons: Structure–reactivity relationships and environmental implications. *Environmental Science & Technology*, 54(4), 2489-2499.

- Bogdan, D. (2019). *Perfluorobutane sulfonic acid (PFBS) chemistry, production, uses, and environmental fate in michigan*.
https://www.michigan.gov/documents/pfasresponse/Perfluorobutane_Sulfonic_Acid_PFBS_Chemistry_Production_Uses_and_Environmental_Fate_704238_7.pdf
- Bonefeld-Jørgensen, E. C., Long, M., Fredslund, S. O., Bossi, R., & Olsen, J. (2014). Breast cancer risk after exposure to perfluorinated compounds in Danish women: a case-control study nested in the Danish National Birth Cohort. *Cancer Causes & Control*, 25(11), 1439-1448.
- Bossi, R., Strand, J., Sortkjaer, O., & Larsen, M. (2008). Perfluoroalkyl compounds in Danish wastewater treatment plants and aquatic environments. *Environment international*, 34(4), 443-450.
- Boulanger, B., Vargo, J., Schnoor, J. L., & Hornbuckle, K. C. (2004). Detection of perfluorooctane surfactants in Great Lakes water. *Environmental Science & Technology*, 38(15), 4064-4070.
- Brandsma, S., Koekkoek, J., van Velzen, M., & de Boer, J. (2019). The PFOA substitute GenX detected in the environment near a fluoropolymer manufacturing plant in the Netherlands. *Chemosphere*, 220, 493-500.
- Brendel, S., Fetter, É., Staude, C., Vierke, L., & Biegel-Engler, A. (2018). Short-chain perfluoroalkyl acids: environmental concerns and a regulatory strategy under REACH. *Environmental Sciences Europe*, 30(1), 1-11.
- Brusseau, M. L., Anderson, R. H., & Guo, B. (2020). PFAS concentrations in soils: Background levels versus contaminated sites. *Science of The Total Environment*, 740, 140017.
- Buck, R. C., Franklin, J., Berger, U., Conder, J. M., Cousins, I. T., De Voogt, P., Jensen, A. A., Kannan, K., Mabury, S. A., & van Leeuwen, S. P. (2011). Perfluoroalkyl and polyfluoroalkyl substances in the environment: terminology, classification, and origins. *Integrated environmental assessment and management*, 7(4), 513-541.
- Cai, M., Yang, H., Xie, Z., Zhao, Z., Wang, F., Lu, Z., Sturm, R., & Ebinghaus, R. (2012). Per- and polyfluoroalkyl substances in snow, lake, surface runoff water and coastal seawater in Fildes Peninsula, King George Island, Antarctica. *Journal of hazardous materials*, 209, 335-342.

- Cai, M., Zhao, Z., Yang, H., Yin, Z., Hong, Q., Sturm, R., Ebinghaus, R., Ahrens, L., Cai, M., & He, J. (2012). Spatial distribution of per-and polyfluoroalkyl compounds in coastal waters from the East to South China Sea. *Environmental Pollution*, *161*, 162-169.
- Calafat, A. M., Wong, L.-Y., Kuklennyik, Z., Reidy, J. A., & Needham, L. L. (2007). Polyfluoroalkyl chemicals in the US population: data from the National Health and Nutrition Examination Survey (NHANES) 2003–2004 and comparisons with NHANES 1999–2000. *Environmental health perspectives*, *115*(11), 1596-1602.
- Campo, J., Lorenzo, M., Pérez, F., Picó, Y., la Farré, M., & Barceló, D. (2016). Analysis of the presence of perfluoroalkyl substances in water, sediment and biota of the Jucar River (E Spain). Sources, partitioning and relationships with water physical characteristics. *Environmental research*, *147*, 503-512.
- Chen, H., Han, J., Zhang, C., Cheng, J., Sun, R., Wang, X., Han, G., Yang, W., & He, X. (2017). Occurrence and seasonal variations of per-and polyfluoroalkyl substances (PFASs) including fluorinated alternatives in rivers, drain outlets and the receiving Bohai Sea of China. *Environmental Pollution*, *231*, 1223-1231.
- Chen, M., Wang, Q., Shan, G., Zhu, L., Yang, L., & Liu, M. (2018). Occurrence, partitioning and bioaccumulation of emerging and legacy per-and polyfluoroalkyl substances in Taihu Lake, China. *Science of The Total Environment*, *634*, 251-259.
- Chen, X., Zhu, L., Pan, X., Fang, S., Zhang, Y., & Yang, L. (2015). Isomeric specific partitioning behaviors of perfluoroalkyl substances in water dissolved phase, suspended particulate matters and sediments in Liao River Basin and Taihu Lake, China. *Water Research*, *80*, 235-244.
- Cheremisinoff, N. P. (2016). *Perfluorinated chemicals (PFCs): contaminants of concern*. John Wiley & Sons.
- Chu, S., & Letcher, R. J. (2014). In vitro metabolic formation of perfluoroalkyl sulfonamides from copolymer surfactants of pre-and post-2002 scotchgard fabric protector products. *Environmental Science & Technology*, *48*(11), 6184-6191.
- Codling, G., Vogt, A., Jones, P. D., Wang, T., Wang, P., Lu, Y.-L., Corcoran, M., Bonina, S., Li, A., & Sturchio, N. C. (2014). Historical trends of inorganic and organic fluorine in sediments of Lake Michigan. *Chemosphere*, *114*, 203-209.
- Coggan, T. L., Anumol, T., Pyke, J., Shimeta, J., & Clarke, B. O. (2019). A single analytical method for the determination of 53 legacy and emerging per-and polyfluoroalkyl

- substances (PFAS) in aqueous matrices. *Analytical and bioanalytical chemistry*, 411(16), 3507-3520.
- Cooke, M. (2017). Technical fact sheet—perfluorooctane sulfonate (PFOS) and perfluorooctanoic acid (PFOA). *Emergency, O. o. L. a., ed., United States Environmental Protection Agency*.
- D'Agostino, L. A., & Mabury, S. A. (2017). Certain perfluoroalkyl and polyfluoroalkyl substances associated with aqueous film forming foam are widespread in Canadian surface waters. *Environmental science & technology*, 51(23), 13603-13613.
- Dalton, W. (2018). *General overview of PFAS per-and polyfluoroalkyl substances* 25th International Petroleum Environmental Conference, <https://slideplayer.com/slide/15371792/>
- Dauchy, X., Boiteux, V., Colin, A., Bach, C., Rosin, C., & Munoz, J.-F. (2019). Poly- and perfluoroalkyl substances in runoff water and wastewater sampled at a firefighter training area. *Archives of environmental contamination and toxicology*, 76(2), 206-215.
- De Voogt, P. (2010). *Reviews of environmental contamination and toxicology volume 208: perfluorinated alkylated substances* (Vol. 208). Springer Science & Business Media.
- Dinglasan, M. J. A., Ye, Y., Edwards, E. A., & Mabury, S. A. (2004). Fluorotelomer alcohol biodegradation yields poly- and perfluorinated acids. *Environmental Science & Technology*, 38(10), 2857-2864.
- Dong, W., Liu, B., Song, Y., Zhang, H., Li, J., & Cui, X. (2018). Occurrence and partition of perfluorinated compounds (PFCs) in Water and Sediment from the Songhua River, China. *Archives of environmental contamination and toxicology*, 74(3), 492-501.
- Commission staff working document poly- and perfluoroalkyl substances (PFAS) accompanying the document communication from the commission to the European parliament, the council, the European economic and social committee and the committee of the regions chemicals strategy for sustainability towards a toxic-free environment, (2020). <https://op.europa.eu/en/publication-detail/-/publication/2614f1f2-0f02-11eb-bc07-01aa75ed71a1>
- Evich, M. G., Davis, M., Weber, E. J., Tebes-Stevens, C., Acrey, B., Henderson, W. M., Goodrow, S., Bergman, E., & Washington, J. W. (2022). Environmental fate of Cl-PFPECA: predicting the formation of PFAS transformation products in New Jersey soils. *Environmental Science & Technology*, 56(12), 7779-7788.

- Fang, S., Chen, X., Zhao, S., Zhang, Y., Jiang, W., Yang, L., & Zhu, L. (2014). Trophic magnification and isomer fractionation of perfluoroalkyl substances in the food web of Taihu Lake, China. *Environmental Science & Technology*, 48(4), 2173-2182.
- Feng, H., Ruan, Y., Zhang, K., & Lam, P. K. (2019). Current analytical methodologies and gaps for per-and polyfluoroalkyl substances determination in the marine environment. *TrAC Trends in Analytical Chemistry*, 121, 115372.
- Frigerio, G., Cafagna, S., Polledri, E., Mercadante, R., & Fustinoni, S. (2022). Development and validation of an LC–MS/MS method for the quantitation of 30 legacy and emerging per- and polyfluoroalkyl substances (PFASs) in human plasma, including HFPO-DA, DONA, and cC6O4. *Analytical and bioanalytical chemistry*, 414, 1259-1278.
- Gebbink, W. A., Glynn, A., & Berger, U. (2015). Temporal changes (1997–2012) of perfluoroalkyl acids and selected precursors (including isomers) in Swedish human serum. *Environmental Pollution*, 199, 166-173.
- Giesy, J. P., & Kannan, K. (2001). Global distribution of perfluorooctane sulfonate in wildlife. *Environmental Science & Technology*, 35(7), 1339-1342.
- Goodrow, S. M., Ruppel, B., Lippincott, R. L., Post, G. B., & Procopio, N. A. (2020). Investigation of levels of perfluoroalkyl substances in surface water, sediment and fish tissue in New Jersey, USA. *Science of The Total Environment*, 729, 138839.
- Gosetti, F., Chiuminatto, U., Zampieri, D., Mazzucco, E., Robotti, E., Calabrese, G., Gennaro, M. C., & Marengo, E. (2010). Determination of perfluorochemicals in biological, environmental and food samples by an automated on-line solid phase extraction ultra high performance liquid chromatography tandem mass spectrometry method. *Journal of Chromatography A*, 1217(50), 7864-7872.
- Greaves, A. K., & Letcher, R. J. (2013). Linear and branched perfluorooctane sulfonate (PFOS) isomer patterns differ among several tissues and blood of polar bears. *Chemosphere*, 93(3), 574-580.
- Gross, J. H. (2006). *Mass spectrometry: a textbook*. Springer Science & Business Media.
- Gross, J. H. (2017). Electrospray ionization. In *Mass spectrometry: a textbook* (pp. 721-778). Springer International Publishing. https://doi.org/10.1007/978-3-319-54398-7_12

- Guy, W., Taves, D. R., & Brey Jr, W. (1976). Organic fluorocompounds in human plasma: Prevalence and characterization. In. ACS Publications.
- Gyllenhammar, I., Benskin, J. P., Sandblom, O., Berger, U., Ahrens, L., Lignell, S., Wiberg, K., & Glynn, A. (2018). Perfluoroalkyl acids (PFAAs) in serum from 2–4-month-old infants: Influence of maternal serum concentration, gestational age, breast-feeding, and contaminated drinking water. *Environmental Science & Technology*, 52(12), 7101-7110.
- Harrata, K. (1995). *Mass spectrometry tutorial*. Iowa State University, Chemical instrument Facility. Retrieved 10/05/2023 from <https://www.cif.iastate.edu/mass-spec/ms-tutorial#Ionization%20Methods>
- Haug, L. S., Huber, S., Schlabach, M., Becher, G., & Thomsen, C. (2011). Investigation on per- and polyfluorinated compounds in paired samples of house dust and indoor air from Norwegian homes. *Environmental Science & Technology*, 45(19), 7991-7998.
- Hayes, J., & Faber, S. (2020). *Updated map: suspected and confirmed PFAS pollution at U.S. military bases*. Retrieved 10/05/2023 from <https://www.ewg.org/news-and-analysis/2020/04/updated-map-suspected-and-confirmed-pfas-pollution-us-military-bases>
- Hayes, J., Faber, S., Andrews, D., & Lothspeich, A. (2019). *PFAS nation: toxic discharges suspected from almost 500 industrial facilities across U.S.* Retrieved 10/05/2023 from <https://www.ewg.org/news-and-analysis/2019/06/pfas-nation-toxic-discharges-suspected-almost-500-industrial-facilities>
- Heydebreck, F., Tang, J., Xie, Z., & Ebinghaus, R. (2015, Jul 21). Alternative and legacy perfluoroalkyl substances: differences between european and chinese river/estuary systems. *Environ Sci Technol*, 49(14), 8386-8395. <https://doi.org/10.1021/acs.est.5b01648>
- Higgins, C. P., & Luthy, R. G. (2006). Sorption of perfluorinated surfactants on sediments. *Environmental Science & Technology*, 40(23), 7251-7256.
- Hitchcock, D. J., Andersen, T., Varpe, Ø., Loonen, M. J., Warner, N. A., Herzke, D., Tombre, I. M., Griffin, L. R., Shimmings, P., & Borgå, K. (2019). Potential effect of migration strategy on pollutant occurrence in eggs of Arctic breeding barnacle geese (*Branta leucopsis*). *Environmental Science & Technology*, 53(9), 5427-5435.
- Houde, M., Czub, G., Small, J. M., Backus, S., Wang, X., Alae, M., & Muir, D. C. (2008). Fractionation and bioaccumulation of perfluorooctane sulfonate (PFOS) isomers in a Lake Ontario food web. *Environmental Science & Technology*, 42(24), 9397-9403.

- Houtz, E., Wang, M., & Park, J.-S. (2018). Identification and fate of aqueous film forming foam derived per-and polyfluoroalkyl substances in a wastewater treatment plant. *Environmental Science & Technology*, 52(22), 13212-13221.
- Houtz, E. F., Higgins, C. P., Field, J. A., & Sedlak, D. L. (2013). Persistence of perfluoroalkyl acid precursors in AFFF-impacted groundwater and soil. *Environmental science & technology*, 47(15), 8187-8195.
- Hu, X. C., Andrews, D. Q., Lindstrom, A. B., Bruton, T. A., Schaidler, L. A., Grandjean, P., Lohmann, R., Carignan, C. C., Blum, A., & Balan, S. A. (2016). Detection of poly-and perfluoroalkyl substances (PFASs) in US drinking water linked to industrial sites, military fire training areas, and wastewater treatment plants. *Environmental Science & Technology Letters*, 3(10), 344-350.
- Hua, X., Luo, J., Zhao, Z., Wang, Q., & Sun, H. (2019). Neutral polyfluoroalkyl and perfluoroalkyl substances in surface water and sediment from the Haihe River and Dagu Drainage Canal deserve more attention. *Environmental Science and Pollution Research*, 26(32), 32911-32918.
- Huerta, B., McHugh, B., & Regan, F. (2022). Development and application of an LC-MS method to the determination of poly-and perfluoroalkyl substances (PFASs) in drinking, sea and surface water samples. *Analytical Methods*, 14(21), 2090-2099.
- Hurley, S., Goldberg, D., Wang, M., Park, J.-S., Petreas, M., Bernstein, L., Anton-Culver, H., Nelson, D. O., & Reynolds, P. (2018). Time trends in per-and polyfluoroalkyl substances (PFASs) in California women: declining serum levels, 2011–2015. *Environmental Science & Technology*, 52(1), 277-287.
- ITRC, I. T. R. C. (2021). *PFAS technical and regulatory guidance document and fact sheets PFAS-1*. <https://pfas-1.itrcweb.org/>
- Jain, R. B. (2018). Time trends over 2003–2014 in the concentrations of selected perfluoroalkyl substances among US adults aged ≥ 20 years: interpretational issues. *Science of The Total Environment*, 645, 946-957.
- Johnson, R. L., Anschutz, A. J., Smolen, J. M., Simcik, M. F., & Penn, R. L. (2007). The adsorption of perfluorooctane sulfonate onto sand, clay, and iron oxide surfaces. *Journal of Chemical & Engineering Data*, 52(4), 1165-1170.

- Kaboré, H. A., Duy, S. V., Munoz, G., Méité, L., Desrosiers, M., Liu, J., Sory, T. K., & Sauvé, S. (2018). Worldwide drinking water occurrence and levels of newly-identified perfluoroalkyl and polyfluoroalkyl substances. *Science of The Total Environment*, 616, 1089-1100.
- Keen, R. (2005). *The life and work of Friedrich Wohler (1800-1882)* (Publication Number ISBN 3-88309-224-X) University College London (University of London)]. Verlag Traugott Bautz GmbH, Nordhausen
- KEMI. (2015). *Occurrence and use of highly fluorinated substances and alternatives*. <https://www.kemi.se/en/publications/reports/2015/report-7-15-occurrence-and-use-of-highly-fluorinated-substances-and-alternatives>
- Koch, A., Aro, R., Wang, T., & Yeung, L. W. (2020). Towards a comprehensive analytical workflow for the chemical characterisation of organofluorine in consumer products and environmental samples. *TrAC Trends in Analytical Chemistry*, 123, 115423.
- Koch, A., Kärman, A., Yeung, L. W., Jonsson, M., Ahrens, L., & Wang, T. (2019). Point source characterization of per- and polyfluoroalkyl substances (PFASs) and extractable organofluorine (EOF) in freshwater and aquatic invertebrates. *Environmental Science: Processes & Impacts*, 21(11), 1887-1898.
- Koch, A., Yukioka, S., Tanaka, S., Yeung, L. W., Kärman, A., & Wang, T. (2021). Characterization of an AFFF impacted freshwater environment using total fluorine, extractable organofluorine and suspect per- and polyfluoroalkyl substance screening analysis. *Chemosphere*, 130179.
- Labadie, P., & Chevreuil, M. (2011). Partitioning behaviour of perfluorinated alkyl contaminants between water, sediment and fish in the Orge River (nearby Paris, France). *Environmental pollution*, 159(2), 391-397.
- Lam, N. H., Cho, C.-R., Kannan, K., & Cho, H.-S. (2017). A nationwide survey of perfluorinated alkyl substances in waters, sediment and biota collected from aquatic environment in Vietnam: distributions and bioconcentration profiles. *Journal of hazardous materials*, 323, 116-127.
- Lassen, C., & Brinch, A. (2017). *Investigation of sources to PFBS in the environment* (A086083). N. E. Agency.

- Lee, J., Lee, H.-K., Lim, J.-E., & Moon, H.-B. (2020). Legacy and emerging per- and polyfluoroalkyl substances (PFASs) in the coastal environment of Korea: Occurrence, spatial distribution, and bioaccumulation potential. *Chemosphere*, 126633.
- Lee, J. W., Lee, H. K., Lim, J. E., & Moon, H. B. (2020, Jul). Legacy and emerging per- and polyfluoroalkyl substances (PFASs) in the coastal environment of Korea: Occurrence, spatial distribution, and bioaccumulation potential. *Chemosphere*, 251, 126633. <https://doi.org/10.1016/j.chemosphere.2020.126633>
- Li, X., Fatoweh, M., Cui, D., & Quinete, N. (2022, Feb 1). Assessment of per- and polyfluoroalkyl substances in Biscayne Bay surface waters and tap waters from South Florida. *Sci Total Environ*, 806(Pt 1), 150393. <https://doi.org/10.1016/j.scitotenv.2021.150393>
- Li, Y., Feng, X., Zhou, J., & Zhu, L. (2020). Occurrence and source apportionment of novel and legacy poly/perfluoroalkyl substances in Hai River basin in China using receptor models and isomeric fingerprints. *Water Research*, 168, 115145.
- Li, Y., Yao, J., Pan, Y., Dai, J., & Tang, J. (2023). Trophic behaviors of PFOA and its alternatives perfluoroalkyl ether carboxylic acids (PFECAs) in a coastal food web. *Journal of hazardous materials*, 452, 131353.
- Li, Y., Yao, J., Zhang, J., Pan, Y., Dai, J., Ji, C., & Tang, J. (2021). First report on the bioaccumulation and trophic transfer of perfluoroalkyl ether carboxylic acids in estuarine food web. *Environmental Science & Technology*, 56(10), 6046-6055.
- Lindstrom, A. B., Strynar, M. J., & Libelo, E. L. (2011). Polyfluorinated compounds: past, present, and future. *Environmental Science & Technology*, 45(19), 7954-7961.
- Liu, H.-S., Wen, L.-L., Chu, P.-L., & Lin, C.-Y. (2018). Association among total serum isomers of perfluorinated chemicals, glucose homeostasis, lipid profiles, serum protein and metabolic syndrome in adults: NHANES, 2013–2014. *Environmental Pollution*, 232, 73-79.
- Liu, Y., D'Agostino, L. A., Qu, G., Jiang, G., & Martin, J. W. (2019). High-resolution mass spectrometry (HRMS) methods for nontarget discovery and characterization of poly- and per-fluoroalkyl substances (PFASs) in environmental and human samples. *TrAC Trends in Analytical Chemistry*, 121, 115420.
- Liu, Y., Zhang, Y., Li, J., Wu, N., Li, W., & Niu, Z. (2019). Distribution, partitioning behavior and positive matrix factorization-based source analysis of legacy and emerging

- polyfluorinated alkyl substances in the dissolved phase, surface sediment and suspended particulate matter around coastal areas of Bohai Bay, China. *Environmental Pollution*, 246, 34-44.
- Liu, Y., Zhang, Y., Li, J., Wu, N., Li, W., & Niu, Z. (2019, Mar). Distribution, partitioning behavior and positive matrix factorization-based source analysis of legacy and emerging polyfluorinated alkyl substances in the dissolved phase, surface sediment and suspended particulate matter around coastal areas of Bohai Bay, China. *Environ Pollut*, 246, 34-44. <https://doi.org/10.1016/j.envpol.2018.11.113>
- Löfstedt Gilljam, J., Leonel, J., Cousins, I. T., & Benskin, J. P. (2016). Is ongoing sulfluramid use in South America a significant source of perfluorooctanesulfonate (PFOS)? Production inventories, environmental fate, and local occurrence. *Environmental Science & Technology*, 50(2), 653-659.
- Loganathan, B. G., Sajwan, K. S., Sinclair, E., Kumar, K. S., & Kannan, K. (2007). Perfluoroalkyl sulfonates and perfluorocarboxylates in two wastewater treatment facilities in Kentucky and Georgia. *Water Research*, 41(20), 4611-4620.
- Loos, R., Tavazzi, S., Mariani, G., Suurkuusk, G., Paracchini, B., & Umlauf, G. (2017). Analysis of emerging organic contaminants in water, fish and suspended particulate matter (SPM) in the Joint Danube Survey using solid-phase extraction followed by UHPLC-MS-MS and GC-MS analysis. *Science of The Total Environment*, 607, 1201-1212.
- Marchiandi, J., Szabo, D., Dagnino, S., Green, M. P., & Clarke, B. O. (2021). Occurrence and fate of legacy and novel per- and polyfluoroalkyl substances (PFASs) in freshwater after an industrial fire of unknown chemical stockpiles. *Environmental Pollution*, 278, 116839.
- Martin, D., Munoz, G., Mejia-Avenidaño, S., Duy, S. V., Yao, Y., Volchek, K., Brown, C. E., Liu, J., & Sauvé, S. (2019). Zwitterionic, cationic, and anionic perfluoroalkyl and polyfluoroalkyl substances integrated into total oxidizable precursor assay of contaminated groundwater. *Talanta*, 195, 533-542.
- Meng, L., Song, B., Zhong, H., Ma, X., Wang, Y., Ma, D., Lu, Y., Gao, W., Wang, Y., & Jiang, G. (2021). Legacy and emerging per- and polyfluoroalkyl substances (PFAS) in the Bohai Sea and its inflow rivers. *Environment International*, 156, 106735.
- Miaz, L. T., Plassmann, M. M., Gyllenhammar, I., Bignert, A., Sandblom, O., Lignell, S., Glynn, A., & Benskin, J. P. (2020). Temporal trends of suspect- and target-per/polyfluoroalkyl substances (PFAS), extractable organic fluorine (EOF) and total fluorine (TF) in pooled serum from first-time mothers in Uppsala, Sweden, 1996–2017. *Environmental Science: Processes & Impacts*, 22(4), 1071-1083.

- Michael J. Parent, P. M. S., Richard M. Flynn (2004). *Fluorinated surfactants for buffered acid etch solutions* (US Patent No. US7169323B2).
- Milinic, J., Lacorte, S., Vidal, M., & Rigol, A. (2015). Sorption behaviour of perfluoroalkyl substances in soils. *Science of The Total Environment*, 511, 63-71.
- Moody, C. A., Kwan, W. C., Martin, J. W., Muir, D. C., & Mabury, S. A. (2001). Determination of perfluorinated surfactants in surface water samples by two independent analytical techniques: liquid chromatography/tandem mass spectrometry and ¹⁹F NMR. *Analytical chemistry*, 73(10), 2200-2206.
- Mulabagal, V., Liu, L., Qi, J., Wilson, C., & Hayworth, J. S. (2018, 2018/12/01/). A rapid UHPLC-MS/MS method for simultaneous quantitation of 23 perfluoroalkyl substances (PFAS) in estuarine water. *Talanta*, 190, 95-102.
<https://doi.org/https://doi.org/10.1016/j.talanta.2018.07.053>
- Munoz, G., Giraudel, J.-L., Botta, F., Lestremau, F., Dévier, M.-H., Budzinski, H., & Labadie, P. (2015). Spatial distribution and partitioning behavior of selected poly-and perfluoroalkyl substances in freshwater ecosystems: a French nationwide survey. *Science of The Total Environment*, 517, 48-56.
- Munoz, G., Labadie, P., Botta, F., Lestremau, F., Lopez, B., Geneste, E., Pardon, P., Dévier, M.-H., & Budzinski, H. (2017). Occurrence survey and spatial distribution of perfluoroalkyl and polyfluoroalkyl surfactants in groundwater, surface water, and sediments from tropical environments. *Science of The Total Environment*, 607, 243-252.
- Munoz, G., Ray, P., Mejia-Avenida, S., Duy, S. V., Do, D. T., Liu, J., & Sauvé, S. (2018). Optimization of extraction methods for comprehensive profiling of perfluoroalkyl and polyfluoroalkyl substances in firefighting foam impacted soils. *Analytica chimica acta*, 1034, 74-84.
- Naile, J. E., Khim, J. S., Wang, T., Chen, C., Luo, W., Kwon, B.-O., Park, J., Koh, C.-H., Jones, P. D., Lu, Y., & Giesy, J. P. (2010, 2010/05/01/). Perfluorinated compounds in water, sediment, soil and biota from estuarine and coastal areas of Korea. *Environmental Pollution*, 158(5), 1237-1244.
<https://doi.org/https://doi.org/10.1016/j.envpol.2010.01.023>
- Nakata, H., Kannan, K., Nasu, T., Cho, H.-S., Sinclair, E., & Takemura, A. (2006). Perfluorinated contaminants in sediments and aquatic organisms collected from shallow water and tidal flat areas of the Ariake Sea, Japan: environmental fate of perfluorooctane

- sulfonate in aquatic ecosystems. *Environmental Science & Technology*, 40(16), 4916-4921.
- Nakayama, S. F., Strynar, M. J., Reiner, J. L., Delinsky, A. D., & Lindstrom, A. B. (2010). Determination of perfluorinated compounds in the Upper Mississippi River Basin. *Environmental Science & Technology*, 44(11), 4103-4109.
- Nakayama, S. F., Yoshikane, M., Onoda, Y., Nishihama, Y., Iwai-Shimada, M., Takagi, M., Kobayashi, Y., & Isobe, T. (2019a). Worldwide trends in tracing poly-and perfluoroalkyl substances (PFAS) in the environment. *TrAC Trends in Analytical Chemistry*, 121, 115410.
- Nakayama, S. F., Yoshikane, M., Onoda, Y., Nishihama, Y., Iwai-Shimada, M., Takagi, M., Kobayashi, Y., & Isobe, T. J. T. T. i. A. C. (2019b). Worldwide trends in tracing poly-and perfluoroalkyl substances (PFAS) in the environment. *121*, 115410.
- Nascimento, R. A., Nunoo, D. B., Bizkarguenaga, E., Schultes, L., Zabaleta, I., Benskin, J. P., Spanó, S., & Leonel, J. (2018). Sulfloramid use in Brazilian agriculture: A source of per-and polyfluoroalkyl substances (PFASs) to the environment. *Environmental Pollution*, 242, 1436-1443.
- Nassazzi, W., Lai, F. Y., & Ahrens, L. (2022). A novel method for extraction, clean-up and analysis of per-and polyfluoroalkyl substances (PFAS) in different plant matrices using LC-MS/MS. *Journal of Chromatography B*, 1212, 123514.
- Nguyen, M. A., Wiberg, K., Ribeli, E., Josefsson, S., Futter, M., Gustavsson, J., & Ahrens, L. (2017). Spatial distribution and source tracing of per-and polyfluoroalkyl substances (PFASs) in surface water in Northern Europe. *Environmental Pollution*, 220, 1438-1446.
- Nian, M., Li, Q.-Q., Bloom, M., Qian, Z. M., Syberg, K. M., Vaughn, M. G., Wang, S.-Q., Wei, Q., Zeeshan, M., & Gurram, N. (2019). Liver function biomarkers disorder is associated with exposure to perfluoroalkyl acids in adults: Isomers of C8 Health Project in China. *Environmental research*, 172, 81-88.
- Nilsson, H., Kärrman, A., Rotander, A., van Bavel, B., Lindström, G., & Westberg, H. (2013). Biotransformation of fluorotelomer compound to perfluorocarboxylates in humans. *Environment international*, 51, 8-12.
- O'Brien, J. M., Kennedy, S. W., Chu, S., & Letcher, R. J. (2011). Isomer-specific accumulation of perfluorooctane sulfonate in the liver of chicken embryos exposed in ovo to a technical mixture. *Environmental Toxicology and Chemistry*, 30(1), 226-231.

- Pan, C.-G., Ying, G.-G., Zhao, J.-L., Liu, Y.-S., Jiang, Y.-X., & Zhang, Q.-Q. (2014). Spatiotemporal distribution and mass loadings of perfluoroalkyl substances in the Yangtze River of China. *Science of The Total Environment*, 493, 580-587.
- Pan, C.-G., Yu, K.-F., Wang, Y.-H., Zhang, W., Zhang, J., & Guo, J. (2019). Perfluoroalkyl substances in the riverine and coastal water of the Beibu Gulf, South China: Spatiotemporal distribution and source identification. *Science of The Total Environment*, 660, 297-305.
- Pan, Y., Zhang, H., Cui, Q., Sheng, N., Yeung, L. W., Sun, Y., Guo, Y., & Dai, J. (2018). Worldwide distribution of novel perfluoroether carboxylic and sulfonic acids in surface water. *Environmental Science & Technology*, 52(14), 7621-7629.
- Paul, A. G., Jones, K. C., & Sweetman, A. J. (2009). A first global production, emission, and environmental inventory for perfluorooctane sulfonate. *Environmental Science & Technology*, 43(2), 386-392.
- Pereira, H. C., Ullberg, M., Kleja, D. B., Gustafsson, J. P., & Ahrens, L. (2018). Sorption of perfluoroalkyl substances (PFASs) to an organic soil horizon—Effect of cation composition and pH. *Chemosphere*, 207, 183-191.
- Picard, J.-C., Munoz, G., Duy, S. V., & Sauvé, S. (2021). Longitudinal and vertical variations of waterborne emerging contaminants in the St. Lawrence Estuary and Gulf during winter conditions. *Science of The Total Environment*, 777, 146073.
- Pitt, J. J. (2009). Principles and applications of liquid chromatography-mass spectrometry in clinical biochemistry. *The Clinical Biochemist Reviews*, 30(1), 19.
- Pizzurro, D. M., Seeley, M., Kerper, L. E., & Beck, B. D. (2019). Interspecies differences in perfluoroalkyl substances (PFAS) toxicokinetics and application to health-based criteria. *Regulatory Toxicology and Pharmacology*, 106, 239-250.
- Plunkett, R. J. (1986). The history of polytetrafluoroethylene: discovery and development. High Performance Polymers: Their Origin and Development: Proceedings of the Symposium on the History of High Performance Polymers at the American Chemical Society Meeting held in New York, April 15–18, 1986,
- Poothong, S., Thomsen, C., Padilla-Sanchez, J. A., Papadopoulou, E., & Haug, L. S. (2017). Distribution of novel and well-known poly-and perfluoroalkyl substances (PFASs) in

- human serum, plasma, and whole blood. *Environmental Science & Technology*, 51(22), 13388-13396.
- Prevedouros, K., Cousins, I. T., Buck, R. C., & Korzeniowski, S. H. (2006). Sources, fate and transport of perfluorocarboxylates. *Environmental Science & Technology*, 40(1), 32-44.
- QldGov. (2018). *Firefighting foam policy waste disposal plan advisory (fluorinated organic compounds)*. Retrieved 10/04/2023 from https://www.qld.gov.au/_data/assets/pdf_file/0033/68982/firefighting-foam-waste-disposal-plan-advisory.pdf
- Rayne, S., Forest, K., & Friesen, K. J. (2008). Congener-specific numbering systems for the environmentally relevant C4 through C8 perfluorinated homologue groups of alkyl sulfonates, carboxylates, telomer alcohols, olefins, and acids, and their derivatives. *Journal of Environmental Science and Health Part A*, 43(12), 1391-1401.
- Reagen, W., Lindstrom, K., Jacoby, C., Purcell, R., Kestner, T., Payfer, R., & Miller, J. (2007). Environmental characterization of 3M electrochemical fluorination derived perfluorooctanoate and perfluorooctanesulfonate. Abstracts of the Society of Environmental Toxicology and Chemistry North America 28th Annual Meeting; 2007 November 11-15; Milwaukee, Wisconsin, USA.,
- Ritter, E. E., Dickinson, M. E., Harron, J. P., Lunderberg, D. M., DeYoung, P. A., Robel, A. E., Field, J. A., & Peaslee, G. F. (2017). PIGE as a screening tool for Per-and polyfluorinated substances in papers and textiles. *Nuclear Instruments and Methods in Physics Research Section B: Beam Interactions with Materials and Atoms*, 407, 47-54.
- Robel, A. E., Marshall, K., Dickinson, M., Lunderberg, D., Butt, C., Peaslee, G., Stapleton, H. M., & Field, J. A. (2017). Closing the mass balance on fluorine on papers and textiles. *Environmental Science & Technology*, 51(16), 9022-9032.
- Rosenblum, L., & Wendelken, S. (2019). Method 533: determination of per-and polyfluoroalkyl substances in drinking water by isotope dilution anion exchange solid phase extraction and liquid chromatography/tandem mass spectrometry. *Tandem Mass Spectrometry*, 52.
- Schaider, L. A., Balan, S. A., Blum, A., Andrews, D. Q., Strynar, M. J., Dickinson, M. E., Lunderberg, D. M., Lang, J. R., & Peaslee, G. F. (2017). Fluorinated compounds in US fast food packaging. *Environmental Science & Technology Letters*, 4(3), 105-111.

- Schnellmann, R. G., & Manning, R. O. (1990). Perfluorooctane sulfonamide: a structurally novel uncoupler of oxidative phosphorylation. *Biochimica et Biophysica Acta (BBA)-Bioenergetics*, 1016(3), 344-348.
- Schultz, M. M., Barofsky, D. F., & Field, J. A. (2006). Quantitative determination of fluorinated alkyl substances by large-volume-injection liquid chromatography tandem mass spectrometry characterization of municipal wastewaters. *Environmental Science & Technology*, 40(1), 289-295.
- Schulz, K., Silva, M. R., & Klaper, R. (2020). Distribution and effects of branched versus linear isomers of PFOA, PFOS, and PFHxS: A review of recent literature. *Science of The Total Environment*, 733, 139186.
- Semerád, J., Hatasová, N., Grasserová, A., Černá, T., Filipová, A., Hanč, A., Innemanová, P., Pivokonský, M., & Cajthaml, T. (2020). Screening for 32 per-and polyfluoroalkyl substances (PFAS) including GenX in sludges from 43 WWTPs located in the Czech Republic-Evaluation of potential accumulation in vegetables after application of biosolids. *Chemosphere*, 261, 128018.
- Seow, J., Alper, H., Laine, P., & Callaghan, P. (2020). *PFAS – regulatory trends worldwide*. Retrieved 10/09/2023 from <https://www.filtnews.com/pfas-regulatory-trends-worldwide/>
- Sharma, B. M., Bharat, G. K., Tayal, S., Larssen, T., Bečanová, J., Karásková, P., Whitehead, P. G., Futter, M. N., Butterfield, D., & Nizzetto, L. (2016). Perfluoroalkyl substances (PFAS) in river and ground/drinking water of the Ganges River basin: emissions and implications for human exposure. *Environmental Pollution*, 208, 704-713.
- Shibley, J. M., Hurst, C. H., Tanaka, S. S., DeRoos, F. L., Butenhoff, J. L., Seacat, A. M., & Waxman, D. J. (2004). Trans-activation of PPAR α and induction of PPAR α target genes by perfluorooctane-based chemicals. *Toxicological sciences*, 80(1), 151-160.
- Siegemund, G., Schwertfeger, W., Feiring, A., Smart, B., Behr, F., Vogel, H., & McKusick, B. (2000). Fluorine compounds, organic. *Ullmann's Encyclopedia of Industrial Chemistry*.
- Slotkin, T. A., MacKillop, E. A., Melnick, R. L., Thayer, K. A., & Seidler, F. J. (2008). Developmental neurotoxicity of perfluorinated chemicals modeled in vitro. *Environmental health perspectives*, 116(6), 716-722.
- Snyder, L. R., Kirkland, J. J., & Dolan, J. W. (2009). Introduction. In *Introduction to modern liquid chromatography* (pp. 1-17). <https://doi.org/https://doi.org/10.1002/9780470508183.ch1>

- Song, X., Tang, S., Zhu, H., Chen, Z., Zang, Z., Zhang, Y., Niu, X., Wang, X., Yin, H., & Zeng, F. (2018). Biomonitoring PFAAs in blood and semen samples: investigation of a potential link between PFAAs exposure and semen mobility in China. *Environment international*, *113*, 50-54.
- Starkov, A. A., & Wallace, K. B. (2002). Structural determinants of fluorochemical-induced mitochondrial dysfunction. *Toxicological sciences*, *66*(2), 244-252.
<https://doi.org/10.1093/toxsci/66.2.244>
- Taniyasu, S., Kannan, K., So, M. K., Gulkowska, A., Sinclair, E., Okazawa, T., & Yamashita, N. (2005). Analysis of fluorotelomer alcohols, fluorotelomer acids, and short-and long-chain perfluorinated acids in water and biota. *Journal of Chromatography A*, *1093*(1-2), 89-97.
- Theobald, N., Caliebe, C., Gerwinski, W., Hühnerfuss, H., & Lepom, P. (2011). Occurrence of perfluorinated organic acids in the North and Baltic seas. Part 1: distribution in sea water. *Environmental Science and Pollution Research*, *18*, 1057-1069.
- ThermoFisher. (2006). *Ionization source technology overview*. Retrieved 10/09/2023 from <https://www.thermofisher.com/us/en/home/industrial/mass-spectrometry/mass-spectrometry-learning-center/mass-spectrometry-technology-overview/ionization-source-technology-overview.html>
- Theurillat, X., Mujahid, C., Eriksen, B., Griffin, A., Savage, A., Delatour, T., & Mottier, P. (2023). An LC-MS/MS method for the quantitative determination of 57 per-and polyfluoroalkyl substances at ng/kg levels in different food matrices. *Food Additives & Contaminants: Part A*, 1-16.
- Tian, Y.-P., Zeng, X.-W., Bloom, M. S., Lin, S., Wang, S.-Q., Yim, S. H. L., Yang, M., Chu, C., Gurram, N., & Hu, L.-W. (2019). Isomers of perfluoroalkyl substances and overweight status among Chinese by sex status: Isomers of C8 Health Project in China. *Environment international*, *124*, 130-138.
- Toms, L.-M. L., Calafat, A. M., Kato, K., Thompson, J., Harden, F., Hobson, P., Sjodin, A., & Mueller, J. F. (2009). Polyfluoroalkyl chemicals in pooled blood serum from infants, children, and adults in Australia. *Environmental Science & Technology*, *43*(11), 4194-4199.
- Toxic timeline: A brief history of PFAS*. (2019). Retrieved 10/06/2023 from https://www.santafenewmexican.com/news/local_news/toxic-timeline-a-brief-history-of-pfas/article_20609664-48c7-574e-a9f7-1fb813e9a13e.html

- Turner, D. (2021). *Gas chromatography – how a gas chromatography machine works, how to read a chromatograph and GCxGC*. Retrieved 10/09/2023 from <https://www.technologynetworks.com/analysis/articles/gas-chromatography-how-a-gas-chromatography-machine-works-how-to-read-a-chromatograph-and-gcxgc-335168>
- USEPA. (1996). *Monitoring unregulated drinking water contaminants, first unregulated contaminant monitoring rule*. Retrieved 10/09/2023 from <https://www.epa.gov/dwucmr/first-unregulated-contaminant-monitoring-rule>
- USEPA. (2002). *Risk management for per- and polyfluoroalkyl substances (PFAS) under TSCA, overview*. Retrieved 10/09/2023 from <https://www.epa.gov/assessing-and-managing-chemicals-under-tsca/risk-management-and-polyfluoroalkyl-substances-pfas>
- USEPA. (2006). *Risk management for per and polyfluoroalkyl substances (PFAS) under TSCA, PFOA stewardship program*. Retrieved 10/09/2023 from <https://www.epa.gov/assessing-and-managing-chemicals-under-tsca/risk-management-and-polyfluoroalkyl-substances-pfas>
- USEPA. (2009). *Provisional health advisories for perfluorooctanoic acid (PFOA) and perfluorooctane sulfonate (PFOS)*. Retrieved 10/09/2023 from <https://www.epa.gov/sdwa/provisional-health-advisories-perfluorooctanoic-acid-pfoa-and-perfluorooctane-sulfonate-pfos>
- USEPA. (2012). *UCMR3 fact sheet: searching for emerging contaminants in drinking water*. <https://www.epa.gov/dwucmr/fact-sheets-about-third-unregulated-contaminant-monitoring-rule-ucmr-3>
- USEPA. (2016). *Fact sheet: PFOA & PFOS drinking water health advisories*. Retrieved 10/09/2023 from https://www.epa.gov/sites/production/files/2016-06/documents/drinkingwaterhealthadvisories_pfoa_pfos_updated_5.31.16.pdf
- USEPA. (2017). *EPA's non-CBI summary tables for 2015 company progress reports (final progress reports)*. Retrieved 10/09/2023 from <https://www.epa.gov/assessing-and-managing-chemicals-under-tsca/epas-non-cbi-summary-tables-2015-company-progress>
- USEPA. (2018). *Human health toxicity values for perfluorobutane sulfonic acid (CASRN 375-73-5) and related compound potassium perfluorobutane sulfonate (CASRN 29420 49 3)*. https://www.epa.gov/sites/default/files/2018-11/documents/pfbs_public_comment_draft_toxicity_assessment_nov2018-508.pdf

- USEPA. (2019). *EPA's per-and polyfluoroalkyl substances (PFAS) action plan*. Retrieved 10/10/2023 from <https://www.epa.gov/pfas/epas-pfas-action-plan>
- USEPA. (2022a). Drinking water health advisories for PFAS: fact sheet for communities. <https://www.epa.gov/system/files/documents/2022-06/drinking-water-ha-pfas-factsheet-communities.pdf>
- USEPA. (2022b). *National overview: facts and figures on materials, wastes and recycling*. Retrieved 10/10/2023 from <https://www.epa.gov/facts-and-figures-about-materials-waste-and-recycling/national-overview-facts-and-figures-materials#NationalPicture>
- USEPA. (2023a). *Hazardous waste management facilities and units*. Retrieved 10/10/2023 from <https://www.epa.gov/hwpermitting/hazardous-waste-management-facilities-and-units#landfills>
- USEPA. (2023b). *Per- and polyfluoroalkyl substances (PFAS) proposed PFAS national primary drinking water regulation*. Retrieved 10/10/2023 from <https://www.epa.gov/sdwa/and-polyfluoroalkyl-substances-pfas>
- Walker, B. (2018). *Update: mapping the expanding PFAS crisis*. Retrieved 10/06/2023 from <https://www.ewg.org/research/update-mapping-expanding-pfas-crisis>
- Wang, F., Zhao, C., Gao, Y., Fu, J., Gao, K., Lv, K., Wang, K., Yue, H., Lan, X., & Liang, Y. (2019). Protein-specific distribution patterns of perfluoroalkyl acids in egg yolk and albumen samples around a fluorochemical facility. *Science of The Total Environment*, 650, 2697-2704.
- Wang, N., Szostek, B., Buck, R. C., Folsom, P. W., Sulecki, L. M., Capka, V., Berti, W. R., & Gannon, J. T. (2005). Fluorotelomer alcohol biodegradation direct evidence that perfluorinated carbon chains breakdown. *Environmental Science & Technology*, 39(19), 7516-7528.
- Wang, N., Szostek, B., Folsom, P. W., Sulecki, L. M., Capka, V., Buck, R. C., Berti, W. R., & Gannon, J. T. (2005). Aerobic biotransformation of ¹⁴C-labeled 8-2 telomer B alcohol by activated sludge from a domestic sewage treatment plant. *Environmental Science & Technology*, 39(2), 531-538.
- Wang, X., Yu, N., Qian, Y., Shi, W., Zhang, X., Geng, J., Yu, H., & Wei, S. (2020). Non-target and suspect screening of per-and polyfluoroalkyl substances in Chinese municipal wastewater treatment plants. *Water Research*, 183, 115989.

- Wang, Y., Zhang, L., Teng, Y., Zhang, J., Yang, L., Li, J., Lai, J., Zhao, Y., & Wu, Y. (2018). Association of serum levels of perfluoroalkyl substances with gestational diabetes mellitus and postpartum blood glucose. *Journal of environmental sciences*, 69, 5-11.
- Wang, Z., DeWitt, J. C., Higgins, C. P., & Cousins, I. T. (2017). A never-ending story of per-and polyfluoroalkyl substances (PFASs)?
- White, N. D., Balthis, L., Kannan, K., De Silva, A. O., Wu, Q., French, K. M., Daugomah, J., Spencer, C., & Fair, P. A. (2015). Elevated levels of perfluoroalkyl substances in estuarine sediments of Charleston, SC. *Science of The Total Environment*, 521, 79-89.
- Xie, Z., Wang, Z., Mi, W., Möller, A., Wolschke, H., & Ebinghaus, R. (2015). Neutral poly-/perfluoroalkyl substances in air and snow from the Arctic. *Scientific reports*, 5(1), 1-6.
- Yamazaki, E., Falandysz, J., Taniyasu, S., Hui, G., Jurkiewicz, G., Yamashita, N., Yang, Y.-L., & Lam, P. K. (2016). Perfluorinated carboxylic and sulphonic acids in surface water media from the regions of Tibetan Plateau: Indirect evidence on photochemical degradation? *Journal of Environmental Science and Health, Part A*, 51(1), 63-69.
- Yao, J., Pan, Y., Huan, Y., & Dai, J. (2021). Occurrence of novel perfluoroalkyl ether carboxylic acids in river water and human urine quantified by a simple liquid–liquid microextraction approach coupled with LC–MS/MS. *Environmental Science & Technology Letters*, 8(9), 773-778.
- Yao, J., Pan, Y., Sheng, N., Su, Z., Guo, Y., Wang, J., & Dai, J. (2020). Novel perfluoroalkyl ether carboxylic acids (PFECAs) and sulfonic acids (PFESAs): occurrence and association with serum biochemical parameters in residents living near a fluorochemical plant in China. *Environmental Science & Technology*, 54(21), 13389-13398.
- Ye, X., Kato, K., Wong, L.-Y., Jia, T., Kalathil, A., Latremouille, J., & Calafat, A. M. (2018). Per-and polyfluoroalkyl substances in sera from children 3 to 11 years of age participating in the National Health and Nutrition Examination Survey 2013–2014. *International journal of hygiene and environmental health*, 221(1), 9-16.
- Yeung, L. W., De Silva, A. O., Loi, E. I., Marvin, C. H., Taniyasu, S., Yamashita, N., Mabury, S. A., Muir, D. C., & Lam, P. K. (2013). Perfluoroalkyl substances and extractable organic fluorine in surface sediments and cores from Lake Ontario. *Environment international*, 59, 389-397.

- Yu, C. H., Riker, C. D., Lu, S.-e., & Fan, Z. T. (2020). Biomonitoring of emerging contaminants, perfluoroalkyl and polyfluoroalkyl substances (PFAS), in New Jersey adults in 2016–2018. *International journal of hygiene and environmental health*, 223(1), 34-44.
- Zabaleta, I., Bizkarguenaga, E., Nunoo, D. B., Schultes, L., Leonel, J., Prieto, A., Zuloaga, O., & Benskin, J. P. (2018). Biodegradation and uptake of the pesticide sulfluramid in a soil–carrot mesocosm. *Environmental Science & Technology*, 52(5), 2603-2611.
- Zeng, X.-W., Lodge, C. J., Dharmage, S. C., Bloom, M. S., Yu, Y., Yang, M., Chu, C., Li, Q.-Q., Hu, L.-W., & Liu, K.-K. (2019). Isomers of per-and polyfluoroalkyl substances and uric acid in adults: Isomers of C8 Health Project in China. *Environment international*, 133, 105160.
- Zhang, W., Pang, S., Lin, Z., Mishra, S., Bhatt, P., & Chen, S. (2020). Biotransformation of perfluoroalkyl acid precursors from various environmental systems: advances and perspectives. *Environmental Pollution*, 115908.
- Zhao, L., Zhang, Y., Zhu, L., Ma, X., Wang, Y., Sun, H., & Luo, Y. (2017). Isomer-specific transplacental efficiencies of perfluoroalkyl substances in human whole blood. *Environmental Science & Technology Letters*, 4(10), 391-398.
- Zhao, P., Xia, X., Dong, J., Xia, N., Jiang, X., Li, Y., & Zhu, Y. (2016). Short-and long-chain perfluoroalkyl substances in the water, suspended particulate matter, and surface sediment of a turbid river. *Science of The Total Environment*, 568, 57-65.
- Zhao, S.-Y., Zhou, T., Wang, B.-H., Liang, T.-K., & Liu, L.-F. (2018). Isolation, identification, and biodegradation behaviors of a perfluorooctane sulfonic acid precursor (PreFOSs) degrading bacterium from contaminated soil. *Huanjing kexue*, 39(7), 3321-3328.
- Zhao, Z., Cheng, X., Hua, X., Jiang, B., Tian, C., Tang, J., Li, Q., Sun, H., Lin, T., & Liao, Y. (2020). Emerging and legacy per-and polyfluoroalkyl substances in water, sediment, and air of the Bohai Sea and its surrounding rivers. *Environmental Pollution*, 114391.
- Zhao, Z., Tang, J., Mi, L., Tian, C., Zhong, G., Zhang, G., Wang, S., Li, Q., Ebinghaus, R., & Xie, Z. (2017). Perfluoroalkyl and polyfluoroalkyl substances in the lower atmosphere and surface waters of the Chinese Bohai Sea, Yellow Sea, and Yangtze River estuary. *Science of The Total Environment*, 599, 114-123.
- Zhao, Z., Xie, Z., Tang, J., Zhang, G., & Ebinghaus, R. (2015). Spatial distribution of perfluoroalkyl acids in surface sediments of the German Bight, North Sea. *Science of The Total Environment*, 511, 145-152.

Zhou, J., Li, S., Liang, X., Feng, X., Wang, T., Li, Z., & Zhu, L. (2021). First report on the sources, vertical distribution and human health risks of legacy and novel per-and polyfluoroalkyl substances in groundwater from the Loess Plateau, China. *Journal of hazardous materials*, 404, 124134.

Zhu, P., Ling, X., Liu, W., Kong, L., & Yao, Y. (2016). Simple and fast determination of perfluorinated compounds in Taihu Lake by SPE-UHPLC–MS/MS. *Journal of Chromatography B*, 1031, 61-67.

Zhu, Z., Wang, T., Wang, P., Lu, Y., & Giesy, J. P. (2014). Perfluoroalkyl and polyfluoroalkyl substances in sediments from South Bohai coastal watersheds, China. *Marine pollution bulletin*, 85(2), 619-627.